69-10,600

HSIA, Jen-chang, 1938-
DEVELOPMENT OF SINGLE AND DOUBLE SPIN-LABELING METHODS AND THEIR APPLICATIONS TO THE STUDY OF ANTIBODY ACTIVE SITES.

University of Hawaii, Ph.D., 1968
Biophysics, general

University Microfilms, Inc., Ann Arbor, Michigan

This dissertation has been
microfilmed exactly as received

69-10,600

HSIA, Jen-chang, 1938-

Please note: Name also appears as Carleton Jen-chang Hsia.

University Microfilms, Inc., Ann Arbor, Michigan

DEVELOPMENT OF SINGLE AND DOUBLE SPIN-LABELING METHODS AND THEIR APPLICATIONS TO THE STUDY OF ANTIBODY ACTIVE SITES

A THESIS SUBMITTED TO THE GRADUATE DIVISION OF THE
UNIVERSITY OF HAWAII IN PARTIAL FULFILLMENT
OF THE REQUIREMENTS FOR THE DEGREE OF

DOCTOR OF PHILOSOPHY

IN BIOPHYSICS

SEPTEMBER 1968

By

Jen-chang Hsia

Thesis Committee

Lawrence H. Piette, Chairman
Kerry T. Yasunobu
Robert H. McKay
Morton Mandel
J. Adin Mann, Jr.

ABSTRACT

DEVELOPMENT OF SINGLE AND DOUBLE SPIN-LABELING METHODS AND THEIR APPLICATIONS TO THE STUDY OF ANTIBODY ACTIVE SITES

Two specific methods have been developed, utilizing the electron spin resonance (ESR) spin-labeling technique, to probe the dimensional and structural nature of the macromolecular active site and to determine the correlation of active site structure with its biological specificities. The hapten combining sites (HCS) of rabbit anti-dinitrophenyl antibodies have been studied using two classes of twenty-two specifically prepared spin-labeled haptens.

The single spin-labeling method employs a hapten labeled with only one spin. The hapten may be either a monovalent or bivalent homologous hapten, or a cross reacting hapten. The line-width and maximum splitting of the anisotropic ESR spectrum of the spin-label is a function of its correlation time τ_c. The spectral variation is very sensitive to changes in τ_c within the range of 1 to 100 nanoseconds. This range is most suitable for studying dimensional variations of antibody HCS in solution since 100 nanoseconds is approximately the average rotational diffusion time of the antibodies. Pertinent results obtained with this method are: (1) the dominant contribution to the correlation time τ_c was found to be associated with freedom of rotation about a single

bond for the bound spin label; (2) the average depth of HCS was determined to be 10 Å, and heterogeneity of depth was observed; (3) differences in specificity of antibodies isolated with homologous and cross reacting antigens were found due to structural and dimensional differences at the HCS; (4) homologous haptens form a rigid complex and/or have preferred orientation at HCS, however, cross reacting haptens form a less rigid complex; (5) rotational relaxation time (ρ) for antibody monomer and dimer was determined; (6) a sensitive method has been developed in determining antibody hapten affinity, taking advantage of the complete separation of ESR absorption spectrum of the bound and free spin-label; (7) affinity spin-labels have been demonstrated to be able to distinguish specific and non-specific labeling.

Double spin-labeled haptens have two unpaired electrons per molecule. The intensities of the isotropic hyperfine and maximum splitting of the anisotropic ESR spectra are very sensitive to electron-electron exchange and dipolar interactions as well as to the relative orientation to the hyperfine tensors of the two electrons. The anisotropic spectra of the bound labels were only slightly perturbed. This may indicate that the HCS is quite flexible. However, the same spin-labeled hapten containing only one electron was rigidly immobilized at the antibody HCS.

From the results of this work, the HCS was found to be

dimensionally heterogeneous and probably consists of an inner rigid charge transfer complex region of approximately 5~6 Å with a flexible outer region of 4~5 Å which is partially hydrophobic.

TABLE OF CONTENTS PAGE

LIST OF FIGURES AND TABLES PAGE

LIST OF FIGURES AND TABLES (cont.) PAGE

LIST OF FIGURES AND TABLES (cont.) PAGE

ABBREVIATIONS

DNP-5-A:	(N-1-oxyl-2,2,5,5-tetramethyl-3-pyrrolidinyl)-2,4-dinitrobenzene
ONP-5-A:	(N-1-oxyl-2,2,5,5-tetramethyl-3-pyrrolidinyl)-o-nitrobenzene
PNP-5-A:	(N-1-oxyl-2,2,5,5-tetramethyl-3-pyrrolidinyl)-p-nitrobenzene
TNP-5-A:	(N-1-oxyl-2,2,5,5-tetramethyl-3-pyrrolidinyl)-2,4,6-trinitrobenzene
DNP-6-A:	(N-1-oxyl-2,2,6,6-tetramethyl-4-piperidinyl)-2,4-dinitrobenzene
DNP-6-H:	1-(1-oxyl-2,2,6,6-tetramethyl-4-piperidone)-2,4-dinitrophenyl hydrazone
DSL-Y and DSL-R:	1,5-di-(N-1-oxyl-2,2,5,5-tetramethyl-3-pyrrolidinyl)-2,4-dinitrobenzene
Mix-DSL:	1-(N-2,2,6,6-tetramethyl-4-piperidinyl)-5-(N-1-oxyl-2,2,5,5-tetramethyl-3-pyrrolidine)-2,4-dinitrobenzene
DNP-α-Gly-SL or α-Gly:	α-N-2,4-dinitrophenyl-(1-oxyl-2,2,6,6-tetramethyl-4-piperidinyl)-glycinate
DNP-β-Ala-SL or β-Ala:	β-N-2,4-dinitrophenyl-(1-oxyl-2,2,6,6-tetramethyl-4-piperidinyl)-alaninate

ABBREVIATIONS (cont.)

DNP-γ-But-SL or γ-But:	γ-N-2,4-dinitrophenyl-(1-oxyl-2,2,6,6-tetramethyl-4-piperidinyl)-butyrate
DNP-ε-Cap-SL or ε-Cap:	ε-N-2,4-dinitrophenyl-(1-oxyl-2,2,6,6-tetramethyl-4-piperidinyl)-caproate
Di-DNP-Lys-SL:	α, ε-N,N'-di-2,4-dinitrophenyl-(1-oxyl-2,2,6,6-tetramethyl-4-piperidinyl)-lysinate
FDNB-5-A or F:	1-Fluoro-5-N-(1-oxyl-2,2,5,5-tetramethyl-3-pyrrolidinyl)-2,4-dinitrobenzene
FDNB-5-MA:	1-Fluoro-5-N-(1-oxyl-2,2,5,5-tetramethyl-3-aminomethyl-pyrrolidinyl)-2,4-dinitrobenzene
DANSYL-NA:	1-dimethylamino-naphthalene-5-(N-1-oxyl-2,2,5,5-tetramethyl-3-pyrrolidinyl)-sulfonamide
DSL-5-MA:	1,5-di-(N-1-oxyl-2,2,5,5-tetramethyl-3-aminomethyl-pyrrolidinyl)-2,4-dinitrobenzene
6-Alcohol-NA:	1-oxyl-2,2,6,6-tetramethyl-4-piperidinol
5-Amine-NA:	1-oxyl-2,2,5,5-tetramethyl-3-amino-pyrrolidine
6-Amine-NA:	1-oxyl-2,2,6,6-tetramethyl-4-amino-piperidine
M-6-SL or M:	(N-1-oxyl-2,2,6,6-tetramethyl-4-piperidinyl)-maleimide
5-AM-NA:	1-oxyl-2,2,5,5-tetramethyl-3-aminomethyl-pyrrolidine

ABBREVIATIONS (cont.)

RγG:	Rabbit gamma globulin
HγG:	Human gamma globulin
BγG:	Bovine gamma globulin
BSA:	Bovine serum albumin
HSA:	Human serum albumin
AB-D:	anti-DNP-antibodies immunized with DNP-BγG isolated with DNP-HγG
AB-T:	anti-DNP-antibodies immunized with DNP-BSA isolated with DNP-PNP-TNP-HγG
τ_c:	Rotational correlation time or rotational reorientation time
ρ:	Rotational relaxation time
HCS:	Hapten combining site.
ESR:	Electron Spin Resonance
NMR:	Nuclear magnetic resonance
AEC:	Aminoethyl cellulose
SL:	Spin-label or spin-labels
SSL:	Single Spin-Labels or Single spin-labeled hapten
DSL:	Double spin-labels or double spin-labeled haptens
ASL:	Affinity spin-labels
A_{max}:	Maximum splitting of the anisotropic ESR spectra

CHAPTER I

INTRODUCTION

A general method has been developed utilizing Electron Spin Resonance (ESR) spin labeling technique in probing the dimensional and structural nature of macromolecular active sites and in determining the correlation of structure with biological activity. At present one can obtain detailed structural information from x-ray analysis of homogeneous protein single crystals. These studies are generally difficult, requiring many man-years of work for any one macromolecule. The method developed in the present work is most desirable because it offers an alternative method capable of giving a fairly good approximation of active site structure, with less exhaustive efforts than x-ray, and also can be used to study both homogeneous and heterogeneous systems in solution. The work presented here is an extension of the ESR spin-labeling technique developed by S. Ohnishi and H.M. McConnell (1965) and L. Stryer and O.H. Griffith (1965). Antidinitrophenyl (Anti-DNP) antibodies have been chosen as a model system in the present work in order to verify the method and study the correlation between the active site structure and biological specificity.

Since the multichain structure of immunoglobulins was established many attempts have been made to define the chemical basis of their various biological activities and

especially of that most characteristic property, combining specificity. This problem is greatly complicated by the size of the antibody molecules and, more particularly, by their remarkable chemical heterogeneity which is superimposed upon a constant basic structure. Recent studies have provided further evidence of this complexity reviewed by Gitlin (1966) and Fleischman (1966).

It seems reasonable to assume that the remarkable degree of structural variation of immunoglobulin chains is related to combining specificity, especially since the successful refolding of the antibody molecule in the absence of antigen has provided strong evidence that such specificity is dependent upon covalent structure. However, the analysis of the relationship between combining specificity and primary structure of heavy and light chains has been extremely complex. A physical method of studying this complexity is to measure the flexibility, depth, and shape of the immunoglobulin active site and study their correlation with heterogeneity, cross reactivity, and binding affinity.

(A) PHYSICAL AND CHEMICAL PROPERTIES OF RABBIT ANTI-DNP ANTIBODY (IgG)

The rabbit anti-DNP antibody belongs to the class of IgG immunoglobulins. The 4-chain structure of antibody molecules consisting of 2 heavy and 2 light chains covalently linked by interchain disulfide bonds first proposed by Porter (1962) for rabbit immunoglobulins (IgG), shown in Fig. 1-1, has been found to apply to all vertebrates having recognizable humoral antibodies.

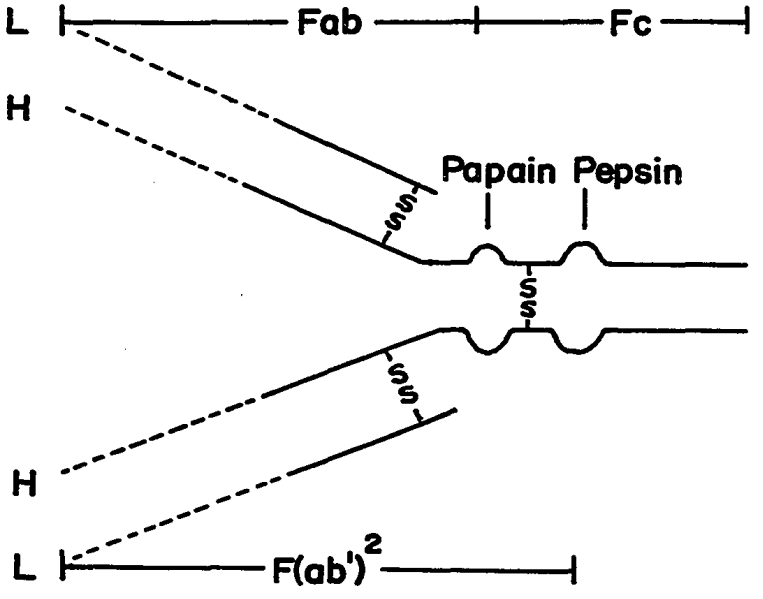

FIG. 1-1
Diagrammatic representation of the 4-chain structure of IgG linked by interchain disulfide bridges. Broken lines show stretches in which heterogeneity occurs (or is presumed) within a given chain type. The undulating portion of the heavy chain indicates the area susceptible to proteolytic digestion giving rise to the fragments indicated.

Preparations of rabbit IgG examined by negative contrast appear as essentially symmetrical particles 80 - 120 Å wide and about 34 Å thick (Feinstein and Rowe, 1965). Electron microscopy of rabbit anti-DNP IgG saturated with a bivalent DNP hapten (bisdinitrophenyl octamethylene diamine) indicates individual antibody molecules are y-shaped and the angle between the two arms can vary from 0 - 180°. Each arm is about 60 Å long and about 35 Å wide.

The isolation of monovalent Fab fragments from papain digestion of IgG antibody molecules (Porter, 1959) proves directly that each 4-chain unit carries two combining sites.

There are constant and variable regions on the rabbit antibodies. The variable portions of heavy and light chains are present in the active Fab fragments which contain the antibody HCS. It is generally assumed that this variability in primary structure is related directly to difference in combining specificity. The best evidence indicating that specificity is dependent on primary sequence comes from experiments in which Fab fragments of various rabbit antibodies, completely reduced in 6 M guanidine-HCl, were shown to regain a significant degree of combining affinity after removal of denaturing and reducing agents. (Buckley et al, 1963; Haber, 1964; Neolken and Tanford, 1964; Whitney and Tanford, 1965a.b.)

(B) IMMUNOLOGICAL SPECIFICITY

Specificity of induced antibodies is believed to be dependent on the chemical structure of portions of the protein antigen molecule. The most decisive discovery for the understanding and later development of immunological specificity was made by Landsteiner and Lampl (1917) through their successful preparation of azoantigens. By the use of these conjugated proteins, it was established (Landsteiner, 1945) that antibodies could be formed against small haptenic groups of known chemical structure. Because of the experimental limitations, the bulk of the research in this area has been limited to the study of the structure of the hapten in relation to the specific reaction.

The structural relation of an antigenic group and its homologous antibody site cannot be studied directly on an atomic scale. However, the antigen-antibody reaction, like the crystallization process, shows a high degree of selectivity but is more adaptable and flexible. Thus an antibody prepared against a particular group could be studied with respect to its capacity to discriminate between this group and other haptens which differ from it in terms of selected chemical and structural variations. In these studies, the process which is basic and therefore common to such investigation is the formation of a soluble complex between the antibody-combining site and the selected haptens. Aside

from kinetic observations, which have been few in number, the information which is potentially available is thermodynamic in nature. This thermodynamic information can be expressed in terms of free energy change (ΔF) for the process which may be written (assuming a monovalent hapten and two binding sites are equivalent)

$$H + S \rightleftharpoons HS$$

In this equation, H represents the hapten and S is a combining site of the antibody. Since the association constant K_A for this process is almost invariably calculated using molar concentrations, the free energy deduced from the equation

$$K_A = e^{-\Delta F/RT}$$

is the usual standard free energy (ΔF^{o}).

An important aspect of the interaction between antibody and hapten, as well as of the production of antibody, is the energetic heterogeneity of the antibody, which is best treated with Sip's (1948) distribution function developed for the heterogeneous catalyst surface. By using Sip's function, the resulting binding equation may be written as

$$r/n = \frac{(K_oC)^a}{1 + (K_oC)^a} \qquad (1\text{-}1)$$

where the number of combining sites per antibody molecule is n, r is the average number of sites occupied at the concentration C of free hapten, and a, the index of heterogeneity, may range from 0 to 1. K_o is the average intrinsic association constant when antibody sites are half saturated. The experimental suitability of equation (1-1) and the determination of a can be facilitated by the use of the following equation readily derived from the above:

$$\log \left(\frac{r}{n-r}\right) = a \log c + a \log K_o \qquad (1\text{-}2)$$

A plot of $\log \left(\frac{r}{n-r}\right)$ versus log c covering a sufficient range of c will test the adequacy of the Sip's distribution. If the plot is linear, then the value of a and K_o can be directly established.

(C) SIZE OF THE ANTIBODY-COMBINING REGION

The extent of the combining region of the antibody is an aspect of immunological behavior that has an important bearing on such properties of the antibody-hapten reaction as affinity, heterogeneity, and cross reactivity. The combining region can be defined, of course, only with respect to the ligand with which it interacts. Since the discovery of anti-hapten antibodies, it has been clear that the combination of antibody with a test antigen, to yield, e.g., a specific precipitate, need involve the interaction of only a small portion of the antibody molecule. The early experiments of Hooker and Boyd (1933) served to show that, for a small haptenic group, such as p-azophenylarsonate, the antibody site extended beyond this to include at least the residue to which the azo group was attached. On the other hand, from a hapten inhibition study with an antibody homologous to the p-azosuccinanilate group, Pressman, et al. (1948) concluded that "the combining region of the antibody is complementary in structure to succinanilate and also to the benzene ring, but that it does not extend much further along the haptenic group."

The extent of the antibody site has been elucidated by Kabat (1954, 1956, 1960) through the use of the hapten inhibition method applied to human anti-dextran antiserum. These studies were largely concerned with human anti-dextran

of 1-6 specificity and the inhibition of its precipitation with oligosaccharides of the isomaltose series ranging from glucose to isomaltoheptaose. Since the antibody was introduced by an antigen consisting of long chains of 1-6 linked α-D-glucopyranose units, it was possible to explore the size of the antigenic determinant with these homologous oligosaccharides.

From a comparison of the hapten inhibition curves obtained with six individual human anti-dextran sera and the five compounds--isomaltoheptaose, isomaltohexaose, isomaltopentaose, isomaltotetraose, isomaltotriose--two interesting conclusions have been obtained (Kabat, 1961). (1) Increasing inhibition per mole of compound was observed between the triose and the hexaose, but the incremental increase declined with increasing length. (2) Maximum inhibition was observed with the hexaose indicating that this represented the limit of the size of antigenic determinant to which the antibody can be complementary. The extent of the antibody-combining region inferred from this result fits in well with the more approximate estimates made in the foregoing.

A marked heterogeneity was revealed by differences in the relative effectiveness of the homologous inhibitors among the several human antisera. (Kabat, 1956) This heterogeneity was attributed to the existence of mixed

populations of antibody with combining regions of different size or to the overlapping notion that the degree of complementarity to each of the six units varies from one antibody molecule to another. A choice between these extreme alternatives was not possible.

(D) HETEROGENEITY OF ANTI-DNP ANTIBODIES

The variation of association constants of anti-DNP antibodies against DNP-Lysin was found to be as large as 1,000 fold, which is related to the difference in the immunization procedure. In an early study (Carsten and Eisen, 1955), multiple intravenous injections of the soluble antigen were used. K_o was found to be 2.3×10^5 liter/mole. In a later work (Velick et al., 1960), a much smaller amount of antigen in Freund's adjuvant was administered in the foot pad and K_o was found to be 2×10^8 liter/mole. This variation in affinity during the immune response was further investigated by Eisen and Siskind (1964) where all populations of anti-DNP molecules examined, whether isolated from pooled sera or from single bleedings of individual rabbits, were heterogeneous in respect to affinity for nitrobenzenes. Fractional precipitation of antibody from serum, by addition of limited amounts of antigen, yielded from the serum of individual rabbits anti-DNP populations that differed as much as 10,000 fold (from 10^5-10^9) in K_o. The K_o increased progressively with time after immunization. It was inferred from the low affinity of antibodies isolated early after immunization that their specific binding sites are poorly adapted to the dinitroanilino group and insensitive to the norleucine moiety of the ε-DNP-Lysine. In contrast, antibodies isolated late after immunization bind ε-DNP-Lysine

strongly and from their interaction with a variety of dinitrobenzenes, it was inferred that their binding sites, on the average, are just about large enough to accommodate ε-DNP-L-Lysine. At the same time, affinity of antibodies was found to be dependent on purification procedures (Eisen and Siskind, 1964). This variation in affinity was also found to be related to hapten conjugated antigens used in the isolation procedure whether it is an homologous or a cross reacting hapten antigen (Cheng and Talmage, 1965). Fractionation of heterogeneous antibodies according to their binding affinity was achieved by Cheng and Talmage in 1966. This energetic heterogeneity is thought to couple with a structural heterogeneity of the HCS which is in turn related to the primary amino acid sequence of the variable region of the heavy and light chain near the active site.

(E) SPIN-LABELING TECHNIQUE

(1) Introduction

In the original experimental work of H. McConnell and co-workers, it was found that the attachment of paramagnetic species to large molecules may be used to obtain information about the behavior of these molecules in solution. This technique, called "spin-labeling", makes use of the strong motional dependence of the electron spin resonance (ESR) spectra of a class of stable nitroxide free radicals in solution. Most of the experimental work to date has used various forms of these radicals, shown schematically as (I), as the spin labels, which contain a protected nitroxide group, where the nitrogen atom is bound to two tertiary carbon atoms and R is a group that is used to bind the radical to the macromolecule.

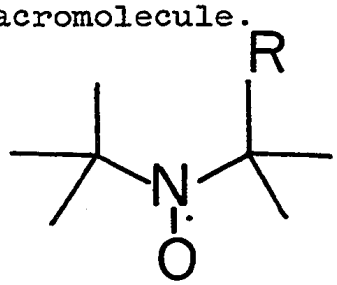

(I)

These radicals are quite stable in solution and exhibit sharp, well-resolved ESR spectra which are quite sensitive to molecular motion. The first stable saturated nitroxide radical was prepared by A.K. Hoffman. The chemistry of these radicals has been subsequently developed extensively by Dupeyre and co-workers (1964, 1965, 1966) and by Rozantzev,

Neiman, and co-workers (1962-1967). Some of these radicals have been prepared as single crystal solid solutions in an inert solvent and their ESR spectra have been taken as relative orientations of the crystallographic and external-magnetic-field axes (Griffith and co-workers, 1965). For all orientations, the spectra are well resolved and consist of three sharp lines whose separation is a function of orientation. From these spectra, one may conclude that the hyperfine interaction between the electron (S = 1/2) and the nitrogen nucleus (I = 1), on which most of the electron spin is presumed to be localized, is anisotropic.

(2) The Spin Hamiltonian

The spin Hamiltonian for a typical nitroxide spin-label is:

$$\mathcal{H} = |\beta| \, \hat{\underset{\sim}{S}} \cdot \underset{\approx}{g} \cdot \underset{\sim}{H} + \hat{\underset{\sim}{S}} \cdot \underset{\approx}{T} \cdot \hat{\underset{\sim}{I}} \qquad (1\text{-}3)$$

The Hamiltonian is expressed in units of $\hbar$ and the two right-hand terms are, respectively, Zeeman and hyperfine energies where β, $\hat{\underset{\sim}{S}}$, $\underset{\approx}{g}$, $\underset{\sim}{H}$, $\underset{\approx}{T}$ and $\hat{\underset{\sim}{I}}$ are the electron Bohr magneton, the g tensor, the electron spin operator, the external magnetic field, the hyperfine tensor and the nuclear spin operator, respectively. Representative elements of the g and hyperfine tensor are:

$T_z \simeq 90$ Mc $\qquad g_{xx} = 2.009$

$T_x \simeq T_y \simeq 15$ Mc $\qquad g_{yy} = 2.006$

$g_{zz} = 2.0027$

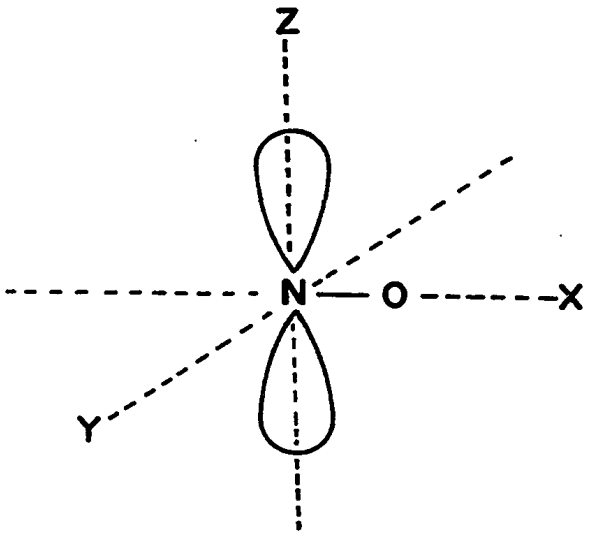

FIG. 1-2
Principle axis system for the sterically protected nitroxide group

The observed elements of the anisotropic hyperfine tensor, together with the known magnitude of the isotropic hyperfine interaction ($a = 1/3\ (Tx + Ty + Tz)$) shows that the odd electron is confined largely to a $2p\pi$ atomic orbital on the nitrogen atom, whose evident near cylindrical symmetry ($Tx \simeq Ty$) is parallel to the z axis in Fig. 1-2. Stereochemical considerations, as well as the single crystal studies indicate that the two tertiary carbon atoms, the nitrogen atom and oxygen atom all lie in a common plane (xy) in Fig. 1-2.

If one prepares a solution of one of these spin-labels in a low-viscosity solvent, the ESR spectrum becomes a sharp

three-line spectrum, which, of course, is independent of the orientation of the sample in the magnetic field. The observed splittings in solution are approximately equal to the average of the principle axis splitting observed in the single crystals (implying that the three principle axis components all have the same sign). If one now increases the viscosity, the three lines begin to broaden, with the high field line broadening most rapidly. As one increases the viscosity of the solution still more, the lines begin to overlap, the spectrum becomes unsymmetric and the total width of the spectrum approaches the maximum principle axis splitting.

(3) Method of Determining τ_c

If one attaches a "spin label" on to a biomacromolecule via a biofunctional group, the product ESR spectrum in a low viscosity solution appears to be anisotropic. For most cases, the spectra correspond to two categories: (1) strongly-immobilized spin, and (2) weakly-immobilized spin.

(1) For the strongly-immobilized spins, the experimental technique of Stryer and Griffith (1965) has been used to estimate the rotational correlation time from the ESR spectrum of the nitroxide. In their experiment, a radical containing both a paramagnetic spin label and a fluorescent chromophore was prepared. For solutions of various viscosity,

the fluorescent depolarization of the chromophore is measured and used to calculate the rotational correlation time. The ESR spectrum is also measured and, assuming that the chromophore and the spin label are rigidly bound together, one can obtain a chart of the ESR spectrum as a function of correlation time.

(2) For the weakly-immobilized spins, where there is only a small deviation from a complete averaging by rapid tumbling and small anisotropy, the quantitative theory of Kivelson (1960) is adequate to estimate the correlation time of the nitroxide. According to the theory developed by Kivelson, the line width of a paramagnetic resonance absorption of a free radical in solution may be expressed as a polynomial in the nuclear spin quantum number M_I. Assuming a Lorentzin line shape, Kivelson's expression is

$$\delta\nu(M) = \pi\sqrt{3}\left[(T_1')^{-1} + (T_2')^{-1}\right] = \pi\sqrt{3}\,(a_1 + a_2 M_I + a_3 M_I)$$

where $\delta\nu(M)$ is the peak-to-peak line width of the absorption derivative, and T_1' and T_2' are the longitudinal and transverse relaxation times of the Bloch equations, respectively. For a single nucleus of I = 1, assuming an axially symmetric spin Hamiltonian, the a_i can be determined. This provides information about the magnetic interaction anisotropy and the re-orientational correlation time τ_c. τ_c is the correlation time for the orientation of the molecular axis with respect to the external magnetic field. From the

linear term in M_I

$$\tau_c = \frac{\delta\nu(M_{-1})+\delta\nu(M_{+1})}{\delta\nu(M_0)} \left\{ \frac{15\pi}{8} \frac{3\delta(M_0)}{b\Delta\gamma H} \right\} \qquad (1\text{-}4)$$

From the quadratic term in M_I

$$\tau_c = \left\{ \frac{\delta\nu(M_{-1})+\delta\nu(M_{+1})}{\delta\nu(M_0)} - 2 \right\} \left\{ \frac{4\pi\sqrt{3}\,\delta\nu(M_0)}{b^2} \right\} \qquad (1\text{-}5)$$

where $\Delta\gamma = \frac{-|\beta|}{\hbar}\left[g_z - \frac{1}{2}(g_x+g_y)\right]$, $b = 4\pi/3(T_z - T_x)$

and the assumption of slow molecular tumbling is made, i.e. $\omega\tau_c \gg 1$ where $\omega = g|\beta|T_x\hbar^{-1}$

Very recently, Itzkowitz (1967) was able to use the exact and approximate solutions to the nitroxide Hamiltonian to simulate spectra from orientated samples, by performing calculations of orientation averages to obtain simulated polycrystalline spectra, and developed a Monte Carlo scheme to evaluate the spectrum for a variety of tumbling rates. His method is expected to obtain τ_c for all the anisotropic ESR spectra of the nitroxide spin labels.

(4) Success of the Method as a Probe

A number of significant papers have now appeared on spin-labeled macromolecules in solution. Their attention is focused on the following three areas.

(1) Conformation change of macromolecules

(a) Proteins:

Oxygen-linked conformational changes in horse

hemoglobin was detected by (spin-labeling technique) Ogawa and McConnell (1967) with SH specific spin label. It was later confirmed by spin-labeled subunit and recombination studies of human hemoglobin by Ohnishi and co-workers (1968).

(b) Poly nucleotide:

Spin-labeled Poly A and Poly G was found to exist in only two forms in the pH range of the transition from a highly ordered to a disordered conformation by Ian C.P. Smith and Tetsuo Yamane (1967).

(2) Spin-labeled substrate for enzymes

A spin label acyl-α-chymotrypsin intermediate was isolated by Berliner and McConnell (1966). The label was found to be strongly immobilized at the active site and the rate constant of deacylaton was determined.

(3) Spin-labeled hapten

Dinitrophenyl hydrozone nitroxide, a spin-labeled hapten, was used by Stryer and Griffith (1965) to study the rigidity of the antibody combining sites. Using combined studies of ESR and polarization fluorescence, they have estimated the rotational correlation time (ρ) for the bound spin label to be 36 nanoseconds.

It is now quite clear that the paramagnetic resonance of synthetic spin labels offers a powerfully new method for investigating a number of features of the structure, motion, and chemistry of biological macromolecules. But the sensitivity of the nitroxide spin label has not been fully utilized; namely, the spin label has only been used to distinguish two different states, bound vs free, weakly immobilized to strongly immobilized. A close examination of anisotropy of the nuclear hyperfine interaction of the nitroxide spin label indicates that systematic modifications of specific labels may develop into a general method to measure various dimensional and structural properties of protein active site in solution.

CHAPTER II

EXTENSION OF THE SINGLE SPIN-LABELING TECHNIQUE

(A) Introduction

Most protein molecules have an approximate average rotational relaxation time between 10 to 100 nanoseconds in their hydrodynamic state while specific biological reactions take place. Their active site configuration, structure, and dimensions are most interesting to scientists in the elucidation of biological specificities. These properties can be studied with a series of systematically modified molecular probes labeled at the protein active site, which can report their local environment.

(B) Formulation of Research Problem

(1) Method of Studying Longitudinal Dimension of Antibody HCS.

The advancement in magnetic resonance spectroscopy has enabled us to use the anisotropic interaction of electron and nuclear moments as a magnetic probe to investigate the dimensional and structural properties of a protein active site in solution.

As indicated earlier, the ESR spin-labeling technique was first introduced by Ohnishi and McConnell. Most of the experimental works have used the following two types of spin-labels shown schematically as A and B.

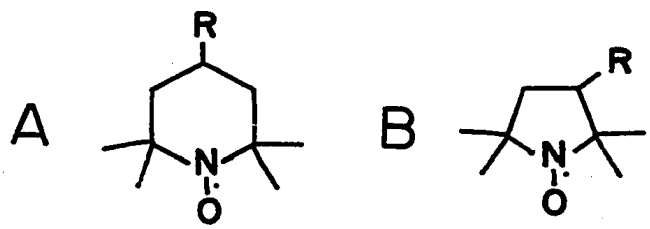

These spin-labels contain a protected nitroxide group, where the nitrogen atom is bound to two tertiary carbon atoms, and R is in the case of antibody studies, the antigenic specific hapten group, or it may be in general studies another biofunctional group. The free radical nitroxide group then serves as the reporter group reflecting its environment via an Electron Resonance Absorption.

In a low viscosity solvent, the tumbling frequency of the spin-label is very fast. The rotational correlation time τ_c for the radical is approximately .01 nanoseconds. Such rapid motion completely averages out the anisotropic hyperfine interaction. If the mobility of the nitroxide is impaired and tumbling is very slow, then the limit for the rotational correlation time τ_c is related to the anisotropy of the nuclear hyperfine interaction in Eq. (1-3) by the approximation

$$\tau_c \simeq |T_z - T_x|^{-1} \simeq 13 \text{ nano-Sec} \qquad (2\text{-}1)$$

FIG. 2-1: ESR spectra of 1-oxyl-2,2,6,6-tetramethyl-4-piperidinol in various weight percent glycerol aqueous solution.

(A) at 0.116 Poise and 283°K

(B) at 0.367 " and 293°K

(C) at 0.523 " and 293°K

(D) at 1.58 " and 283°K

(E) at 5.77 " and 273°K

(F) at 9.42 " and 273°K

The free radical concentration was 1×10^{-4}M. The τ_c were calculated according to equation (2-2) assuming an effective Stoke's radius of 5 Å.

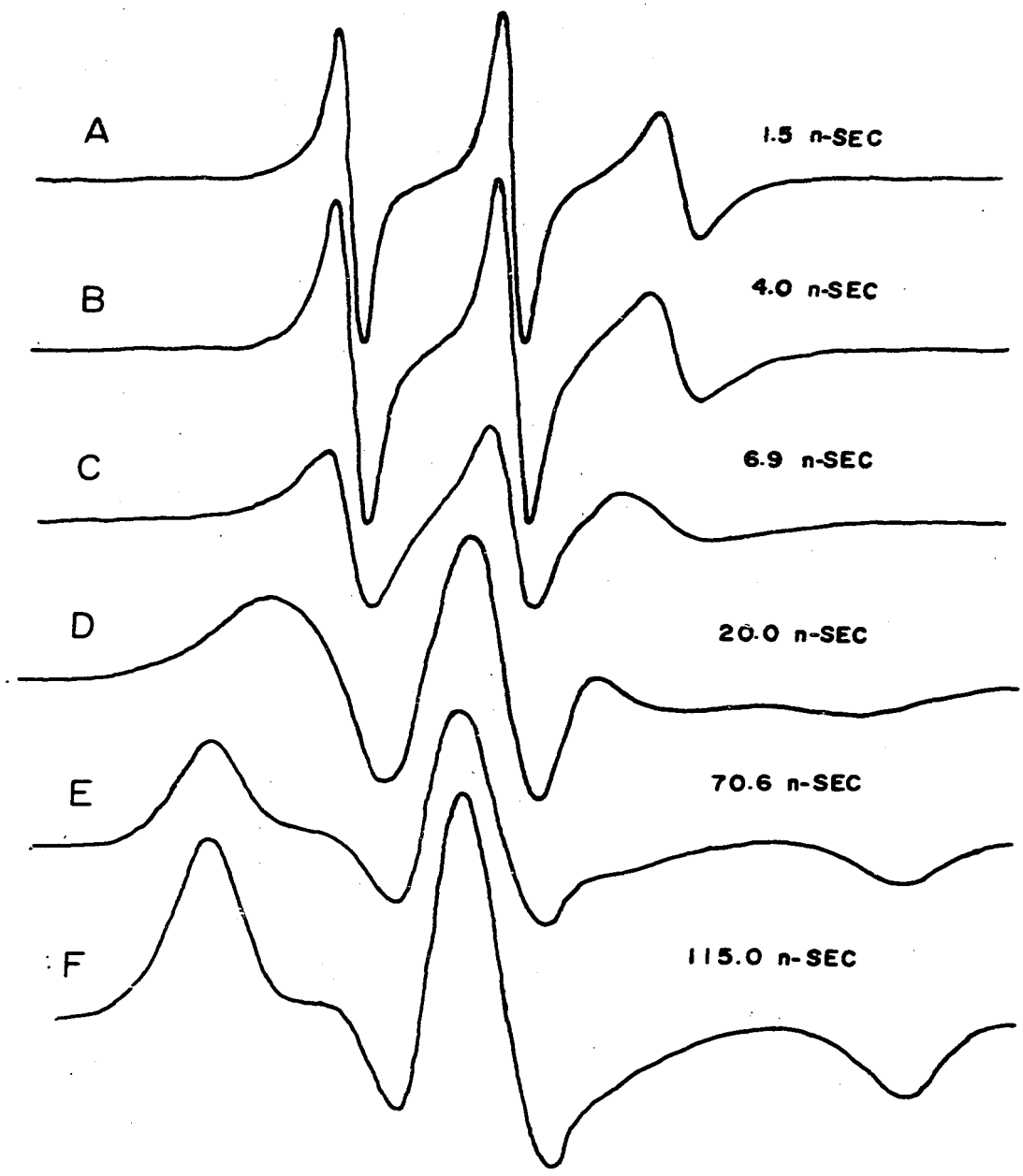
A
1.5 n-SEC
B
4.0 n-SEC
C
6.9 n-SEC
D
20.0 n-SEC
E
70.6 n-SEC
F
115.0 n-SEC

Intermediate correlation times are obtained by slowly changing the tumbling frequency of the molecules. Such variations in tumbling frequencies are easily obtained by variation of the solution viscosity into which the nitroxide is placed.

This variation in τ_c is easily detected in the ESR absorption by observing initially a broadening of the three sharp lines (Fig. 2-1 a, b, and c) obtained from the hyperfine interaction of the N^{14} nucleus with the electron, and a subsequent overlapping of lines (Fig. 2-1 d and e) and finally a redistribution of the lines characteristic of a randomly oriented-free radical in a rigid matrix (Fig. 2-1 f).

The relative tumbling time of the molecule can be conveniently approximated from the Stokes and Einstein's equation,

$$\tau_c = 4\pi\eta\, a_o^3 / 3KT \qquad (2\text{-}2)$$

where η is the viscosity of the medium in poise and $\underline{a}_o$ is the effective radius in Å, $\underline{k}$ the Boltzman constant and T the absolute temperature.

It is evident from Fig. 2-1, that the ESR absorption of these nitroxide spin-labels is extremely sensitive to correlation time variations in the region 1-100 nanoseconds. It is exactly this range of times that

are important in the study of protein macromolecular active sites. A typical protein antibody rotational relaxation time is of the order of 100 nanoseconds, such a time is greater than that approximated for a nitroxide radical in a rigid matrix given by Eq. (2-1). If then a spin-label were attached to an antibody in a manner which would allow no motion of the label relative to the antibody, an ESR absorption would be observed characteristic of a correlation time given by the rotational relaxation time of the antibody and would be similar to that shown in Fig. 2-1 f. If, however, the spin-label were attached to the antibody in a region wherein the label can move with some degree of freedom relative to the protein such as in a very flexible combining site or on the surface of the protein or in an area just outside the binding site, the ESR absorption of the label would reflect this mobility as in Fig. 2-1 a-e.

It can be seen then that this sensitivity of the spin-label to its freedom of motion can be used to map out the dimensions of the combining site of an antibody. If we assume some finite depth to the combining site depicted as

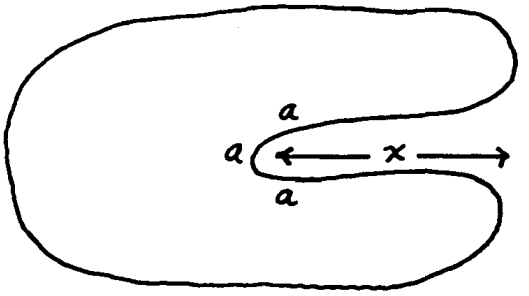

where x represents the depth of the site, and if we further assume binding occurs through the hapten in the general region of a, then by constructing hapten spin-labels of the type

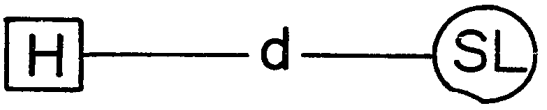

where H represents the hapten as indicated and d is a carbon chain separation which can be varied and SL the spin-label nitroxide moiety, we can easily determine the depth of the site x. When (d + H) is small compared to x and assuming a narrow slit for the combining site, the spin-label nitroxide upon binding will give an ESR absorption characteristic of the protein tumbling rate similar to that in Fig. 2-1 f. As (d + H) becomes large relative to x, the spin-label will be forced out of the combining site and will have mobility independent of the antibody protein and should show an ESR absorption characterized by Fig. 2-1 a-e.

A plot of the correlation time of the spin-label as a function of (d + H) should show a break characteristic of the depth of the combining site x.

Similarly another approach can be taken to determine x. If instead of using a monovalent hapten spin-label, we use a bivalent hapten spin-label depicted as:

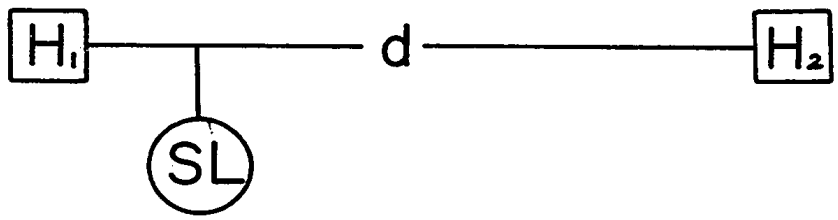

where H, d and SL are previously defined. If H_1 and H_2 are identical haptens, higher conjugates of the antibody can be formed provided $(d + H_1 + H_2)$ is $\geqslant 2x$. If the concentration of antibody is kept low so as to bind only at one hapten namely H_2, then the ESR absorption for the spin-label SL should be characteristic of a spin-label with a high degree of freedom. As more antibody is added so that binding occurs at H_1 to form higher conjugates, the ESR for the spin-label should be similar to that of a completely immobilized spin characterized by Fig. 1 f. The dimerization will not occur if d is much less than 2x. Thus by varying d again, we can verify the dimension x by this alternative method.

(2) Correlation of Energetic and Structural Heterogeneity of HCS.

Anti-DNP antibodies have been long recognized to be heterogeneous. It would be very interesting to correlate this difference in binding affinity to actual dimensional and structural differences of the binding sites. This also would serve as a test of the method in its ability to study heterogeneous systems where small dimensional variations occur.

(3) Mechanism of Cross Reactivity of HCS.

The way in which cross reacting haptens bind to homologous HCS remains an interesting question. To date, this problem can only be studied in terms of their binding affinities. With the use of a motional dependent spin-label, this limit may be extended to include comparative physical studies of the difference in the interactions of spin-labeled homologous and cross reacting haptens with the combining site.

(4) Rotational Relaxation Time of Antibodies and Rigidity of HCS.

The rotational relaxation time of normal globulin has been determined to be 200 nanoseconds by electric birefringence (Krause, S., O'Konski, C.T., 1963) and anti-DNP antibodies to be 36 nanoseconds by DNP-6-H

(dinitrophenyl hydrozone nitroxide) by Stryer, L., and Griffith, O.H. (1965). This discrepancy was attributed by the latter paper due to small rotational flexibility of the nitroxide radical relative to the whole antibody plus free rotation of nitroxide ring relative to the dinitrophenyl group. It appears that a more rigid spin-labeled hapten can be prepared with shorter distance between the hapten and the nitroxide than DNP-6-H. A spin-label of this nature may give us a better estimation of the rigidity of HCS and the rotational relaxation time, ρ, of the rabbit anti-DNP antibody.

(5) Spin-Label Studies of Antibody Affinity.

A considerable number of antibody hapten systems have been studied with haptens which have absorption spectra in the visible region. Usually the hapten which is specifically bound to the antibody has a somewhat different spectrum from that of the hapten which is free in solution, but the spectral shift and the extinction coefficient of the new absorption peak are relatively small (H. Metzger et al, 1963). Furthermore, these types of spectral properties are limited to a single specific case and cannot be applied as a general method.

Taking advantage of the complete separation and narrow line width (i.e. 1 gauss of high field peak of the isotropic spectrum from the anisotropic spectrum), the rigid spin-labeled haptens can be developed into a general method to study the binding affinity and stoichiometry of hapten-antibody complexes, provided the proper spin-labeled haptens can be prepared and the antibody hapten combining site (HCS) has a depth of approximately 2-3 Å deeper than the hapten group.

(6) Affinity Spin-Labeling Studies of the Antibody Active Site.

In the past decade, considerable information about the active sites of a variety of enzymes has been obtained by attaching chemical groups (labels) specifically to some amino acid residue in the active sites. Once a stable linkage is thus formed, the label serves to identify peptide fragments arising from the site upon systematic degradation of the labeled enzymes. A similar method introduced by Leon **Wofsy** and co-workers (1962) is called affinity labeling, where a specific labeling reagent for a given antibody is synthesized which (1) can combine specifically with the particular antibody active sites and (2) possesses a small functional group which can react

readily to form an irreversible covalent bond with one or more amino acid residues. Using this method, tyrosine residue was found to be present at the active site of anti-DNP antibodies (H. Metzger et al, 1963). In the case of labeled tyrosine, heavy chain and light chain are both labeled, and the distribution between the heavy and light chains is almost constant, approximately 2:1 on a molar basis. Analysis of the labeled peptide fragments with counter-current distribution found (1) labeled peptide from both chains appears to be heterogeneous and (2) highly hydrophobic in nature. (Reviewed by S.J. Singer and R.F. Doolittle, 1966). In light of the uncertainty involved in the affinity labeling method (i.e. there is no way of distinguishing between non-specific and specific labeling), it would be useful to prepare a spin-labeled affinity label. Thus, specific and non-specific labeling could be distinguished.

The general formula of an affinity spin-label can be illustrated as follows:

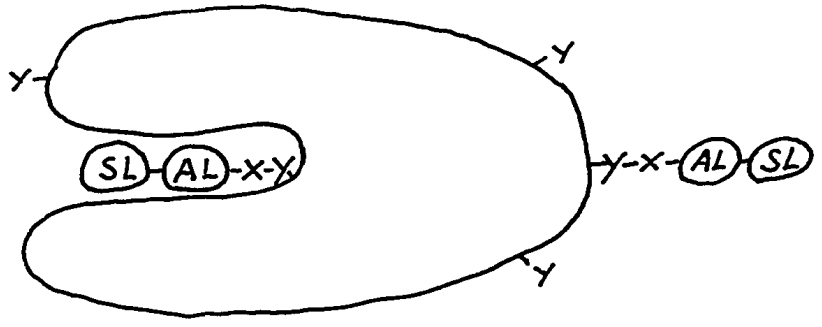

where SL, AL and x are covalently linked spin-label (i.e. nitroxide free radical), affinity label (i.e. hapten for antibodies and inhibitors or substrate for enzymes), and bio-functional group, respectively. y are labeling sites on a protein molecules, specific or non-specific (i.e. SH, NH_2, RNH, R-OH).

(C) Experimental

(1) Instruments and Equipment.

(a) ESR Spectrometer for General Measurements.

The ESR spectra of all the spin-labels were recorded on a 9.5 GHz Varian V4502-13 spectrometer, with a V-4540 variable temperature accessory. The temperatures were calibrated with a thermocouple within $\pm$ 0.1^{o}C.

Fremy salt was used as the standard in the determination of the hyperfine constant of both isotropic and anisotropic ESR spectra of the spin-labels.

The aqueous sample cell used for variable temperature studies was obtained from J.F. Scanlon Co., Whittier, California.

(b) ESR Spectrometer for Titration Measurements.

Spin-labeled hapten titrations of antibody affinity were carried out on a Varian E-3 solid-state spectrometer.

(c) NMR Spectrometer.

A Varian HA-100 spectrometer was used in structure identification of certain diamagnetic intermediate species.

(d) Fluorometer for Polarization Measurement.

Polarization fluorescence measurements were obtained from a spectrophotofluorometer kindly provided by Dr. R.H. McKay.

(e) Spectrophotometer.

Absorbance spectra were obtained from Cary Model 14 recording spectrophotometer using quartz cells with a 10-mm light path.

(f) Melting Points.

Melting points were obtained on a Fisher-Johns Melting Apparatus. The melting points reported were not corrected using calibration standards.

(g) Glassware.

ESR flat cells were cleaned with chromic acid, rinsed many times with distilled water and then rinsed with acetone and vacuum suction dried.

(2) Materials.

(a) Reagents.

2,4-dinitrophenyl sulfonic acid sodium salt, 2,4-dinitrophenyl (Eastman), and ε-DNP-Lysine

(Sigma) were recrystallized three times before use. Analytical grade o-nitrofluorobenzene, p-nitrofluorobenzene, 1,5-difluoro-2,4-dinitrobenzene, 2,4-dinitrofluorobenzene and picryl chloride (Eastman), α-DNP-glycine, β-DNP-alanine, δ-DNP-Butyrate, ε-DNP-Caporate, α,ε-di-DNP-Lysine, α,δ-di-DNP-ornithine (Sigma) were used without further purification. Streptomycin sulfate (Squibb), DEAE cellulose, Dowex-1-anion exchange resin (Sigma), Amberlite IRA-400, Cl^- form (Mallinckrodt Chemicals) and Sephadex G-25, G-200 were ordered from Pharmacia. HγG, RγG, BγG, BSA, and Freund's complete adjuvant were purchased from Pentex Inc. Dansyl sulfonyl chloride, 2,2,6,6-tetramethyl-4-piperidinol, 2,2,6,6-tetramethyl-4-amino-piperidine, 2,2,6,6-tetramethyl-4-piperidinol and triacetonamine were obtained from Aldrich Chem. Co. N-(1-oxyl-2,2,6,6-tetramethyl piperidinyl)-maleimide (M-6-SL) was a gift from Varian Associates. Lithium aluminum hydride was ordered from Alfa Inorganies, Inc.

(b) Preparation of Spin-Labeled Haptens.

1. Spin-Labeled Nitrophenyl Amines.

<u>DNP-5-A (Ia)</u>: N-(1-oxyl 2,2,5,5-tetramethyl pyrrolidinyl-2,4-dinitrobenzene)

2,2,5,5-tetramethyl-3-amino-pyrrolidine-1-oxyl (5-Amine-NA) was prepared by the procedure of Rozantzev and Krinitzkaya (1965). Equal molar solutions of 5-Amine-NA and 1-Fluoro-2,4-dinitrofluorobenzene were reacted in chloroform for 6 hours. Solvent was removed under vacuum and a yellow precipitate was recrystallized from chloroform and ether. Orange crystals were finally obtained with m.p. 205-206°.

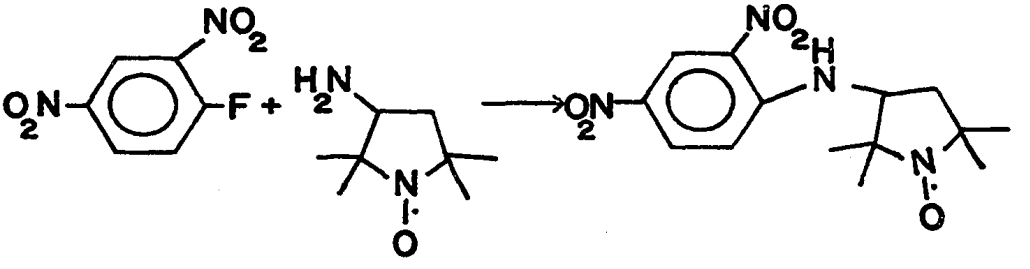

(Ia)

Anal. Ia: Calc. for $C_{14}H_{19}N_4O_5$; C, 52.0; H, 5.8; N, 17.3%

Found: C, 51; H, 5.4; N, 17.3%

<u>ONP-5-A (Ib)</u>: o-Nitrophenyl amine nitroxide (Ib): N-(2,2,5,5-tetramethyl-3-amino-pyrrolidine-1-oxyl)-o-nitrobenzene was prepared in a manner analogous to Ia. m.p. 106-106.5°.

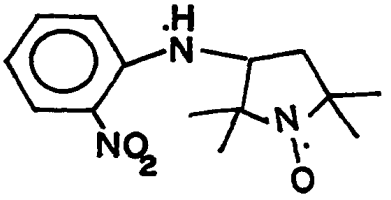

(Ib)

Anal. Ib: Calc. for $C_{14}H_{20}N_3O_3$: C, 60.4; H, 7.2; N, 15.1%

Found: C, 60.4; H, 7.3; N, 15.3%

<u>PNP-5-A (Ic)</u>: p-Nitrophenyl amine nitroxide (Ia): N-(1-oxyl-2,2,5,5-tetramethyl-3-amino-pyrrolidinyl)-p-nitrobenzene was synthesized in a manner analogous to Ia, with a catalytic amount of potassium carbonate. m.p. 187-187.5°.

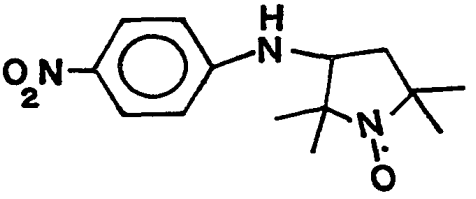

(Ic)

M.W. calc. 278.33

Mass spectral analysis found 278.

<u>TNP-5-A (Id)</u>: N-(1-oxyl-2,2,5,5-tetramethyl-3-amino-pyrrolidine)-2,4,6-trinitrobenzene were prepared according to the procedure of (Ih).

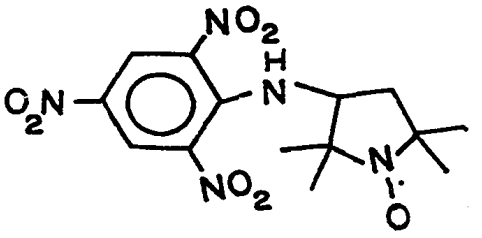

(Id)

Anal. Id: Calc. for $C_{14}H_{18}N_5O_7$: C, 45.7; H, 5.06; N, 19%

Found: C, 45.6; H, 5.05; N, 19%

<u>DNP-5-MA (Ie)</u>: N-(1-oxyl-2,2,5,5-tetramethyl-3-aminomethyl-pyrrolidine)-2,4-dinitrobenzene: 1-oxyl-2,2,5,5-tetramethyl-3-aminomethyl-pyrrolidine (5-AM-NA) was prepared by the reduction of 1-oxyl-2,2,5,5-tetramethyl-3-carboimide-pyrrolidine with equal molar amount of Lithium Aluminum hydride reflex in ether for 24 hours.

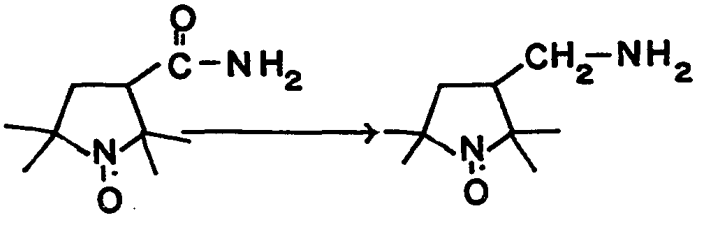

Isolated product (5-AM-NA) was vacuum sublimated yielding a light yellow crystal with a melting point of 97-98°.

The product amine was reacted with 1-Fluoro-2,4-dinitrobenzene according to the procedure of Ia. Recrystallized bright orange-red crystals of Ie with a melting point of between 140-140.5°.

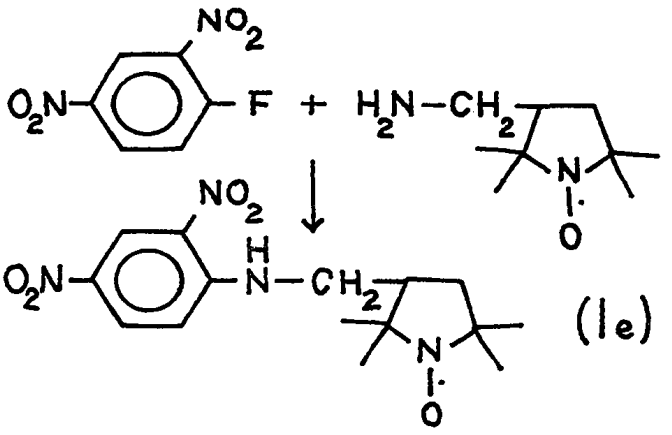

<u>DNP-6-A (If)</u>: N-(1-oxyl-2,2,6,6-tetramethyl-4-piperidinyl)-2,4-dinitrobenzene: Equal molar amounts of 1-Fluoro-2,4-dinitrobenzene

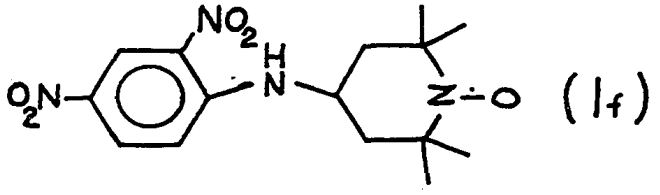

4-Amino-1-oxyl-2,2,6,6-tetramethyl-piperidine (6-Amine-NA) prepared according to the procedure of E.G. Rozantzev and

Yu. V. Kokhanov (1966) were reacted in chloroform overnight. Reaction mixture was filtered; chloroform phase was chromatographed on a silicic acid column. The fast moving yellow band was collected and the solvent stripped under vacuum. Orange crystals were obtained upon recrystallization from chloroform and hexane. m.p. 185-185.5°.

M.W. calc. 337.35. Mass spectral analysis indicated the M.W. to be 337.

Anal. Id: calc. for $C_{15}H_{21}N_4O_5$: C, 53.93; H, 6.0; N, 16.6%

Found: C, 53.8; H, 6.0; N, 16.6%

<u>ONP-6-A (Ig)</u>: N-(1-oxyl-2,2,6,6-tetramethyl-4-piperidine)-o-nitrobenzene was prepared analogously to the procedure of Id. m.p. 160-160.5°.

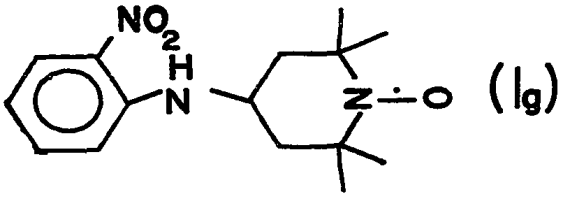

(Ig)

M.W. calc. 291.34. Mass spectral analysis, M.W. 291.

<u>TNP-6-A (Ih)</u>: N-(1-oxyl-2,2,6,6-tetramethyl-4-amino-piperidine)-2,4,6-trinitrobenzene.

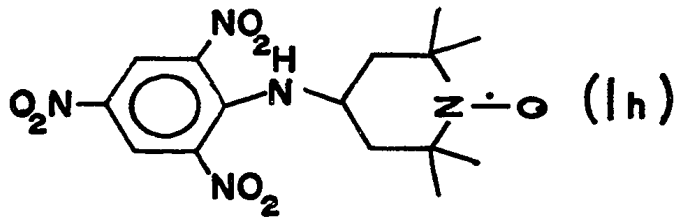

Equal molar of picryl chloride and 6-amine-NA were allowed to react in chloroform with vigorous magnetic stirring overnight. Reaction mixture was filtered; chloroform phase was chromatographed on a silicic acid column. Second yellow band was collected. Orange crystals were obtained after solvent was stripped off in vacuum. After recrystallization in chloroform and ether, metallic brown, flaky crystals were obtained. m.p. 203.5-204°. M.W. calc. 381.34. Mass spectral analysis value, 381.

2. Spin-Labeled Nitrophenyl Hydrazones.

<u>DNP-6-H (IIa)</u>: The 2,4-dinitrophenyl hydrazone of 2,2,6,6-tetramethyl-4-piperidone nitrogen oxide was prepared by the method of Rozantzev and Neiman(1964).

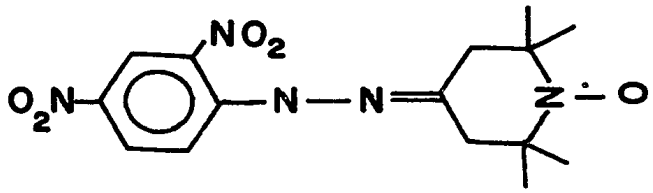

Calc. for: $C_{15}H_{20}N_5O_5$: C, 51.5; H, 5.7; N, 20.0%

Found: C, 51.5; H, 5.6; N, 20.0%

<u>PNP-6-H (IIb)</u>: P-nitrophenyl-hydrazone nitroxide (IIb); 1-(2,2,6,6-tetramethyl-4-piperidone-1-oxyl)-p-nitrophenyl hydrazone was prepared in the same manner as mentioned above, except for the substitution of p-nitrophenyl hydrazine for the 2,4-dinitro compound.

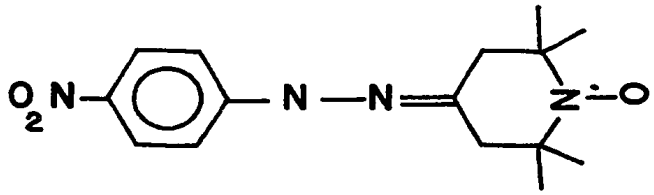

Anal: Calc. for $C_{15}H_{21}N_4O_3$: C, 59.1; H, 6.8; N, 18.4%

Found: C, 58.9; H, 6.8; N, 18.4%

3. Affinity Spin-Label.

<u>FDNB-6-A (IIIa)</u>: 1-Fluoro-5-N-(1-oxyl-2,2,6,6-tetramethyl-4-amino-piperidine)-2,4-dinitrobenzene.

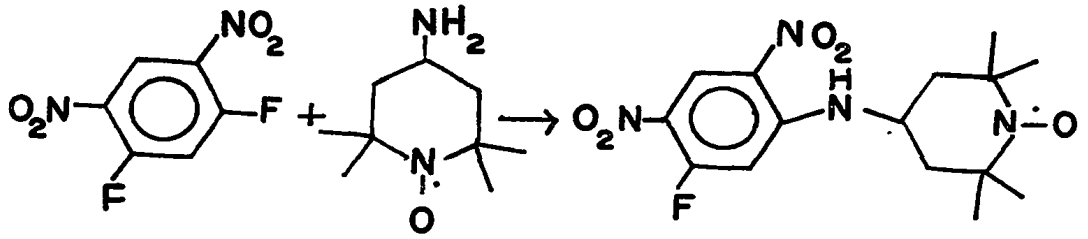

1mM of 6-amino-SL in 5 ml of chloroform was added dropwise into equal molar of 1,5-difluoro-2,4-dinitrobenzene dissolved in 10 ml chloroform. Under vigorous magnetic stirring, it was allowed to react overnight shielded from light. After the solvent was stripped off, yellow precipitate was chromatographed on a silicic acid column eluted with chloroform. Fast moving yellow bands were collected and recrystallization was carried out in chloroform and ether and small amount of hexane. m.p. 198.5-199°. M.W. calc. 355.34. Mass spectral analysis found 355.

<u>FDNB-5-A (IIIb)</u>: 1-Fluoro-5-N-(1-oxyl-2,2,5,5-tetramethyl-3-amino-pyrrolidine)-2,4-dinitrobenzene was prepared using the analogous procedure to IIIa.

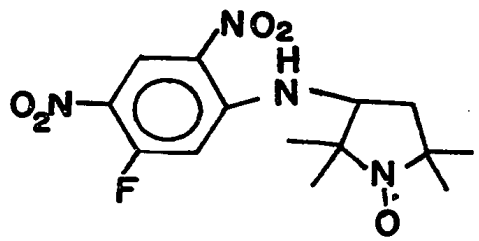

m.p. 214.5-215° M.W. calc. 341. Mass spectral analysis yielded a value of 341.

<u>FDNB-5-MA (IIIc)</u>: 1-Fluoro-5-N-(1-oxyl-2,2,5,5-tetramethyl-3-aminomethyl-pyrrolidine)-2,4-dinitrobenzene was prepared following the procedure of IIIa.

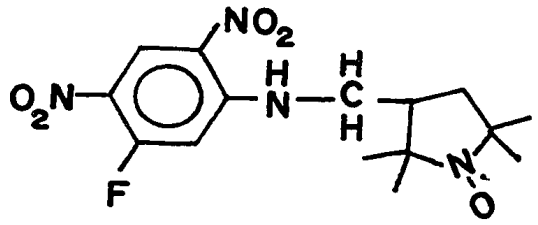

The purified product appears in two crystalling forms: the bright yellow crystals melting at about 154.5-155° and the orange-red crystals melting at about 158.5-159°.

4. Spin-Labeled DNP-Amino Acids.

<u>DNP-Gly-SL (IVa)</u>: α-N-2,4-dinitrophenyl-(1-oxyl-2,2,6,6-tetramethyl-4-piperidinyl) glycinate. The glycinate and other amino

acid derivatives characterized as

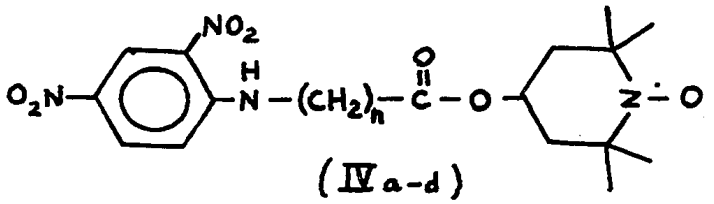

(IVa-d)

where n = 1 glycine derivative IVa, n = 2 β-alanine derivative IVb, n = 3 γ-Butyric derivative IVc, n = 5 Caporic derivative IVd was prepared by the reaction:

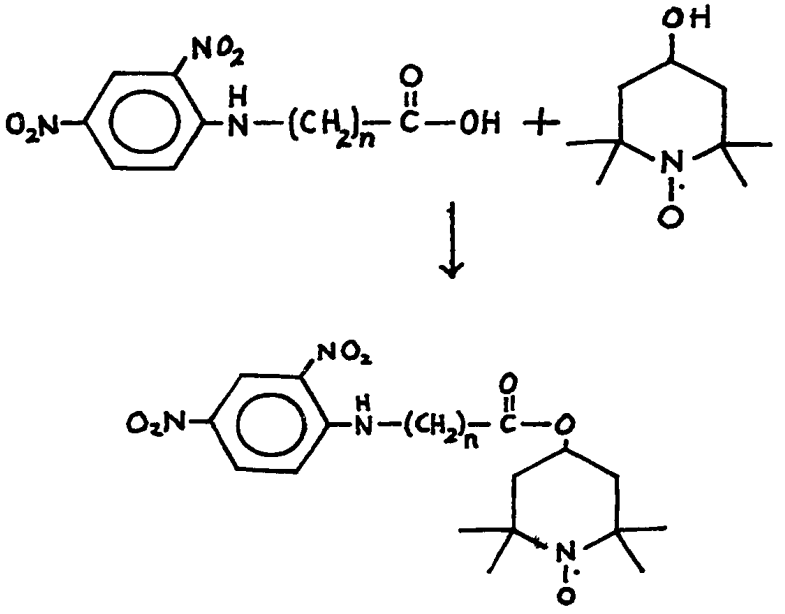

2,2,6,6-Tetramethyl-4-piperidinal-1-oxyl (6-Alcohol-SL) was prepared by the procedure of Rozantzev.(1964) DNP-amino acids were ordered from Sigma. Equal molar concentrations of DNP glycine, 6-Alcohol-

SL and dicyclohexylcarbodiimide were reacted in a manner similar to the methods employed by Zerner et al (1964). The product was purified by chromatography on silica gel using chloroform, which when rechromatographed, gives a final product with a single spot using silica gel thin layer chromatography.

<u>DNP-β-Ala-SL (IVb)</u>: β-N-2,4-dinitrophenyl-(1-oxyl-2,2,6,6-tetramethyl-4-piperidinyl) alaninate.

Anal.: Calc. for $C_9N_3O_6H_8$: C, 52.8; H, 6.1; N, 13.7%

Found: C, 52.8; H, 6.2; N, 13.7%

<u>DNP-γ-But-SL (IVc)</u>: γ-N-2,4-dinitrophenyl-(1-oxyl-2,2,6,6-tetramethyl-4-piperidinyl) Butyrate.

Molecular Weight Analysis MW Calc. 423.4

Found M = 423.

<u>DNP-ε-Cap-SL (IVd)</u>: ε-N-2,4-dinitrophenyl-(1-oxyl-2,2,6,6-tetramethyl-4-piperidinyl) caporate.

Anal.: Calc. for $C_{11}N_3O_6H_{14}$: C, 56; H, 6.9; N, 12.8%

Found: C, 57; H, 6.7; N, 12.7%

<u>Di-DNP-Lys-SL (V)</u>: a,α,ε-N,N'-di-2,4-dinitrophenyl-(1-oxyl-2,2,6,6-tetramethyl-4-piperidinyl)-lysinate was prepared analogous to the procedure outlined in IVa.

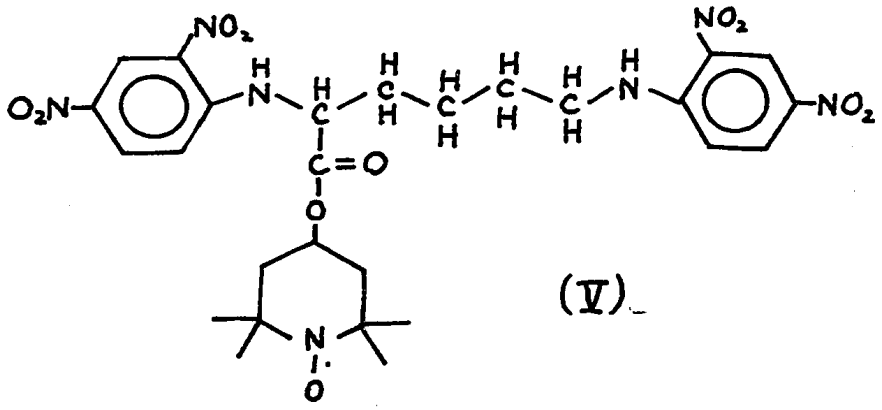

(V)

Anal.: Calc. for $C_{27}H_{35}N_7O_{11}$: C, 51; H, 5.6; N, 15.5%

Found: C, 52; H, 5.5; N, 15.7%

5. Spin-Labeled Chromophore.

<u>Dansyl-nitroxide</u>: 1-dimethylamino-naphthalene-5-(N-1-oxyl-2,2,5,5-tetra-methyl pyrrolidinyl)-sulfonamide was prepared according to the procedure of Stryer and Griffith (1965).

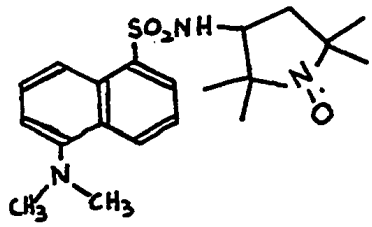

The absorption spectrum of the product in ethanol exhibits maxima at 251 and 337 mμ, with extinction coefficient of 15,000 and 4,200 cm^2/m mole, respectively.

(c) Antibody Preparation and Characterization.

Rabbit anti-DNP antibodies were prepared according to two different procedures.

(1) AB-D was prepared according to the procedure of H.N. Eisen (1962) outlined as follows:

Immunization antigen DNP-B γ G

Antiserum + DNP-H γ G

Precipitate Wash — Supernatant

Precipitate — Washings

1) Extract with 0.1 M-dinitrophenyl pH 7.6, 37°C.
2) Streptomycin sulfate (35 mg/ml)

Supernatant — Residual Precipitate

Dowex 1 column
Cl-form

Effluent

Ammonium sulfate precipitation

Precipitate — Supernate

↓

Dissolve and dialize

(2) AB-T was prepared according to the procedure of Cheng and Talmage (1965) outlined as follows:

Immunizing antigen DNP-BSA

Antiserum + BSA

Supernatant + T-H G — Precipitate

Precipitate Wash — Supernatant

Washed Precipitate — Washings

1) Elution with 0.1 M 2,4-dinitrophenol pH 7.6, 37°
2) Streptomycin sulfate (40 mg/ml)

Supernatant — Residue

1) Sephadex G-25
2) DEAE-cellulose
3) Dowex 1 (Cl^-) column

Effluent

Rabbit blood was obtained by cardiac puncture. Antibodies were isolated from the serum pooled from 16 rabbits. Purified antibodies have an uncorrected sedimentation coefficient in the range of $6.5-7 \times 10^{-13}$ seconds. In addition, immunoelectrophoresis showed a single precipitin band against goat anti-rabbit crude γ-globulin fraction. Antibody concentrations were based on a specific absorption coefficient of 1.46 cm^2/mg and a molecular weight of 160,000 at 278 mμ (Velick, S.F. et al, 1960).

(3) Methods.

ESR Measurements.

The dimensional studies of antibody HCS with spin-labeled DNP derivatives were carried out at antibody concentration 0.8×10^{-4}M in 0.15 M NaCl, 0.02 PO_4 buffer, pH 7.6 to which approximately 2×10^{-4}M spin-labeled haptens in minimum amount of ethanol were added; excess free spins were removed by dialysis against 3 changes of buffer. The final spectra were recorded at room temperature.

ESR titration studies of antibody hapten affinity were carried out using the following setup:

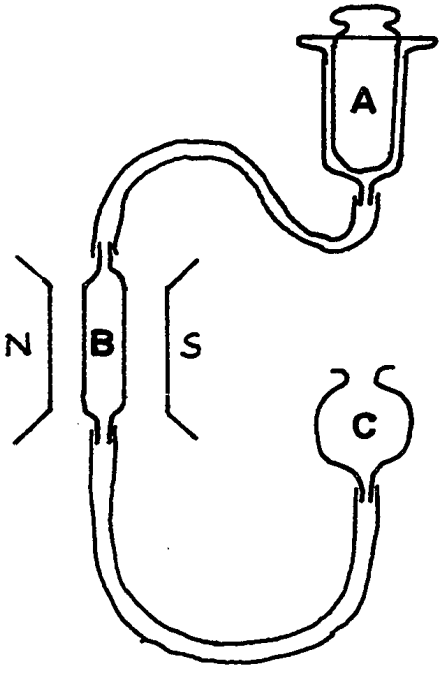

A. Syringe attached to the ESR aqueous flat cell through tefflon tubing can be operated manually to mix the sample during titration.

B. Aqueous flat cell in ESR cavity.

C. Reservoir where titration was carried out in front of the cavity.

Only 0.5—1 ml of sample is needed for one titration experiment. The titration experiment was carried out by fixing the magnetic field at high field peak of the isotropic triplet and its value was calibrated with a standard curve obtained from free spin-label hapten in the presence of normal R γ G in buffer. The bound SLH concentration was obtained by substrate, the detected free SLH, from the total SLH added.

(D) Results and Conclusions

(1) Relaxation Mechanism of the Spin-Label.

Before attempting to analyze the environmental information reported by a spin-label at a specific binding site, it is necessary to have a thorough understanding of the predominant relaxation mechanism of the spin-labels.

After a careful examination of the results accumulated in this field, it appears that the spin-labels give almost identical strongly immobilized spectra

regardless of the molecular weight of the labeled object. For example, α-chymotrypsin (MW, 23,000) (L.J. Berliner and H.M. McConnell, 1966), hemoglobin (MW, 86,000) (Ogawa and McConnell, 1967), anti-DNP antibody (MW,150,000) (Stryer and Griffith, 1965) and cell membranes (H.E. Sandberg and L.H. Piette, 1968) gave almost identical anisotropic spectra. This indicates that the spin-label is sensitive mainly to its local environment, and thus demonstrates the effectiveness of the label in studying low molecular weight protein molecules as well as high molecular weight substances, as long as the rotational correlation time τ_c of the labeled object is greater than 13 nanoseconds according to Eq. 2-1. Therefore, the ESR spectra of the label is a reflection of direct perturbation by the environment. This is shown in Fig. 2-2 and Fig 2-3 where Bovine serum albumin (BSA; MW, 69,000) and Bovine gamma globulin (BγG; MW, 160,000) were labeled with Maleic-6-SL and FDNB-5-A. Contrary to the molecular weight of the two molecules, the labels on the BSA were much more immobilized than on BγG. Almost identical results were found when human gamma globulin and human serum albumin were used. This would indicate that the extent of immobilization of the label is a direct reflection of the rotational restriction exerted upon the label itself, illustrated as follows:

FIG. 2-2: ESR spectra of M-6-SL labeled BSA vs BγG.

(A) M-6-SL labeled BSA.

(B) M-6-SL labeled BγG.

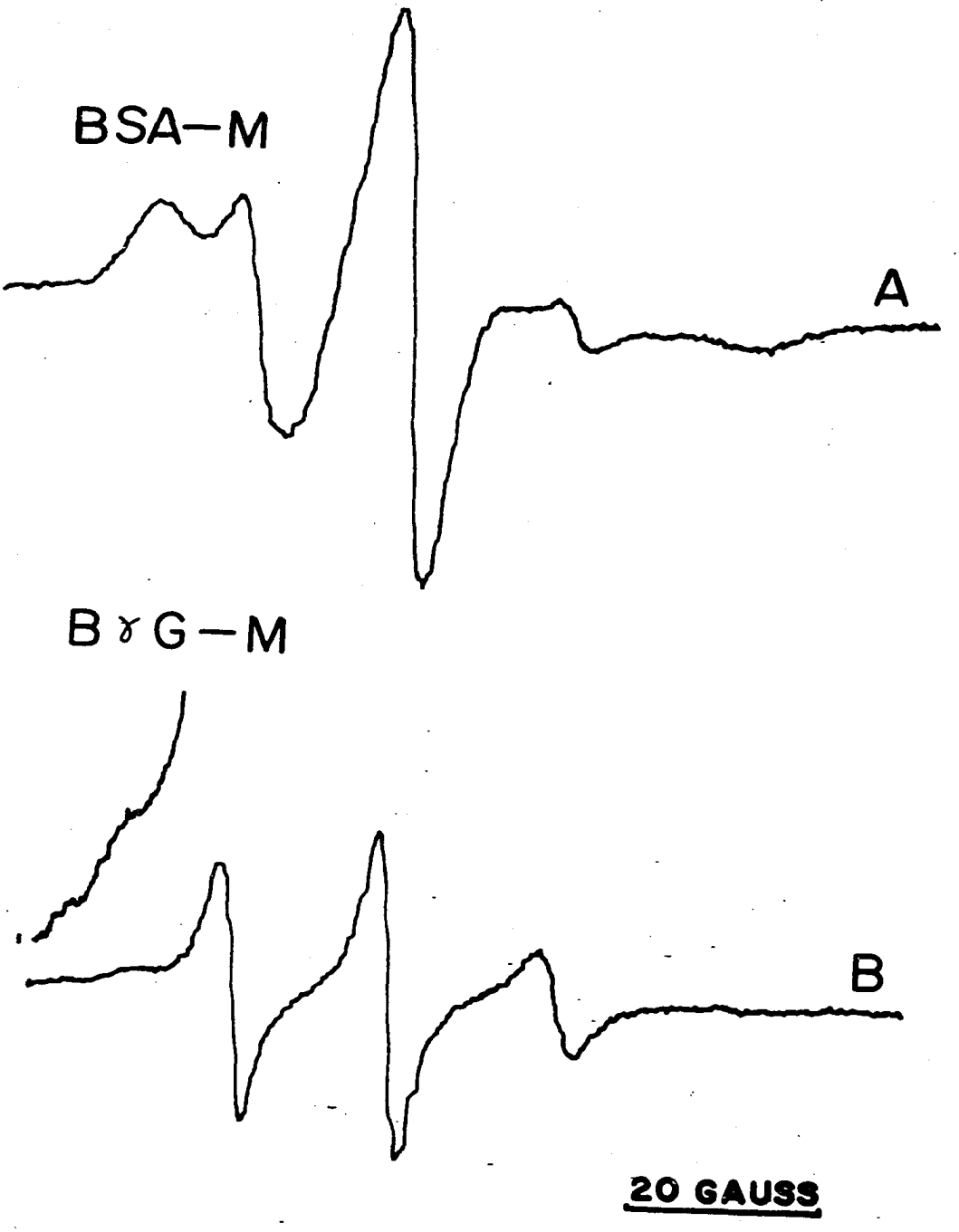
BSA–M
A
BγG–M
B
20 GAUSS

FIG. 2-3: ESR spectra of FDNB-5-A labeled BSA vs BγG.

(A) FDNB-5-A labeled BSA.

(B) FDNB-5-A labeled BγG.

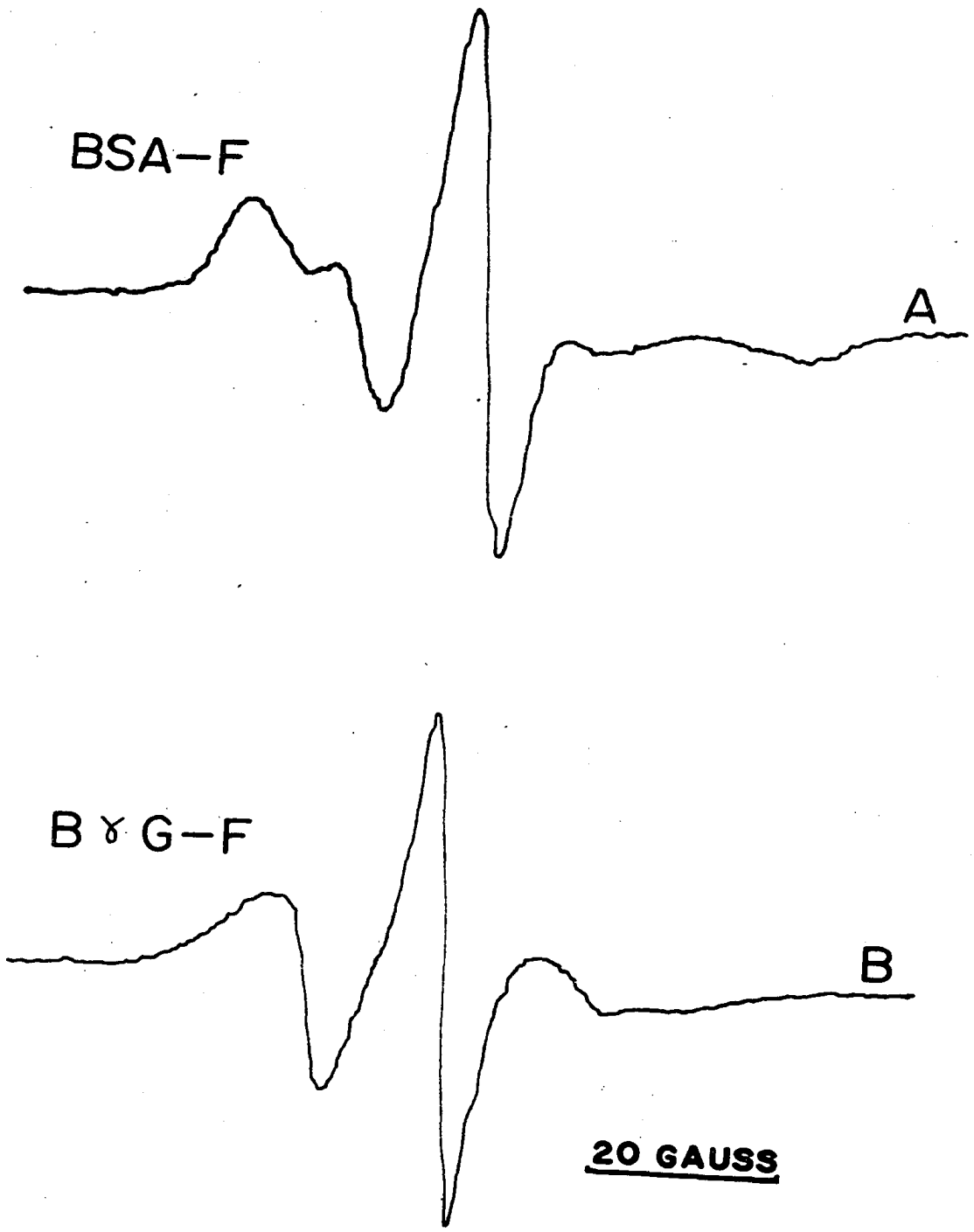
BSA–F
A
B γ G–F
B
20 GAUSS

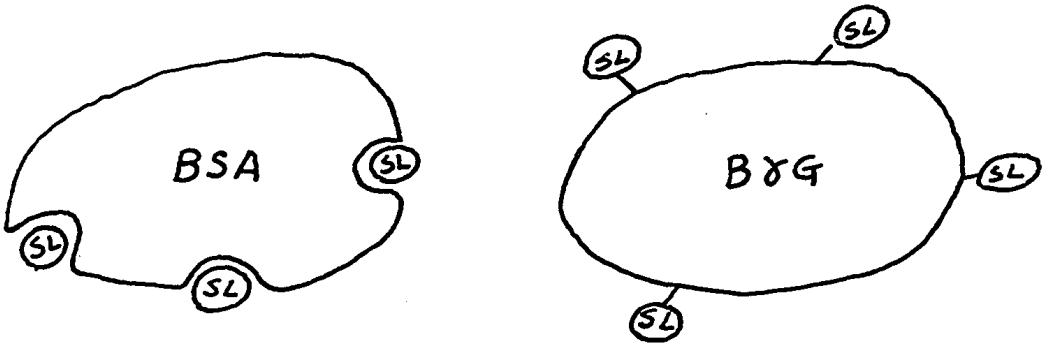

Another aspect of interest is the inherent rotational restriction of some labels currently in use which can often result in somewhat misleading spectra. For example, when the FDNB-5-A and Maleic-6-SL were used to label BSA and BγG (Fig. 2-2 and Fig. 2-3), there was very little difference in the strongly immobilized spectra of labeled BSA. However, the weakly immobilized spectra of BγG were quite different. The FDNB-5-A appears to be more immobilized than Maleic-6-SL, but this could be due to the inherent rotational restriction between the nitroxide and nitrobenzene rings of FDNB-5-A. If this is true, then the predominant relaxation mechanism could be the restriction of the single bond adjacent to the nitroxide spin-label. This finding was further substantiated by using FDNB-5-MA which differs from FDNB-5-A only in its extra methylene group:

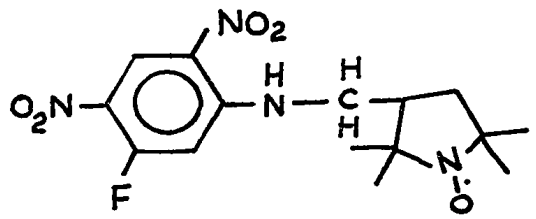

This label was less immobilized than FDNB-5-A (Fig. 2-4 (A)) when labeled onto Amino Ethyl Cellulose (AEC) (Fig. 2-4 (B)) after an extra single bond was introduced.

These findings seem to support the hypothesis outlined in the beginning of this chapter, i.e. that this class of spin-labels, when systematically modified, may be used to map the dimensional properties of a specific macromolecular active site in solution.

(2) Determination of τ_c

In order to calculate τ_c of the specific spin-labels to be used in determining the depth of the HCS, a correlation of the ESR line width and line shape of the labels and their τ_c calculated from Equation (2-2) has to be established. 1-oxyl-2,2,6,6-tetramethyl-4-piperidinol (6-alcohol-NA) was chosen to be the model compound to make this correlation. This molecule is very similar to the actual spin-labeled haptens used in the experiment. It is a desirable model, however, for the determination of fairly accurate τ_c values using the Stokes equation. It has been found that

FIG. 2-4: ESR spectra of FDNB-5-A and FDNB-5-M labeled Aminoethyl cellulose (AEC).

(A) FDNB-5-A Labeled AEC

(B) FDNB-5-MA Labeled AEC

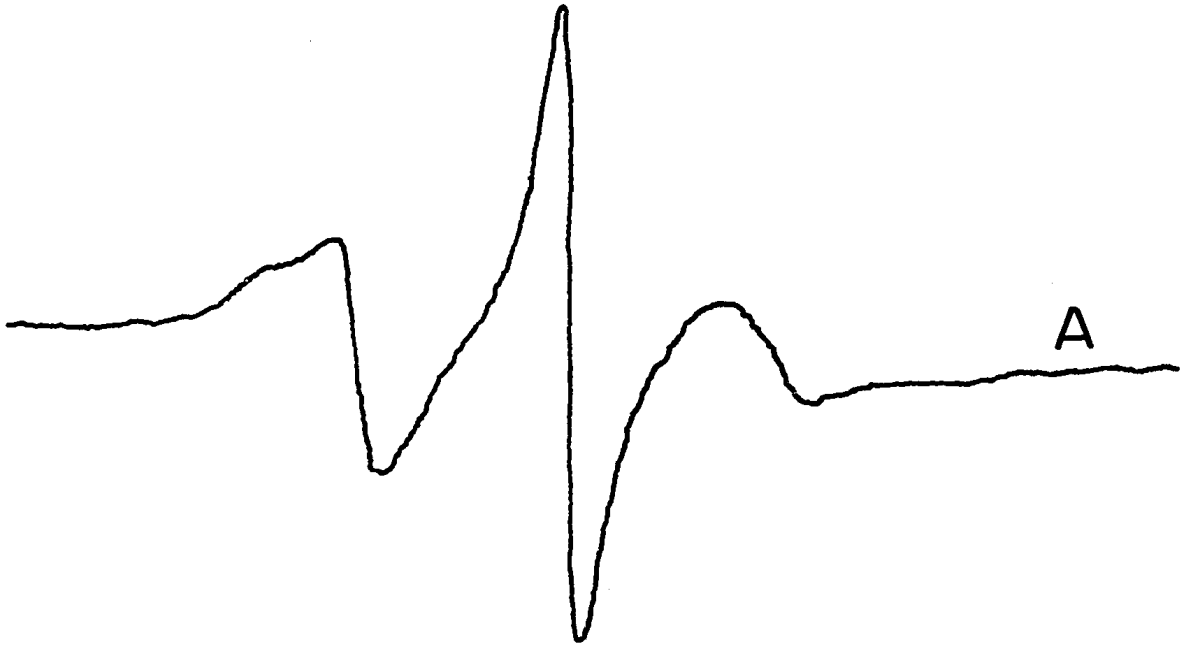
A

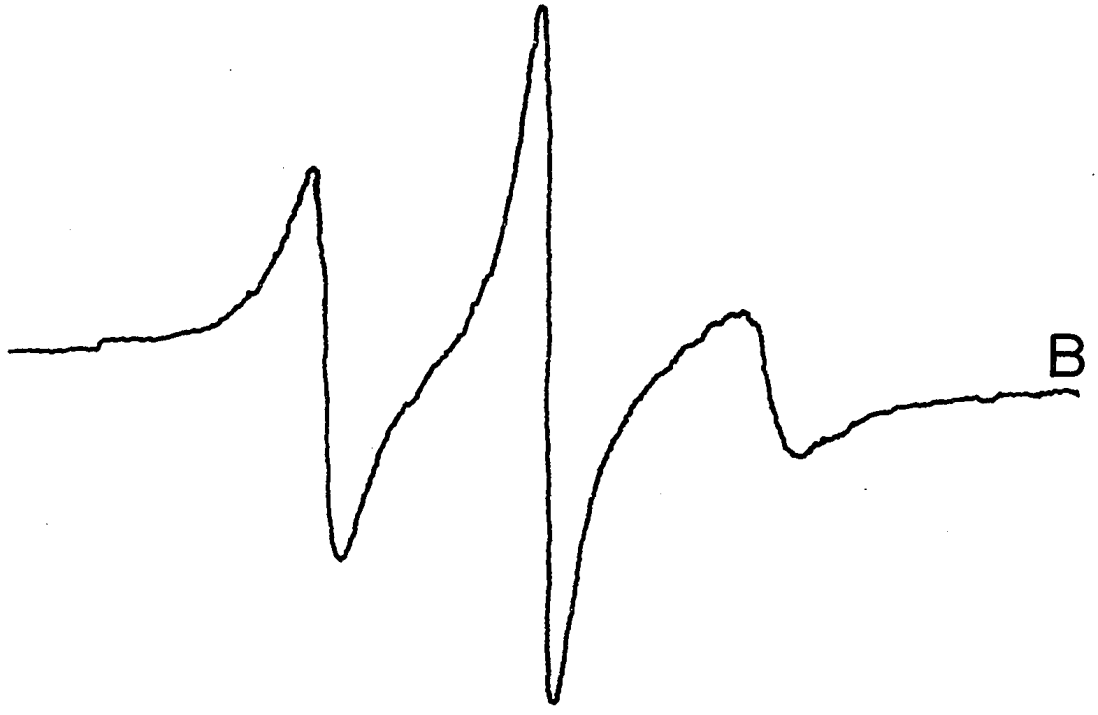
B

FIG. 2-5: Plot of rotational correlation time (τ_c) vs viscosity (η).

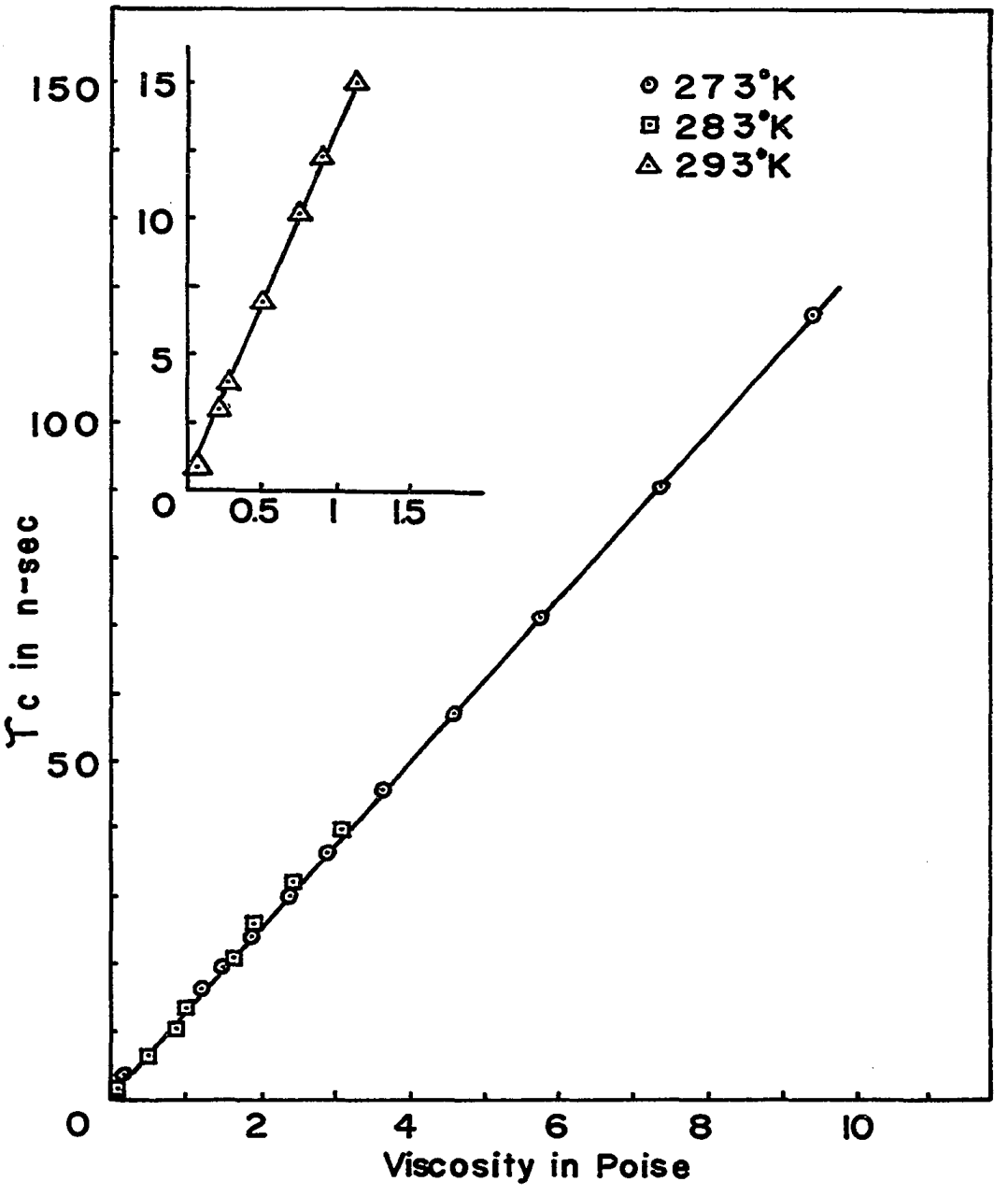
273°K
283°K
293°K
150
100
50
0
15
10
5
0
0.5
1
1.5
τ_c in n-sec
0
2
4
6
8
10
Viscosity in Poise

because of intra-molecular hydrogen bonding, the molecule assumes a more or less spherical configuration, which is an essential assumption in the Stokes expression. τ_c calculations using the Stokes expression depend upon linear viscosity changes. The viscosity was varied by mixing an aqueous solution of the nitroxide with varying weight percent glycerol solutions. The viscosity at a specified temperature was taken from a table given in the Handbook of Chemistry and Physics, 42nd Edition, page 2212. τ_c calculated assuming an effective radius $a_o = 5$ Å for various viscosities are listed in Table (2-1). The linear relation of τ_c and viscosity is plotted in Fig. (2-5) and representative ESR spectra are shown in Fig. (2-1).

(3) Determination of Longitudinal Dimension and Structural Properties of HCS.

(a) Monovalent Hapten Spin-Labels.

Six spin-labeled haptens with increasing distance between the label and the hapten have been used to study the HCS of AB-T. The immobilized spectrum of DNP-6-A is shown in Fig. 2-6 where relative τ_c was estimated to be 39.1 nanoseconds. Fig. 2-7 shows the bound spectrum of DNP-5-MA which gives an almost identical immobilized spectrum to DNP-6-A. The complex spectrum

TABLE 2-1: Determination of τ_c from Aqueous Glycerol Solutions

Glycerol % Wt.	η Viscosity in Poise	τ_c in n-sec	T absolute temperature
80	.060	0.79	293
80	.116	1.47	283
90	.219	2.88	293
80	.225	3.12	273
92	.310	4.07	293
93	.367	4.8	293
94	.437	5.73	293
90	.498	6.3	283
95	.523	6.87	293
96	.624	8.18	293
92	.729	9.22	283
93	.86	10.1	283
94	1.04	13.3	283
99	1.15	15.1	273
95	1.27	16.1	283
96	1.58	20.0	283
92	1.95	23.8	273

Glycerol % Wt.	η Viscosity in Poise	τ_c in n-sec	T absolute temperature
97	1.95	24.7	283
93	2.40	29.4	273
98	2.46	31.2	283
94	2.93	35.8	273
99	3.09	39.1	283
95	3.69	45.1	273
96	4.60	56.3	273
97	5.77	70.6	273
98	7.37	90.0	273
99	9.42	115	273

of DNP-α-Gly shown in Fig. 2-8 appears to be a mixed spectrum consisting of at least two species. The predominant species has a maximum τ_c of approximately 16 nanoseconds, while some (approximately 20-30%) have a τ_c which could be as low as 4.8 nanoseconds. The anisotropic spectrum of DNP-β-Ala shown in Fig. 2-9 also appears to be mixed. Most of the DNP-β-Ala (approximately 90%) have a τ_c of 6.87 nanoseconds and the contribution of $\tau_c \simeq 16.1$ nanoseconds is approximately 10%. The weakly immobilized spectrum of DNP-γ-But is shown in Fig 2-10 where τ_c has a maximum of 5.7 nanoseconds and a minimum of 4.0 nanoseconds. Fig. 2-11 shows the complex spectrum of DNP-ε-Cap where the average τ_c equals 2.7 nanoseconds. The maximum and minimum are 4.07 and 1.47 nanoseconds.

Fig. 2-12 illustrates a plot of the calculated average τ_c versus the distance in angstroms from the oxygen of the para nitro group of the hapten to the C_4 carbon of the nitroxide ring, i.e.

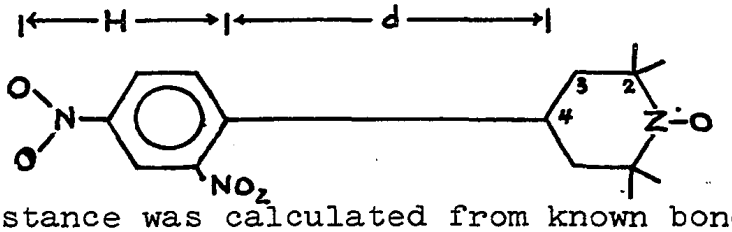

The distance was calculated from known bond angles and bond lengths. The calculated (H + d) for

FIG. 2-6: ESR spectrum of antibody immobilized DNP-6-A (——) and model spectrum of 6-Alcohol-NA in 99% glycerol 1% H_2O at 10°C (·····). Arrows (↓) indicate the superposition of the high and low field peaks of the two spectra.

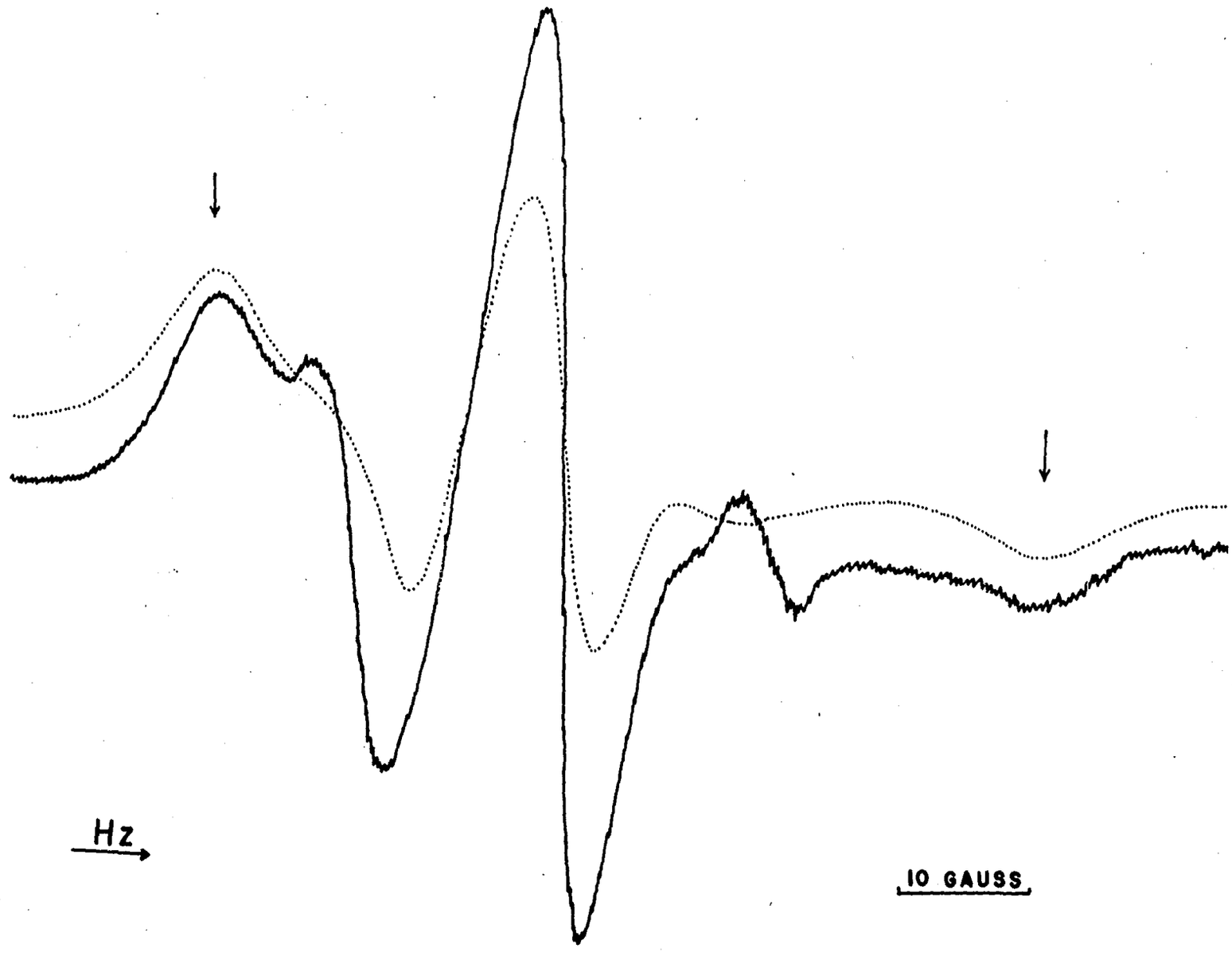
Hz
10 GAUSS

FIG. 2-7: ESR spectra of DNP-5-MA immobilized at antibody active site. The arrows (↓) indicate the maximum splitting is equal to 63~64 gauss.

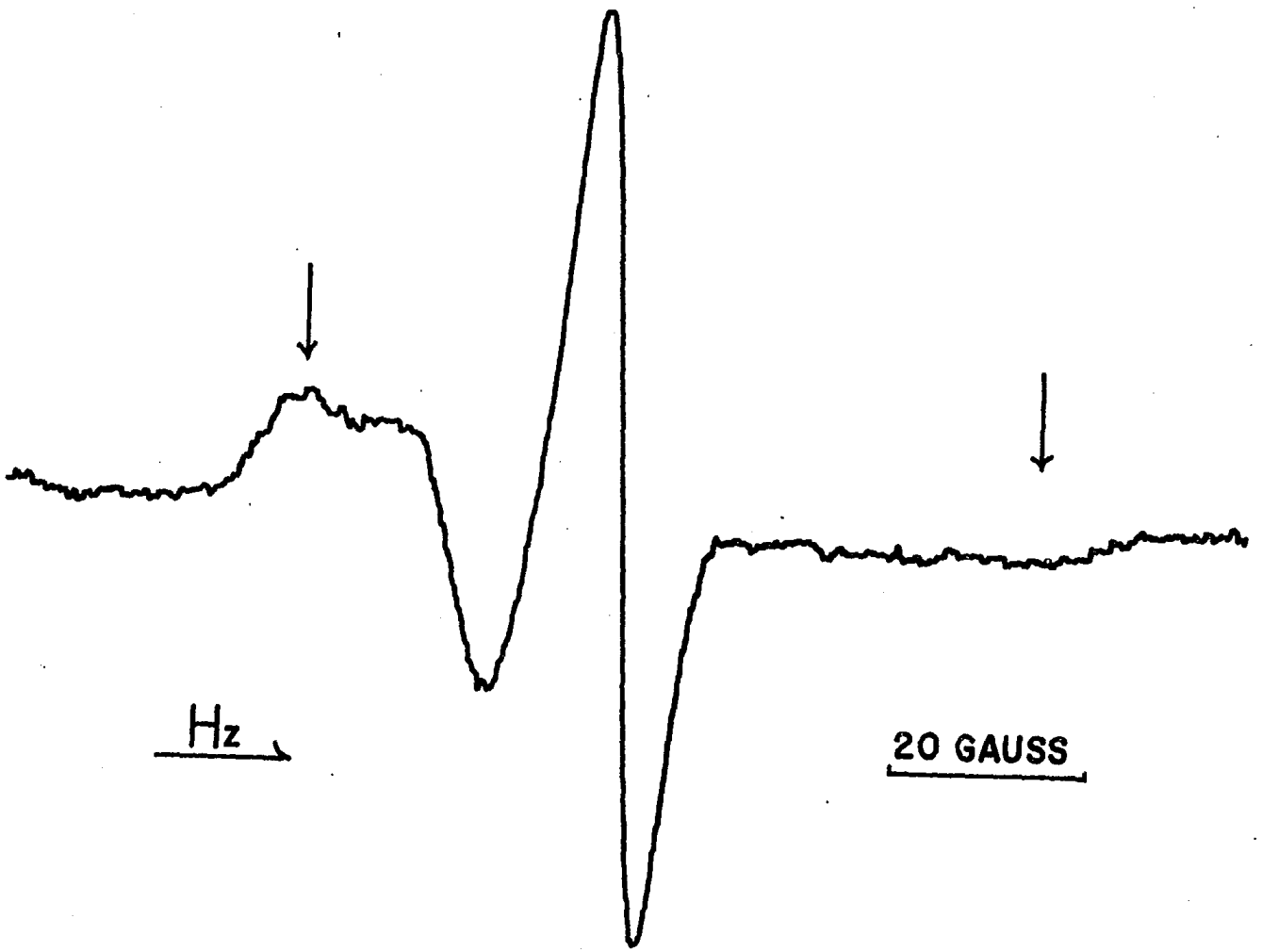
Hz
20 GAUSS

FIG. 2-8: ESR spectra of α-DNP-Gly-SL

(A) Free α-DNP-Gly-SL

(B) Bound at antibody active site (~~~~), and model spectra of 6-Alcohol-NA in 93% glycerol 7% H_2O at 20°C (·····), in 95% glycerol 5% H_2O at 10°C (——).

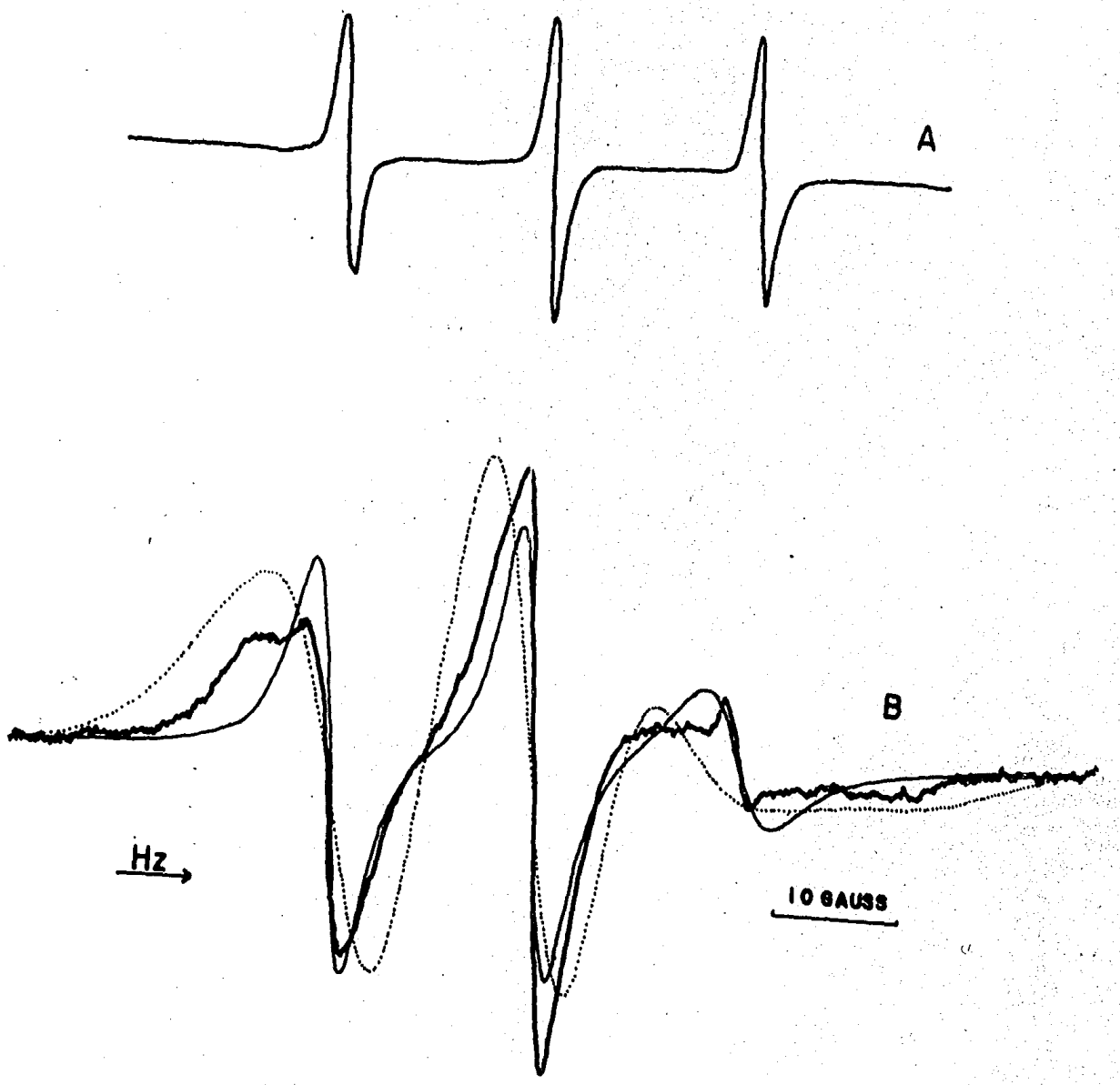
A
B
Hz
10 GAUSS

FIG. 2-9: ESR spectra of β-DNP-Ala-SL.

(A) Free β-DNP-Ala-SL.

(B) ESR spectra of antibody (AB-T) immobilized β-DNP-Ala-SL (——) and 6-Alcohol-NA in 95% glycerol 5% H_2O at 20°C (·····).

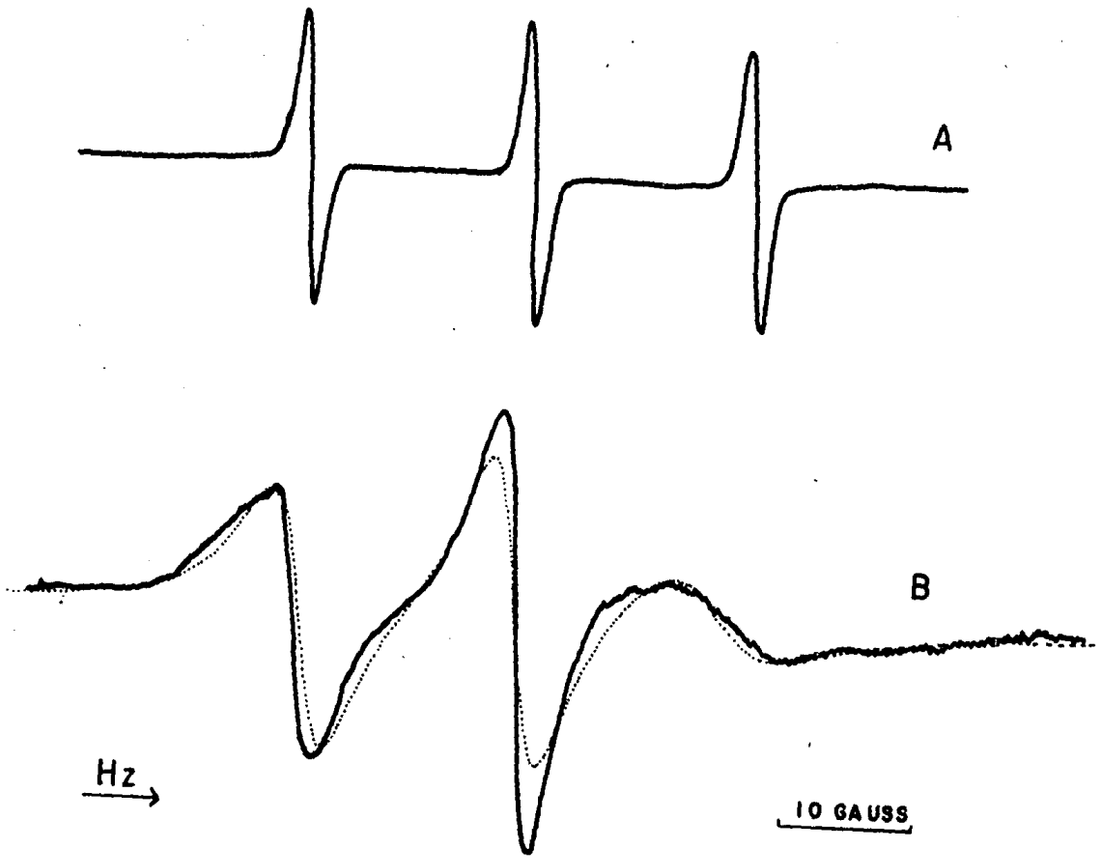
A
B
Hz
10 GAUSS

FIG. 2-10: ESR spectra of γ-DNP-But-SL.

(A) Free γ-DNP-But-SL.

(B) Antibody immobilized γ-DNP-But-SL (—·—·—) 6-Alcohol-NA in 92% glycerol 8% H_2O at 20°C (——) and in 94% glycerol 6% H_2O at 20°C (·····).

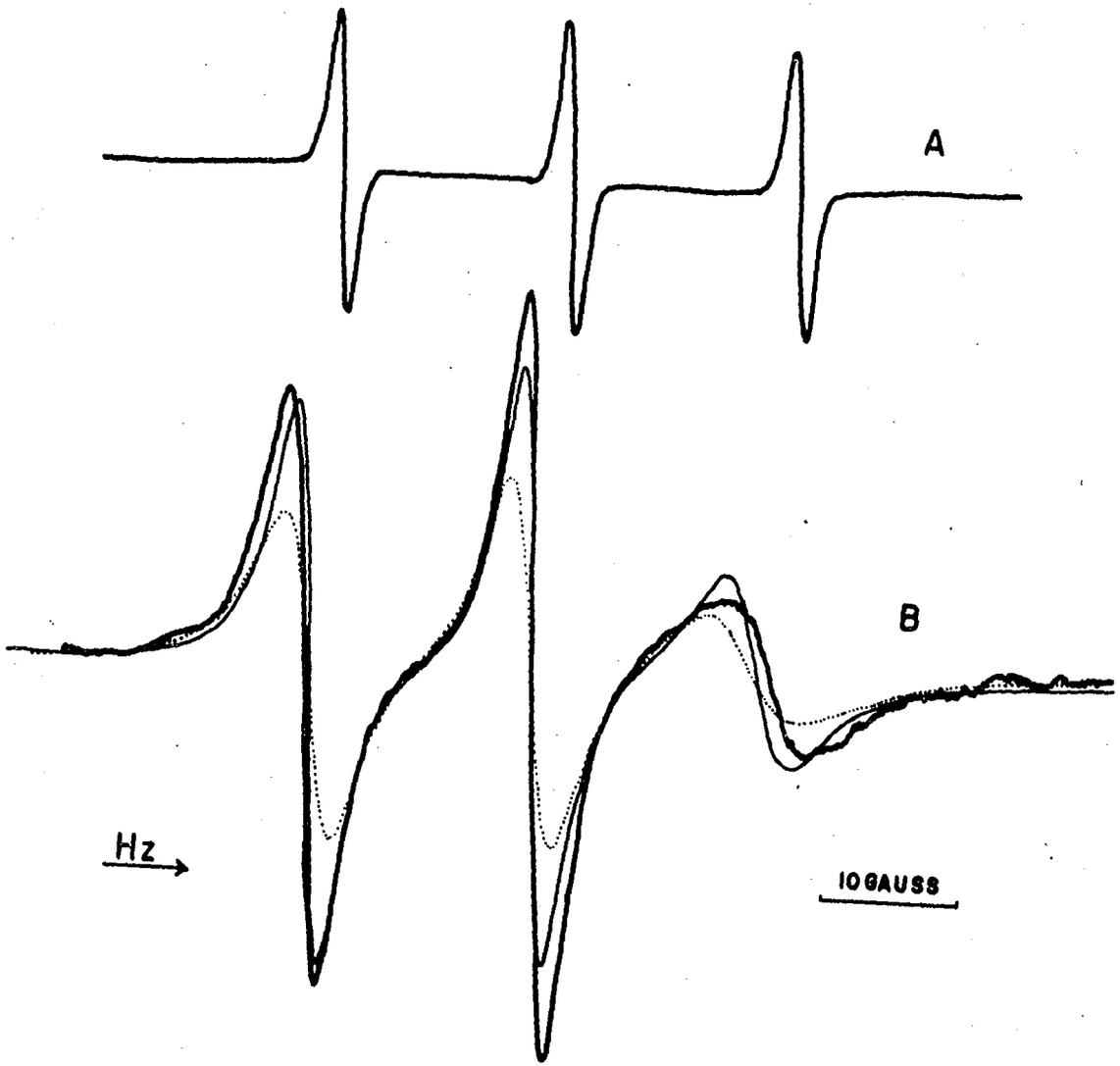
A
B
Hz
10 GAUSS

FIG. 2-11: ESR spectra of ε-DNP-Cap-SL.

(A) Free ε-DNP-Cap-SL.

(B) Antibody bound ε-DNP-Cap-SL spectrum (~~~~~~), 6-Alcohol-NA in 80% glycerol 20% H_2O at 10°C (——), and in 92% glycerol 8% H_2O at 20°C (·····).

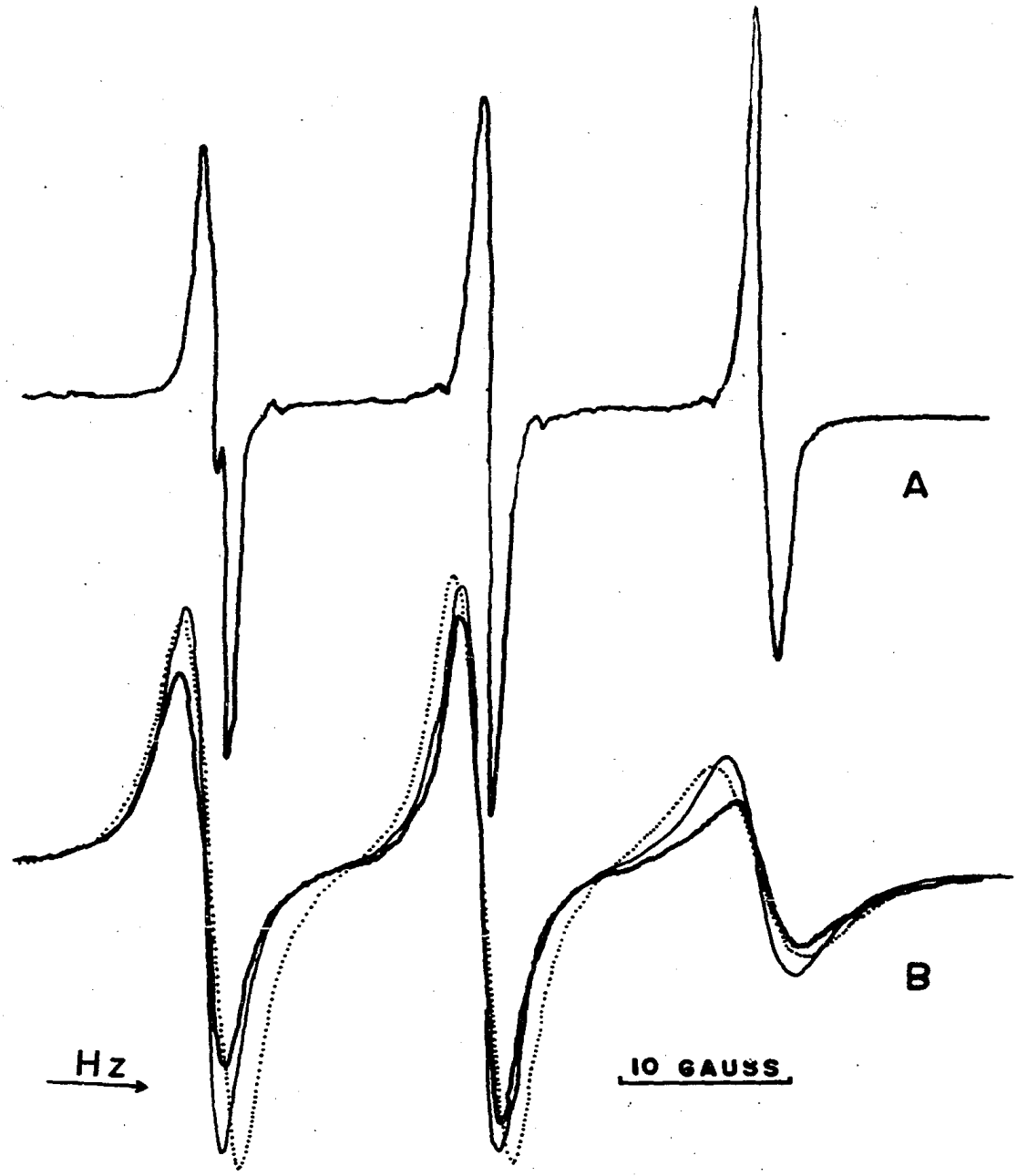
A
B
Hz
10 GAUSS

DNP-6-A was 8 Å, DNP-5-MA: 10 Å, α-Gly: 12 Å, β-Ala: 13.35 Å, γ-But: 14.7 Å, and ε-Cap: 17.4 Å. The curve in Fig. 2-12 shows a sharp break in the range 10-12 Å, and then levels off as the distance is further increased. This would then set an upper limit of about 11~12 Å and a lower limit of about 9 Å with an average depth of 10 Å of the anti-DNP antibody combining site in solution.

(b) Bivalent Hapten Spin-Labels.

In attempting to reduce the uncertainty about the depth of the HCS, the alternative method proposed previously, which relies upon bivalent hapten spin-labels, was used. It has been shown that dimers and higher conjugates of antibodies could be formed by reacting the antibody with varying concentrations of bivalent haptens (Parker, et al, 1962; R.C. Valentine and M.J. Green, 1967).

The bivalent hapten used here was α, ε-di-DNP-Lys-spin-label

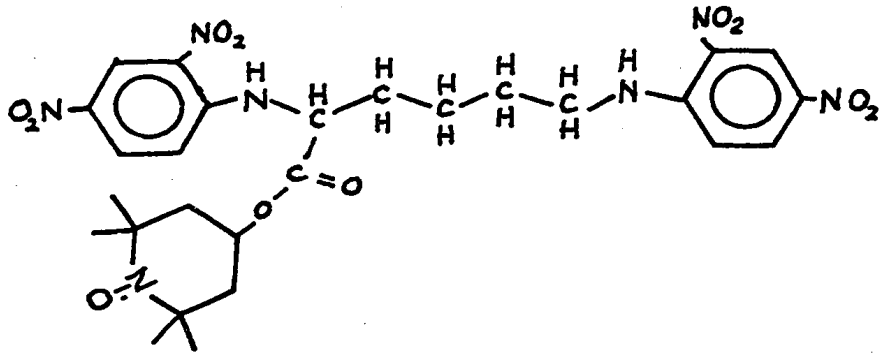

FIG. 2-12: Plot of calculated rotational correlation time (τ_c) for bound labels vs distance (d + H).

(A) DNP-6-A

(B) DNP-5-MA

(C) DNP-α-Gly-SL

(D) DNP-β-Ala-SL

(E) DNP-γ-But-SL

(F) DNP-ε-Cap-SL

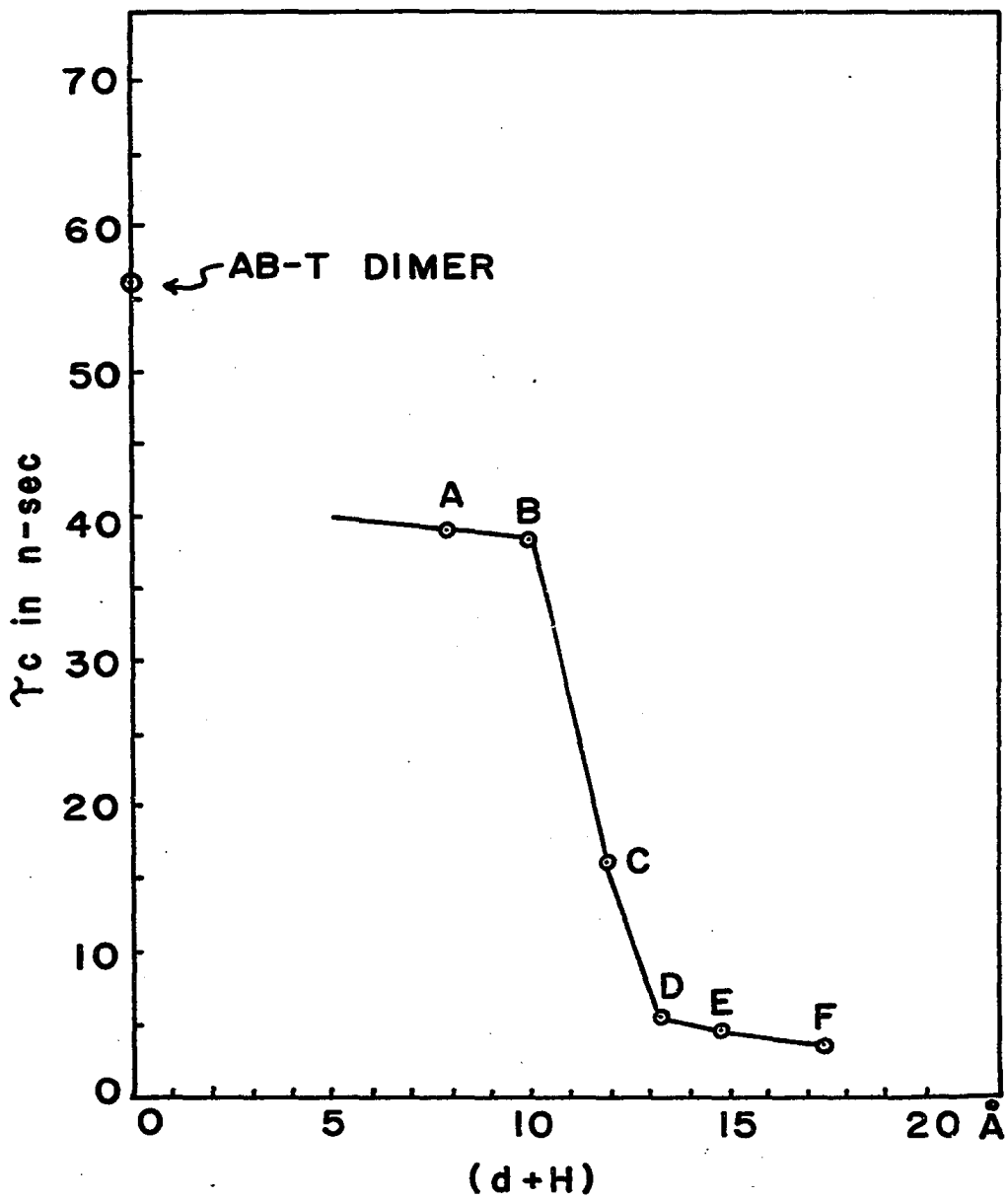
70
60
50
40
30
20
10
0
AB-T DIMER
A
B
C
D
E
F
τc in n-sec
0
5
10
15
20 Å
(d+H)

FIG. 2-13: ESR spectra of ε -DNP antibody complex of α, -di-DNP-Lys-SL (——) and ε -DNP-Cap-SL (.....).

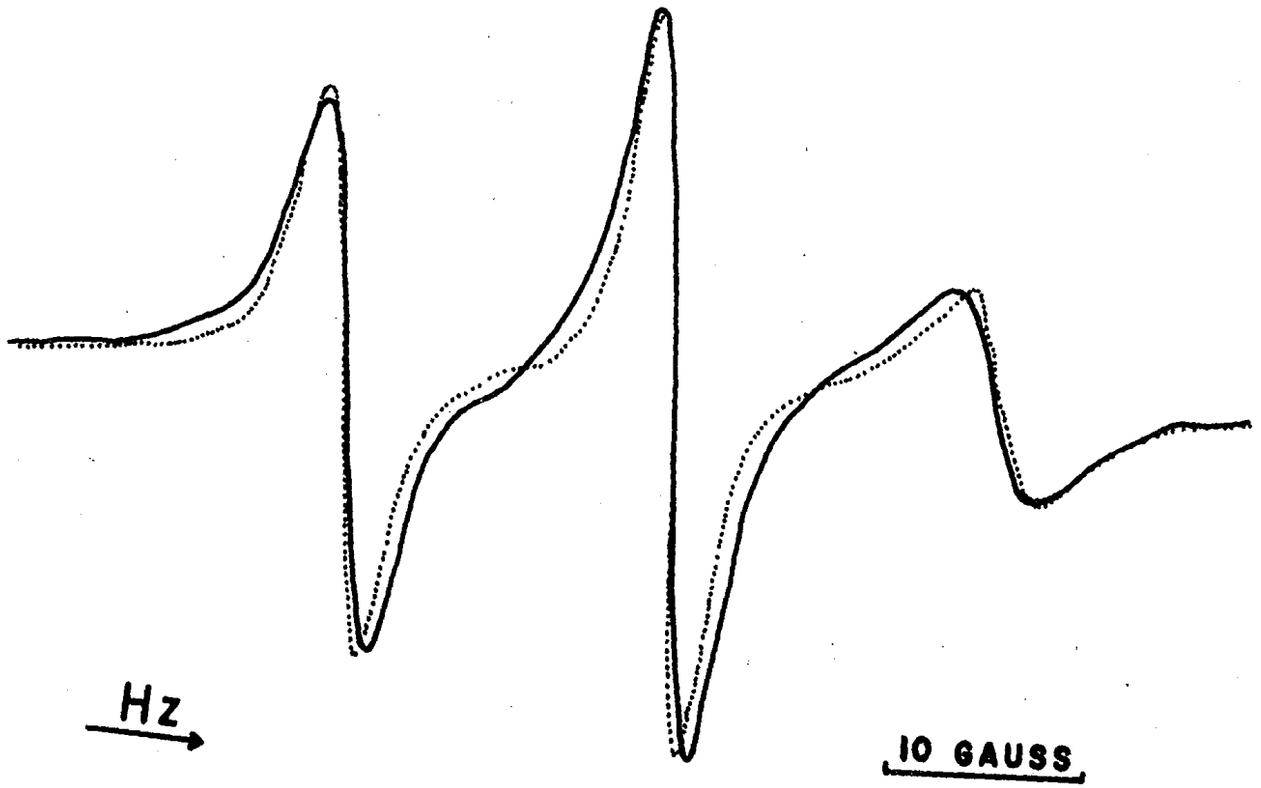
Hz
10 GAUSS

in which the end to end distance calculated between the two hapten groups is 21 Å. When this compound is added to the antibody in an approximately 1:1 molar ratio, the spectrum in Fig. 2-13 is obtained. This ESR spectrum is almost identical to the complex ε-DNP-Cap-SL shown as a dotted line in Fig. 2-13 and thus indicates preferential binding of ε-DNP due to the apolar interaction of the $(CH_2)_4$ group of the ε-DNP moiety with appropriate groups of the antibody active site. (Parker, et al, 1962)

To see if the α-DNP hapten group was available for binding, excess antibody was added yielding the spectrum in Fig. 2-14. It can be seen from this spectrum that the spin-label is completely immobilized, indicating binding at the α-DNP by a second antibody to form the dimer or trimer. The arrow indicates a small amount of the ε-DNP monomer still remains. When additional di-DNP-Lys-SL was added to this solution containing dimer, and excess antibody monomer, the dimer concentration was almost doubled. The enhanced dimer complex formation shown as a solid line spectrum (Fig. 2-15(A)) recorded at approximately half the instrument sensitivity was found

FIG. 2-14: ESR spectrum of predominantly $(AB\text{-}T)_2$-(di-DNP-Lys-SL) complex (——). Antibody concentration was approximately 1.3×10^{-4}M. Model spectrum of 6-Alcohol-NA in 96% glycerol 4% H_2O at 0° (·····). Down arrows (↓) indicate the superposition of the high and low field peaks of the two spectra and up arrow (↑) indicate the presence of ε-DNP-AB-T complex.

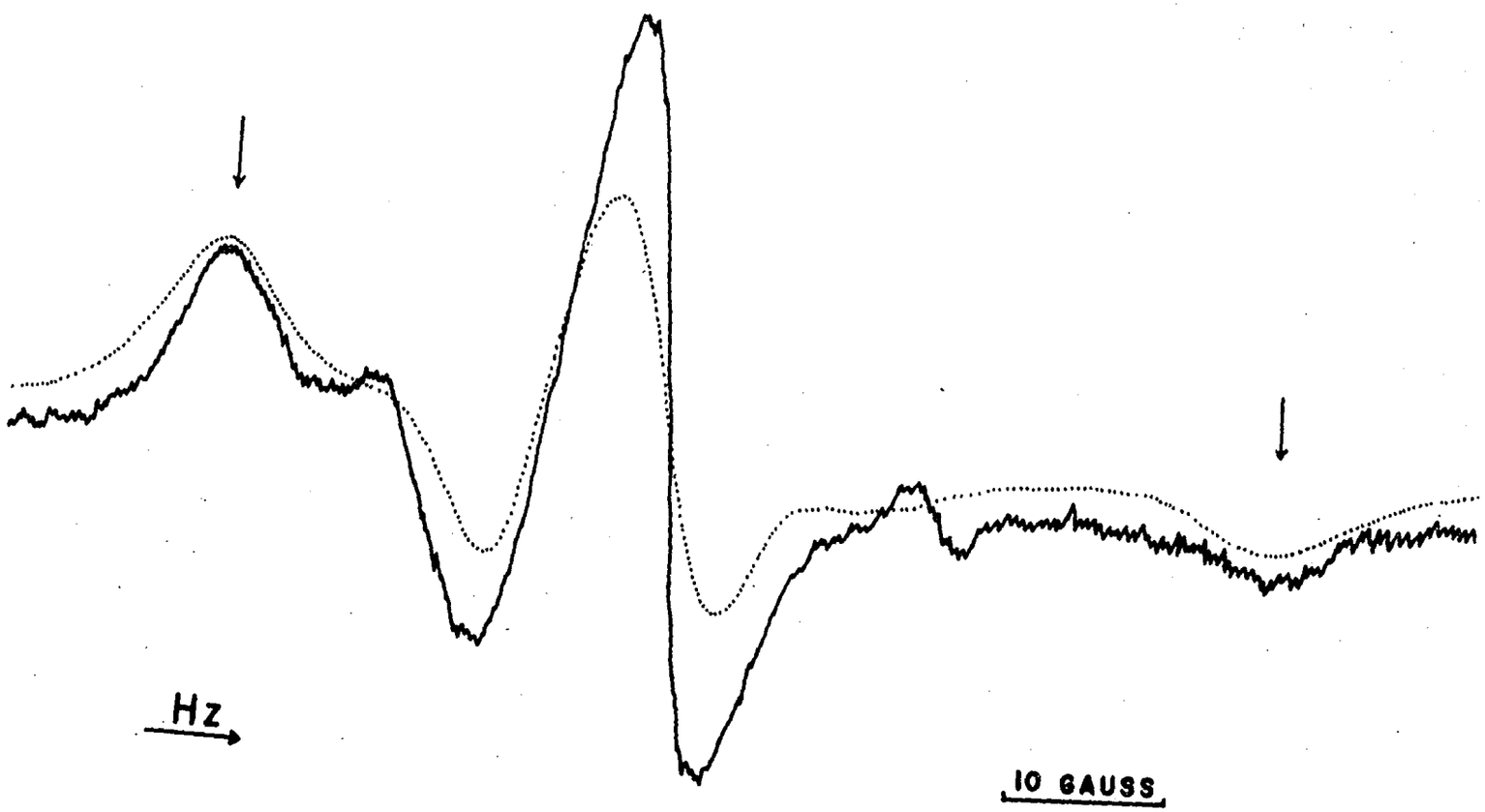
Hz
10 GAUSS

to have identical intensity as the dotted line spectrum (Fig. 2-15 (B)) of pure dimer complex before additional di-DNP-Lysine-SL was added. This value was found to agree fairly well with the estimation made from the comparison of the ultracentrifugation patterns of the two samples. Ultracentrifugation patterns of the purified AB-T are shown in Fig. 2-16 (B). Fig. 2-17 (A) shows the Schlieren patterns of Fig. 2-14 (B); the sedimentation coefficient calculated for the fast moving peak is approximately 10 S which is attributed to the antibody dimers. Fig. 2-17 (B + C) shows the enhanced dimer formation of Fig. 2-15(A). The enhanced dimer preparation was further separated on a sephadex G-200 column and predominant dimers were isolated which gave an identical ESR spectrum of pure dimer complex shown in Fig. 2-15 (B). These conjugates are not disassociable in the presence of excess DNP-Lysine for at least 30 minutes at room temperature. In the presence of 8 M urea, these conjugates are denatured and the ESR spectrum shows a sharp triplet. Attempts were made to form dimers and higher conjugates of di-DNP-ornithine-spin-label haptens without success. The minimum chain length seems to be the lysine

FIG. 2-15: ESR spectrum of monomer and dimer antibody di-DNP-Lysine-SL complex

(A) ESR spectrum of $(AB\text{-}T)_2$-di-DNP-Lysine-SL complex (·····) with excess AB-T monomer before second addition of di-DNP-Lysine-SL. Instrument setting was modulation 800 gain 800. After second addition of di-DNP-Lysine-SL, the ESR spectrum (——) was recorded at modulation 400 gain 800. Arrows under (a) indicate higher conjugation were doubled, (b) existence of ε-DNP-AB-T complex and (c) possible α-DNP-AB-T complex.

(B) ESR spectrum of Sephadex G-200 purified predominant di-DNP-Lysine-SL-$(AB\text{-}T)_2$ complex.

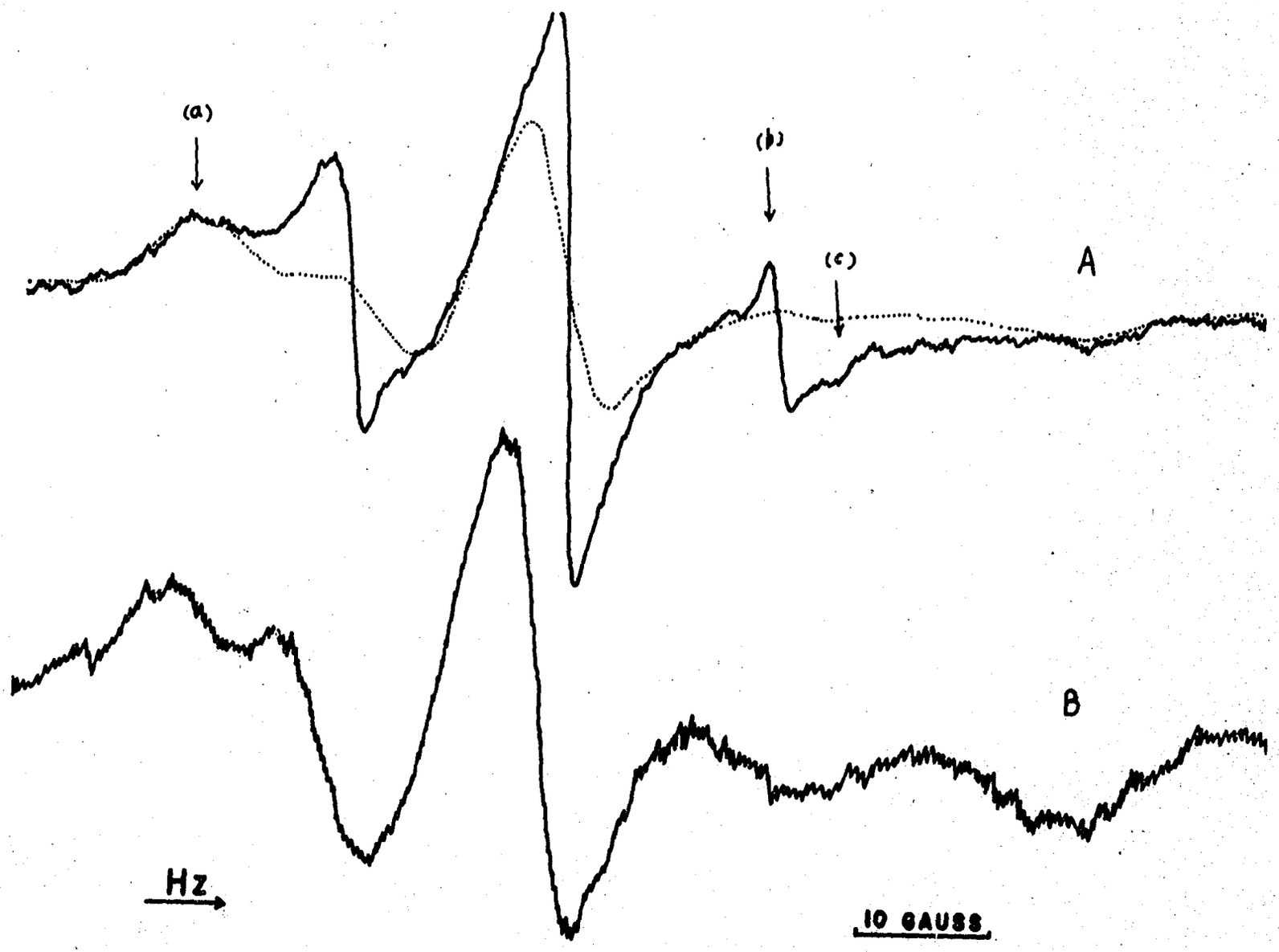
(a)
(b)
(c)
A
B
Hz
10 GAUSS

FIG. 2-16: Ultracentrifugal analysis of purified AB-D and AB-T.

(A) Antibody (AB-D) induced with DNP-BγG isolated with DNP-HγG.

(B) Antibody (AB-T) induced with DNP-BSA isolated with PNP-ONP-TNP-HγG.

The concentration of antibodies were 0.7%. Centrifugation was carried out at 59.780 rpm at 24°C. Schlieren patterns were photographed at 8-minute intervals.

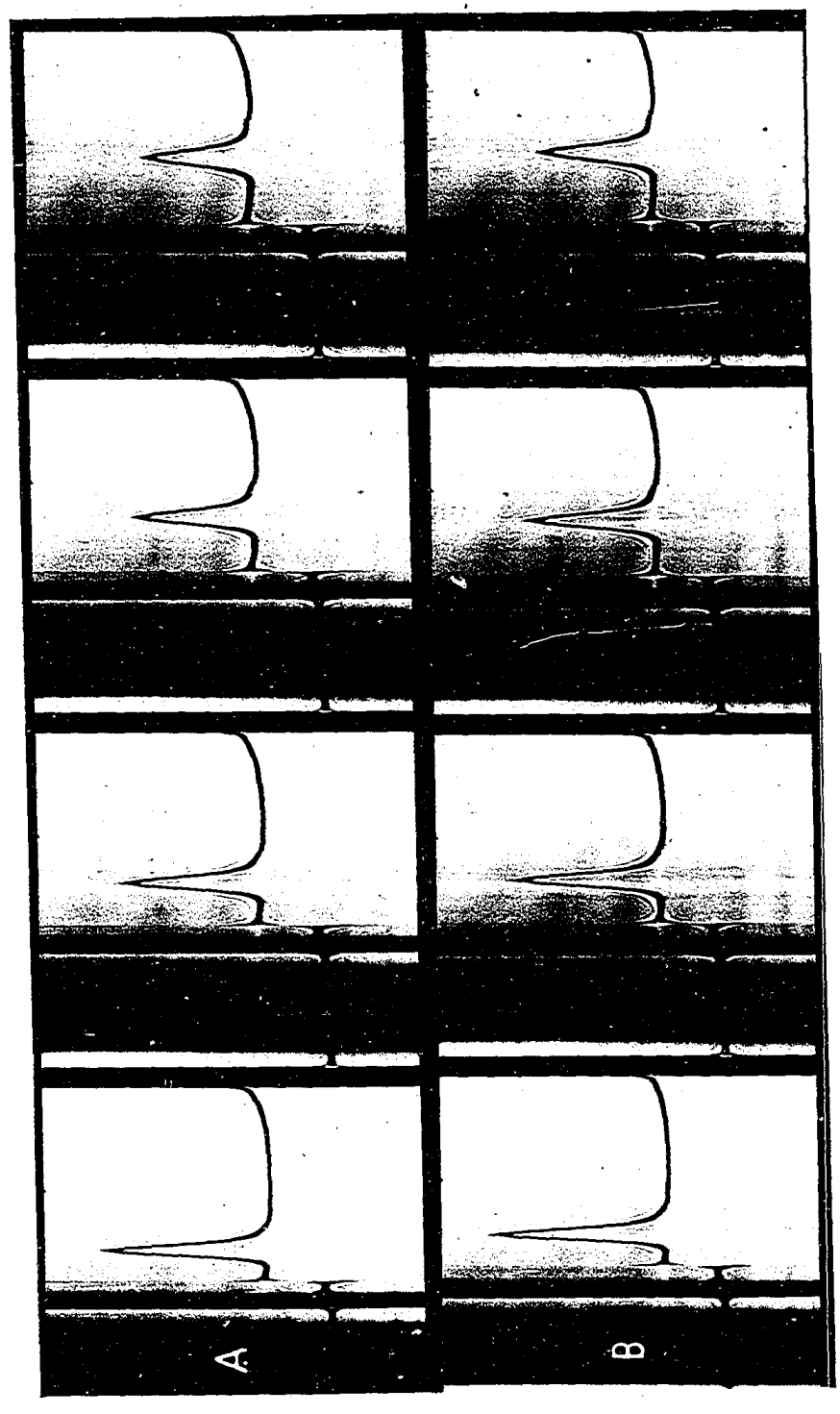
A
B

FIG. 2-17: Ultracentrifugal analysis of the higher conjugates formation of antibodies (AB-T) induced by spin-labeled di-DNP-Lysine.

(A) Schlieren pattern of $(AB\text{-}T)_2$-(di-DNP-Lysine-SL) complex with excess AB-T.

(B) Schlieren pattern of enhanced $(AB\text{-}T)_2$-(di-DNP-Lysine-SL) complex formation after additional di-DNP-Lysine-SL was added to (A).

(C) Was photographed at 57 minutes after reaching full speed.

The concentration of antibodies was approximately 0.3%. Centrifugation was carried out at 59.780 rpm at 24°C. Schlieren patterns were photographed at 8-minute intervals at bar angle 50°. The first pictures of (A) and (B) were taken 16.87 minutes after reaching full speed.

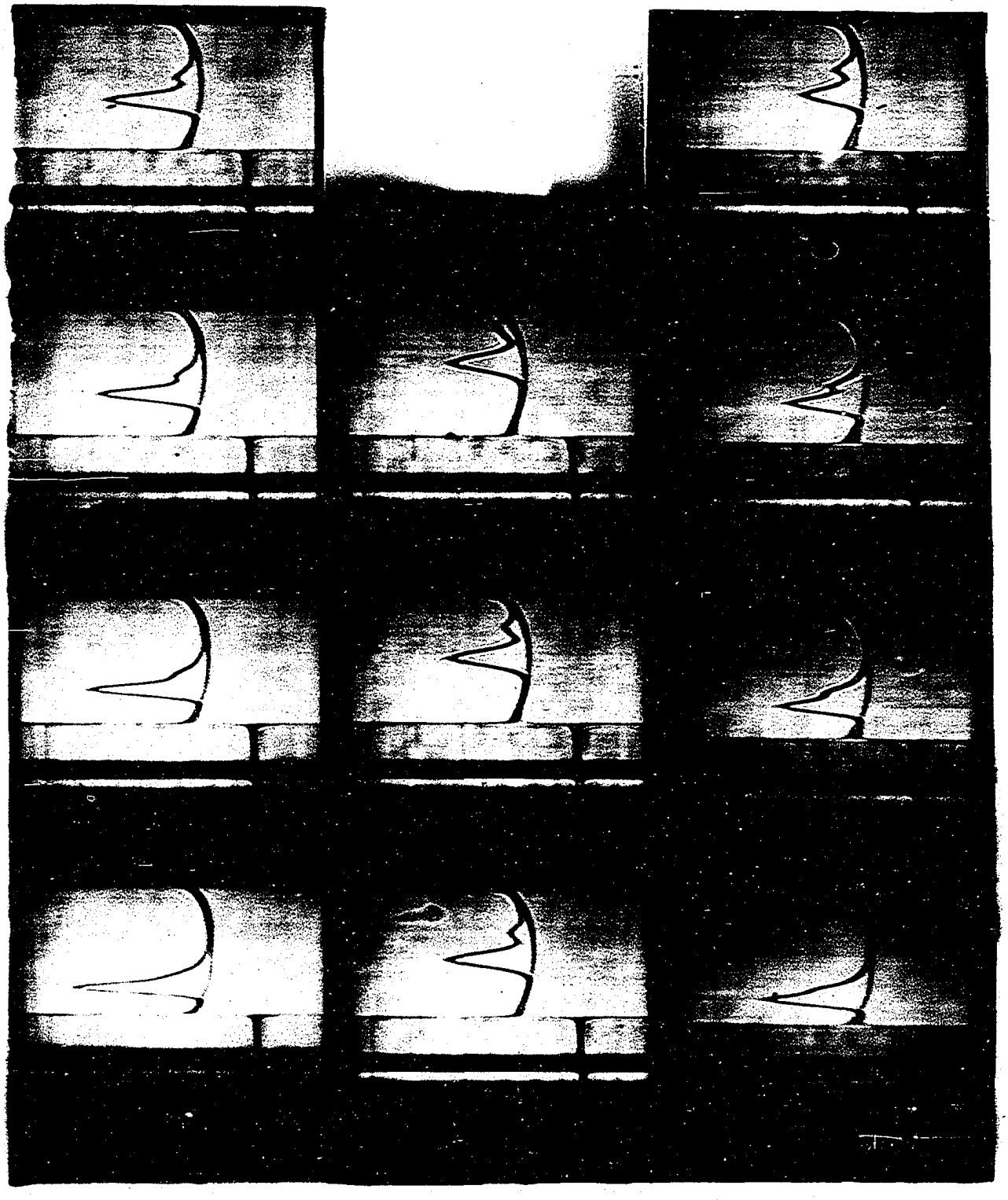

FIG. 2-18: ESR spectra of DNP-5-A and AB-D vs ABT complex. The two spectra were superimposed at their high field peak indicated by an arrow (↓) and the difference is shown at low field peak where T indicated ABT and D indicated ABD. Their difference is estimated to be 62-59 = 3 gauss in maximum splitting.

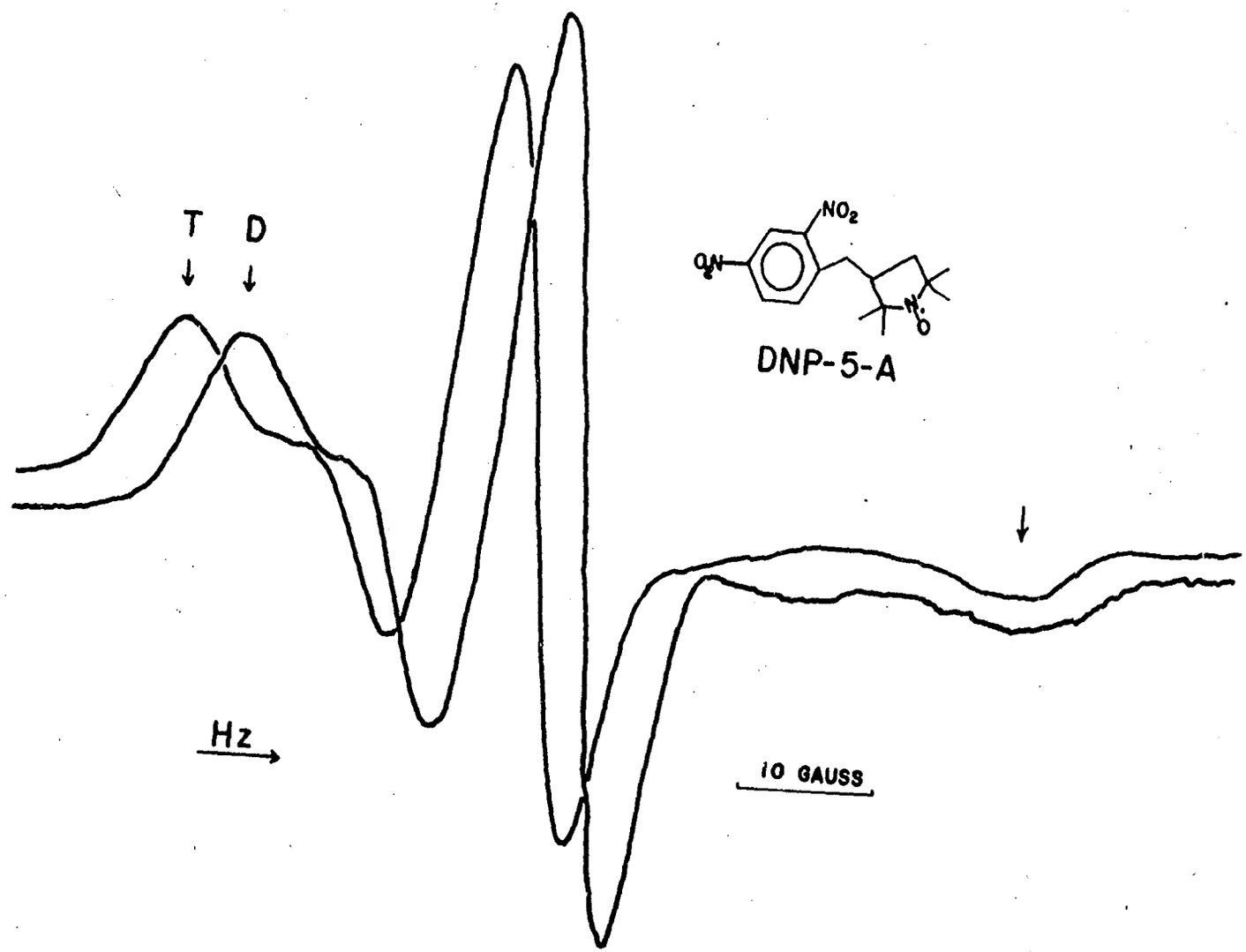
T
D
Hz
10 GAUSS
NO2
O2N
N
O
DNP-5-A

derivative or where the maximum end to end distance is approximately 21 Å. This second method would indicate a possible minimum combining site depth of 10.5 Å for those antibodies able to form dimers.

(4) Studies of HCS Structural Heterogeneity.

Rabbit anti-DNP antibodies isolated with a homologous antigen, i.e. DNP-HγG (denoted as AB-D) using the procedure of Eisen (1964) and those isolated with a cross reacting antigen, i.e. ONP-PNP-TNP-HγG (denoted as AB-T) by Cheng and Talmage (1965) were found to have different specificities by the latter authors. These two antibodies were in this work studied in terms of structural differences of their HCS using a short chain and rigid spin-labeled hapten DNP-5-A. The results are shown in Fig. 2-18.

The anisotropic ESR spectra of DNP-5-A with AB-D and AB-T were lined up at their high field peaks, indicated by an arrow. The difference is shown at their low field peaks. T represents AB-T-DNP-5-A complex spectrum which has a maximum splitting of approximately 62 gauss and D represents AB-D-DNP-5-A complex spectrum having a maximum splitting of 59 gauss. This suggests that the HCS of AB-T is either deeper than or has more hydrophobic interaction than that of AB-D.

(5) Studies of Cross Reactivity of HCS.

Both AB-D and AB-T were studied with spin-labeled homologous hapten DNP-5-A and three cross reacting haptens, ONP-5-A, PNP-5-A, and TNP-5-A.

Fig. 2-19 shows the complex spectra of ONP-5-A, PNP-5-A, and DNP-5-A with AB-D. Their superposition at the high field peaks is indicated by an arrow, with the difference shown at the low field peaks. P represents PNP-5-A-AB-D complex spectrum, which has the largest splitting of approximately 62.5 gauss. O represents ONP-5-A-AB-D complex spectrum with a maximum splitting of 62 gauss and D indicates DNP-5-A-AB-D with a maximum splitting of 59 gauss. These differences were not as pronounced when bound at the HCS of AB-T, but the overall extent of immobilization is increased in all three labeled haptens. The maximum hyperfine splitting observed of the ABT antibody immobilized anisotropic spectra was for PNP-5-A, 64 gauss; ONP-5-A, 63.5 gauss; and DNP-5-A, 62 gauss; as shown in Fig. 2-20, TNP-5-A-AB-T gave 63.5 gauss in splitting which is not shown here.

These results indicate the homologous hapten may form a more rigid complex or has preferred orientation at the HCS thus preventing the direct interaction of the spin-label moiety with the site, while the cross

FIG. 2-19: ESR spectra of PNP-, ONP- and DNP-5-A·AB-D complex were superimposed at their high field peaks indicated by an arrow (↓) and the differences are shown from their low field peaks. P, O, and D represent PNP-5-A, ONP-5-A, and DNP-5-A. The difference in maximum splitting is approximately 62.5-59 = 3.5 gauss for P and D and 3 gauss for O and D.

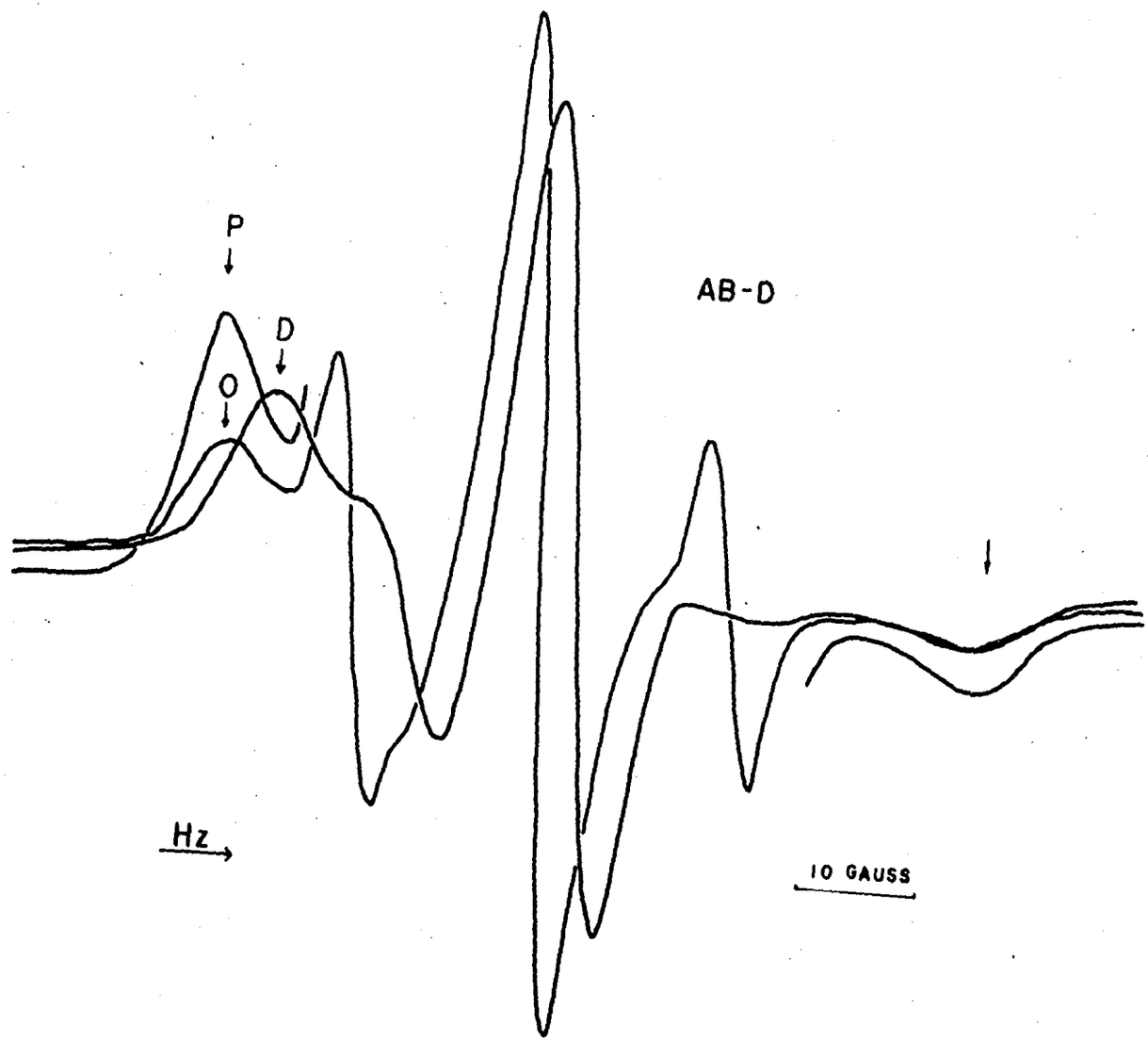
P
D
O
AB-D
Hz
10 GAUSS

FIG. 2-20: Difference in ESR spectra of PNP-5-A, ONP-5-A, and DNP-5-A AB-T complexes.

The three spectra were superimposed at their high field peak indicated by an arrow (↓) and the differences are denoted by P, O, and D at their low field peaks. Differences in maximum splitting are estimated to be 64 vs 63 vs 62 gauss.

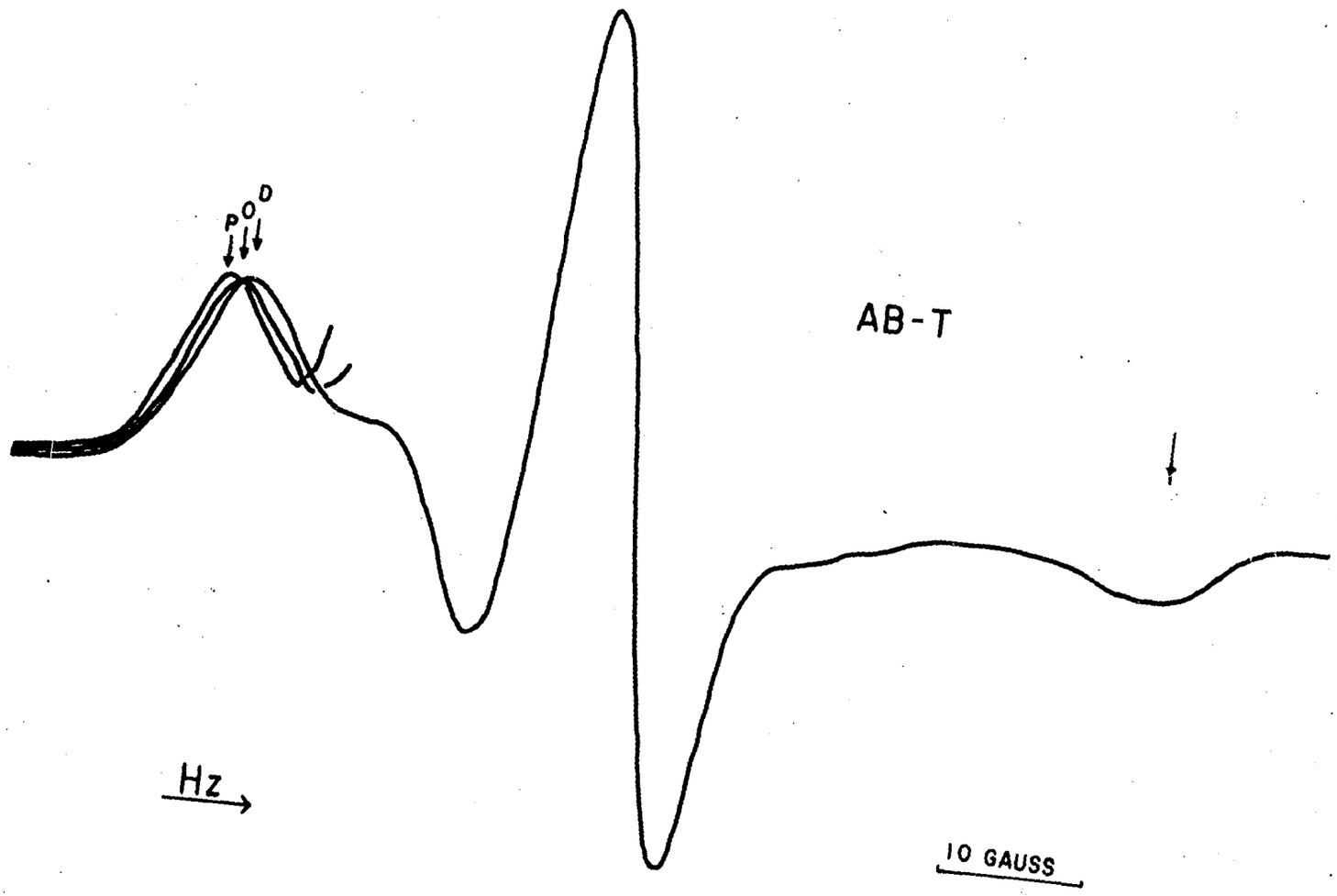
P O D
AB-T
Hz
10 GAUSS

reacting hapten forms a less rigid complex and allows the spin-label moiety more orientational freedom and interacts with hydrophobic region of the binding site to a larger extent than its counterpart.

(6) Studies of the Rotational Relaxation Time of Antibody Monomer and Dimer and the Rigidity of the HCS.

The rotational relaxation time (ρ) of rabbit gamma globulin determined with electric birefringence by Krause and O'Konski (1963) was 200 nanoseconds. O'Konski thinks the result might be off (private communition).

While using DNP-6-H, Stryer and Griffith (1965) have estimated $\rho = 36$ nanoseconds for the spin-label moiety. They attribute this discrepancy to either the flexibility of the hydrazone linkage or the error from indirect polarization fluorescence measurement. In order to narrow this discrepancy, we have attempted to shorten the linkage of the hapten and the spin-label. The result is shown in Fig. 2-21 where the anisotropic AB-T complex spectra of DNP-6-H and DNP-5-A were superimposed at their high field peaks. Differences in maximum splitting are shown at their low field peaks. DNP-6-H-AB-T complex spectrum has a maximum splitting of 54 gauss and DNP-5-A-AB-T is 62 gauss. Therefore,

FIG. 2-21: ESR spectra of DNP-5-A and DNP-6-H, AB-D complex (59 gauss).

(A) DNP-5-A AB-D complex spectrum with a maximum splitting of 59 gauss.

(B) DNP-6-H AB-D complex spectrum with a maximum splitting of 54 gauss.

The two spectra were superimposed at their high field peak and difference in maximum splitting is indicated at their low field peak.

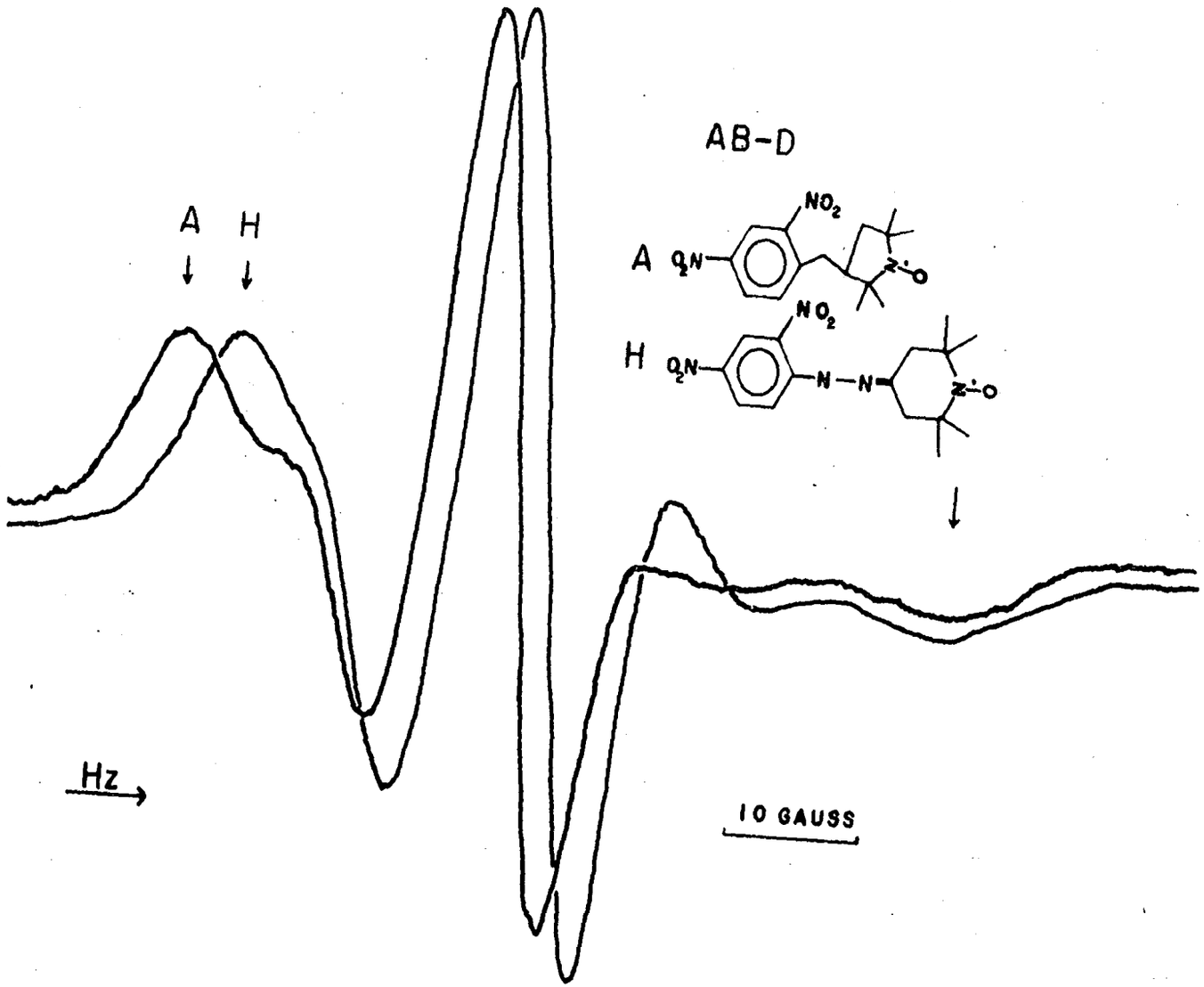
AB-D
A
H
A
H
Hz
10 GAUSS

further immobilization was achieved by replacing DNP-6-H with DNP-5-A, but due to the rigid complex formation of the homologous hapten at the HCS, the spin-label was not completely immobilized in both cases. Therefore, the maximum extent of immobilization is achieved using a spin-labeled cross reacting hapten PNP-5-A where the maximum splitting of the AB-T complex spectrum is approximately 64 gauss, shown in Fig. 2-20. The complex spectrum of an antibody dimer induced by di-DNP-Lysin-SL, where the spin-label is believed to be completely immobilized in between the two antibodies, has a maximum splitting of 66 gauss. (Fig. 2-14). The rotational relaxation time, ρ, is related to the fluorescence polarization by the expression $\rho=3\tau A/A_o-A$, where τ is the excited state life time and A_o is the emission anisotropy in the absence of molecular motion. The emission anisotropy (A. Jablonski, 1960) is defined as $A=I_x-I_y/I_x+2I_y$ where I_x and I_y are the intensities of x and y polarized fluorescence obtained with x-polarized excitation. Using $A_o=0.320$ and $\tau=11.7$ nanoseconds determined by Stryer and Griffith (1965) for the dansyl nitroxide, a plot of emission anisotropy (A) vs rotational relaxation time (ρ) was constructed (Fig. 2-22). The individual emission anisotropy (A) for the antibody immobilized spin-labeled haptens were

obtained from the dansyl moiety when the respective ESR spectra were matched in their maximum splitting. The values of ρ for (a) DNP-6-H, (b) PNP-5-A and (c) di-DNP-Lysine-SL were found to be 32, 80, and 115 nanoseconds respectively (Fig. 2-22).

(7) Spin-Labeled Hapten Studies of Antibody Affinity.

Spin-labeled hapten has been introduced as a general method in determining antibody affinity (equilibrium constant). The ESR spectra of bound and free labels at their high and low field peaks are shown to be completely separated in Fig. 2-23. Crude gamma globulin of immunized rabbit serum was titrated with ONP-5-A. The results are shown in Fig. 2-24. The standard curve of free spin in the presence of normal rabbit gamma globulin (RγG) indicates that this method is capable of detecting free spin concentration as low as 3×10^{-8} mole per liter. This range of sensitivity is sufficient for measuring the binding constant of most of the antibody hapten systems. The binding constant of ONP-5-A to anti-DNP antibodies in crude RγG was estimated to be approximately 1×10^{7} liter per mole, and the amount of antibody present in serum was estimated to be 0.8 mg/ml based on two binding sites per antibody (MW, 160,000).

FIG. 2-22: Plot of rotational relaxation time (ρ) vs emission anisotropy (A).

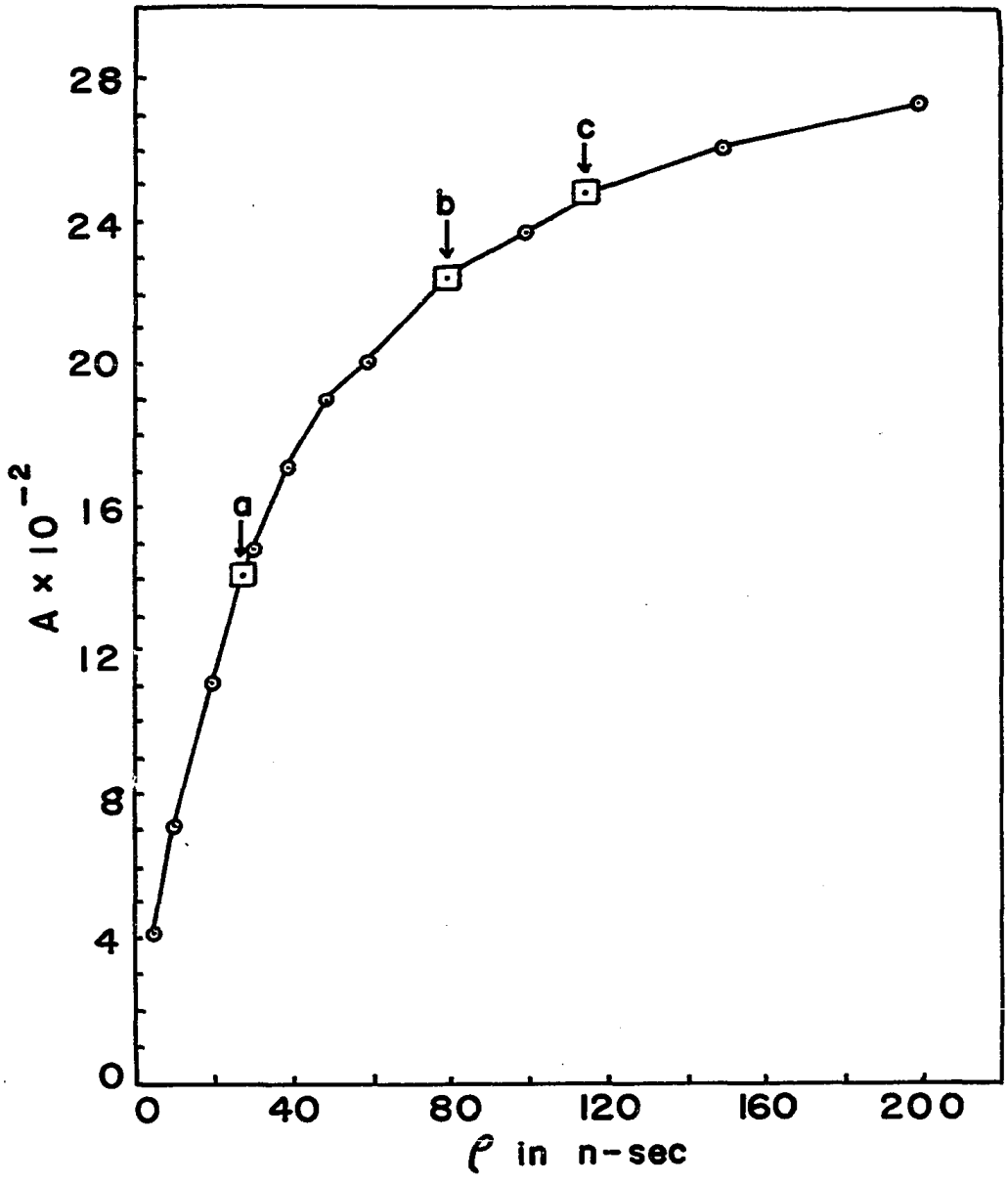
28
24
20
16
12
8
4
0
A x 10^-2
a
b
c
0
40
80
120
160
200
ℓ in n-sec

FIG. 2-23: ESR spectra of antibody bound and free ONP-5-A. The two down-arrows (↓) indicate the antibody bound ONP-5-A and the two up-arrows (↑) indicate free ONP-5-A.

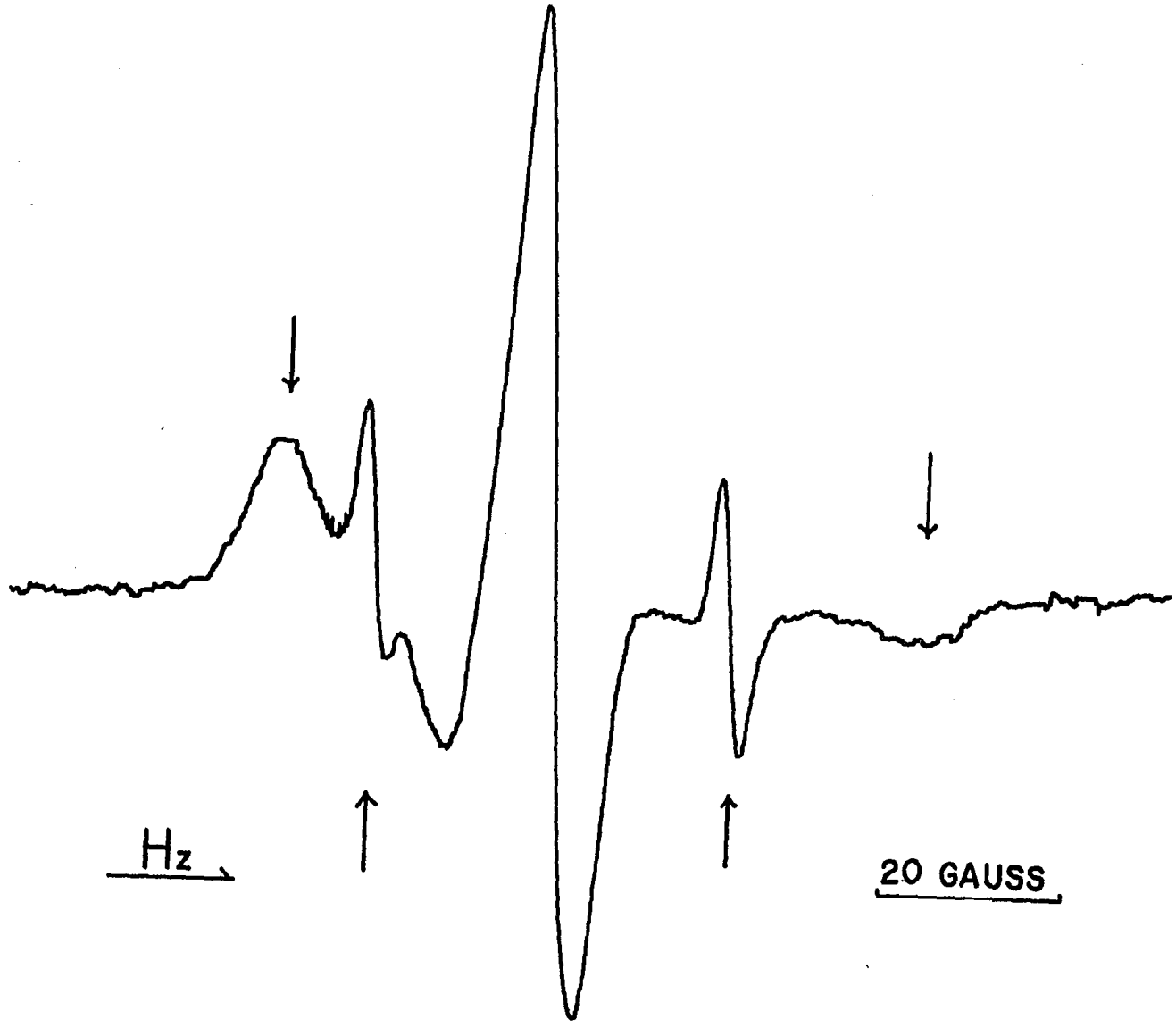
Hz
20 GAUSS

FIG. 2-24: Plot of antibody (in crude RγG) titration with ONP-5-A.

The solid line (———) is a standard curve of free spin concentration normal RγG. The signal was monitored as relative intensity of the high field peak (isotropic spectrum). The bound ONP-5-A (-·-·-·-) was determined from the relative increment of low field peak height of the anisotropic spectra. The free ONP-5-A (-x-x-x-) was determined analogous to the standard curve.

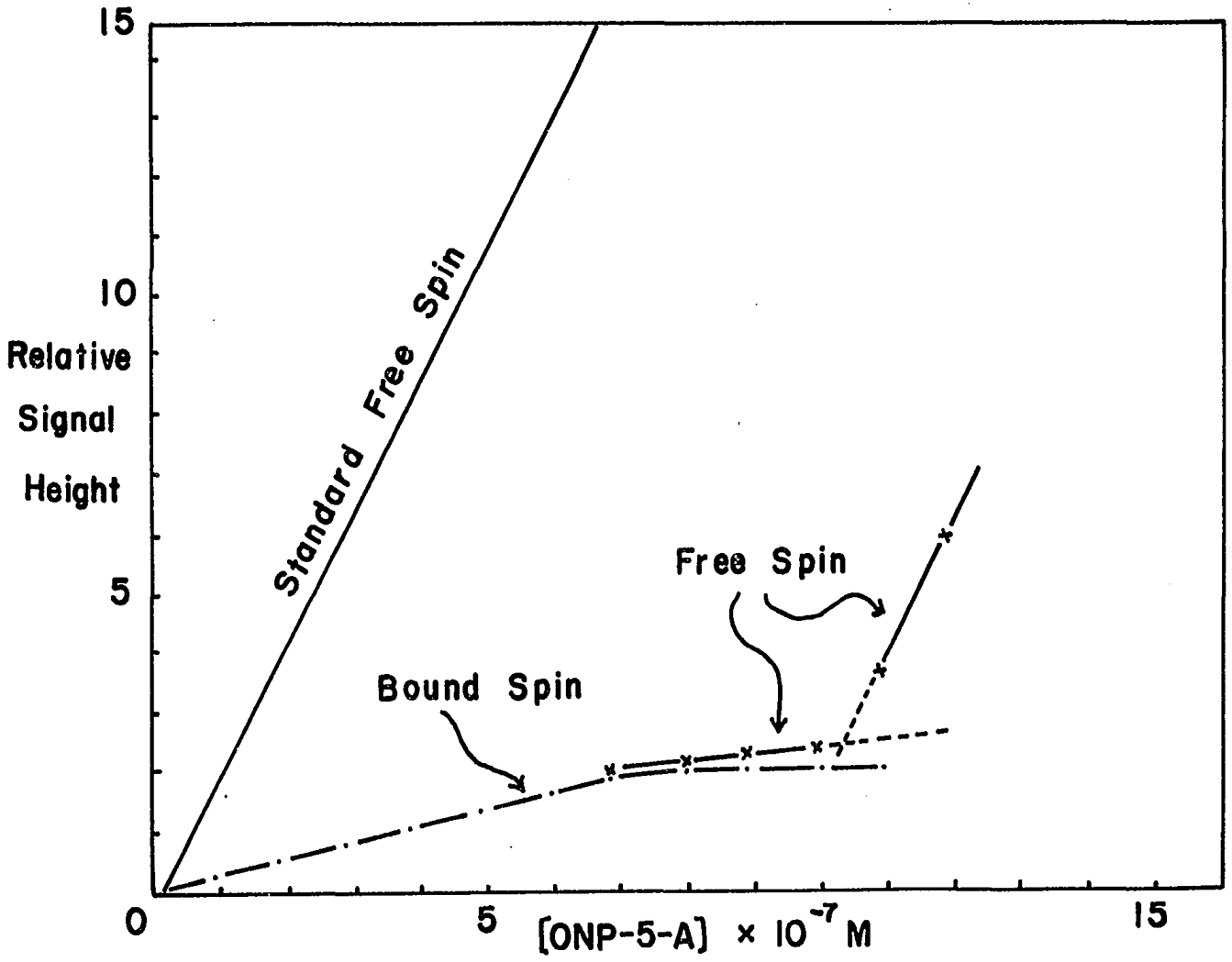
15
10
5
0
Relative
Signal
Height
Standard Free Spin
Free Spin
Bound Spin
5
15
[ONP-5-A] × 10^-7 M

(8) Affinity Spin-Labeling Method.

Two specific affinity spin-labels (ASL) were used in this experiment.

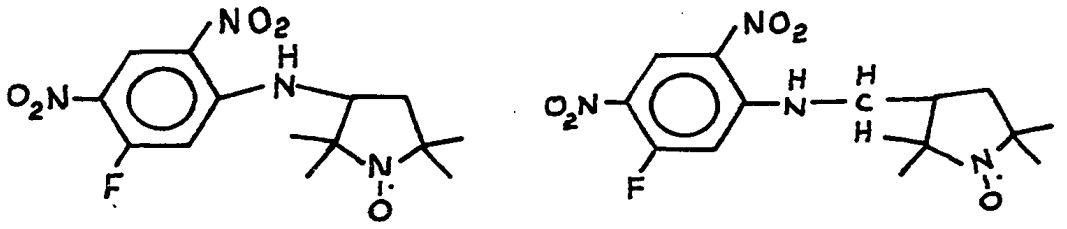

The fluorodinitrobenzene derivatives were known to react with NH_2, SH, tyrosine, OH, and histidine groups on a protein molecule. In order to eliminate non-specific labeling, the ASL were added to AB-T at pH 6.5 at about 2 ASL per site. The ASL were removed by sephadex G-25 column and the pH was subsequently raised to pH 8. The control experiments, using normal RγG (1×10^{-4}M) and the ASL (1×10^{-4}M) were reacted in pH 8.0 buffer. The samples were incubated at 37°C overnight and free ASL was removed by exhaustive dialysis. The resultant spectra of specific and non-specific ASL were found to be drastically different (Fig. 2-25). Both ASL bound at HCS gave identical completely immobilized ESR spectra shown in Fig. 2-25 (A) and the non-specific labeled RγG appears to have considerable motional freedom (Fig. 2-25 (B)), presumably the latter were labeled on the surface of RγG. To examine whether the ASL was covalently labeled at HCS excess DNP-Lysine

FIG. 2-25: ESR spectra of FDNB-5-A labeled AB-T and RγG.

(A) Non-covalent binding of FDNB at HCS of AB-T.

(B) Covalent binding of FDNB on to normal RγG (1×10^{-4} M).

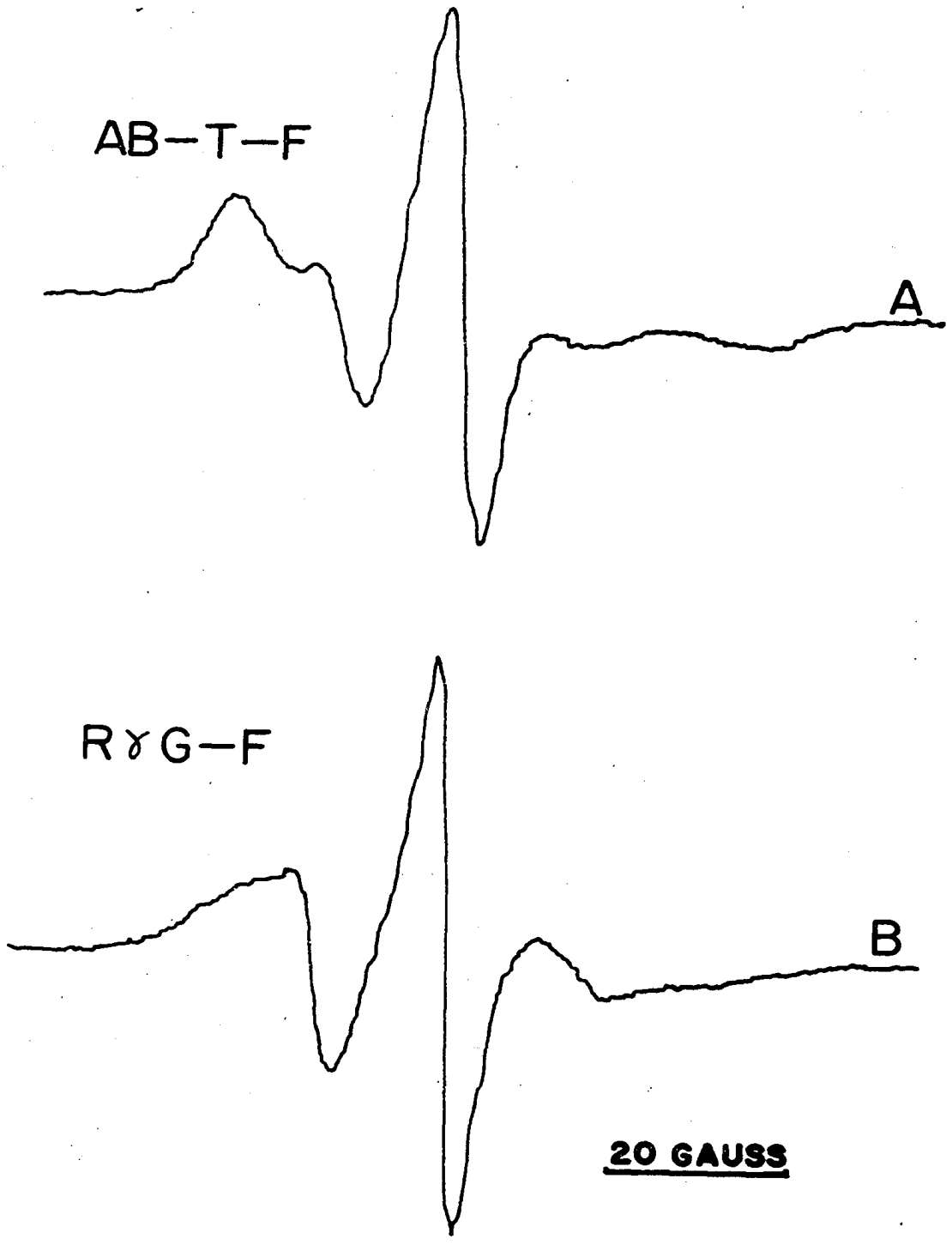
AB—T—F
A
RγG—F
B
20 GAUSS

was added and 90 – 95% of the ASL could be removed. The residue ESR spectra appears to be identical to ASL non-specifically labeled onto normal RγG (Fig. 2-25 (B)). These results demonstrate the usefulness of the ASL method in distinguishing specific and non-specific labeling.

(E) Discussion

(1) The Single Spin-Labeling Technique.

The strong motional dependence of the spin-label spectrum is related to the rotational reorientation time, τ_c, of the molecule. However, the determination of the exact value of τ_c of the label from its ESR spectrum is usually very complicated

In the single spin-labeling studies of the depth of the antibody active site, the exact value of τ_c is not necessary, because the depth of the site will be reflected in a change in τ_c of the various spin-labels as the distance between SL and point of attachment is varied. The relative change in τ_c of the various antibody immobilized spin-labeled haptens was calibrated with a model compound (6-Alcohol-NA) in various weight percent aqueous glycerol media, where line width or maximum splitting of the ESR spectra, i.e. τ_c, is a function of viscosity at constant temperature. The values obtained with this method agree fairly well

with the results from either theoretical calculations or polarization fluorescence measurement As expected, the antibody immobilized spectra and the spectra of the model compound (6-Alcohol-NA) in viscous aqueous glycerol do not match completely in all ranges of τ_c (1-100 nanoseconds). The spectral agreement at high and low τ_c values (Fig. 2-6, 2-7 and 2-11) is quite good in maximum splitting and line width. This is possibly due to the fact that the averaging of the hyperfine anisotropy of both spin-labels is spherical, i.e. when the label is within the active site or when the label is very far away from the active site, and the averaging of the anisotropy is orientation independent. But when the label is just outside of the active site, the predominant averaging mechanism is attributed to the free rotation of the single bond linking the label and the macromolecule. In this case, the rotational frequency of a single bond is much faster than that of the macromolecule itself; thus, the averaging of the hyperfine and g tensor anisotropy is dependent on the angle between the principle axis of the hyperfine and g tensor and the single bond. This is illustrated as follows:

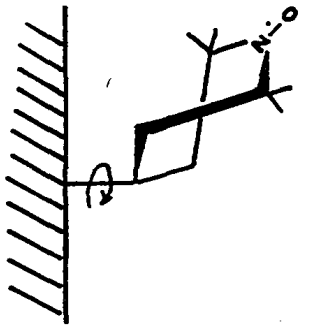

where the macromolecular rotation is taken as stationary (for the sake of simplicity) relative to the single bond rotation. Then the averaging of the hyperfine anisotropy is circularly perpendicular to the single bond. Thus, the splitting of the three peaks in this case does not match very well (see Figs. 2-8-10) with the model spectrum where the averaging is spherical. The estimation of relative τ_c in this case is based on the general line shape of the spectrum rather than relying on a perfect matching of the spectra. This phenomenon is not completely to our disadvantage because the discrepancy of the two spectra further demonstrates that at this distance, the label is just outside of the binding site. Furthermore, the change in τ_c is quite large ($\simeq$40 nanoseconds) between d + H = X and d + H > X. This would eliminate the uncertainties in our estimation of the relative change in τ_c as well

as the depth of the site. Unfortunately, the HCS of anti-DNP are heterogeneous in dimension. Therefore, we have to take into consideration that there could be several or at least two species of immobilization present. However, an upper and a lower limit in τ_c were estimated and the plot of τ_c vs (d + H) was, according to the average weight distribution, between the two limits. The weakly immobilized spectrum of DNP-α-Gly-SL (Fig. 2-8) appears to have two species and both DNP-β-Ala-SL (Fig. 2-9) and DNP-γ-But-SL (Fig. 2-10) show differences in their hyperfine splitting which indicates the motion of the carbonyl group of the DNP amino acids is partially restricted, therefore resulting in deviations from spherical averaging. This effect was not observed in the case of ε-DNP-Cap-SL which indicates that the latter assumes random orientation with respect to the macromolecular active site.

The ε-DNP complex spectra of α, ε-di-DNP-Lysine-SL are not exactly identical to the ε-DNP-Cap-SL (Fig. 2-13). This could be due to equilibrium between the α-DNP and ε-DNP antibody complexes of the bivalent spin-label. This possibility was further substantiated in Fig. 2-15-A(c) indicating the presence of α-DNP antibody complex.

The extent of maximum splitting in the antibody bound spectra of single spin-labels has been used as a criteria for the extent of immobilization of the label inside the HCS. This argument is supported by the fact that A_{max} of the anisotropic spectra is a function of viscosity and thus a function of τ_c. The result is shown in Fig. 2-26 where the spectra were lined up at their high field peaks with the differences shown at their low field peaks. A difference of 2 gauss (66-64 gauss) in A_{max} results in a change of 15 nanoseconds in τ_c and of 60 nanoseconds between 68 and 66 gauss. From the non-linearity relationship between A_{max} and τ_c, the differences in A_{max} of antibody bound spin-labeled cross reacting and homologous hapten spectra with two antibody preparations (AB-D and AB-T) (summarized in Fig. 2-27) could represent small (5 10 nanoseconds) but significant changes in the degree of immobilization of the spin-label moiety and structure or dimensional differences of the two antibody preparations.

(2) Structure, Dimension and Specificity of HCS.

Based on the results of single and double spin-labeling studies of the present work, one can attempt to postulate the structural and dimensional properties of the HCS.

FIG. 2-26: Difference in spectra of 1-oxyl-2,2,6,6-tetramethyl-4-piperidinol in various aqueous glycerol medium.

(A) in 99% glycerol 1% H_2O.

(B) in 96% glycerol 4% H_2O.

(C) in 92% glycerol 8% H_2O.

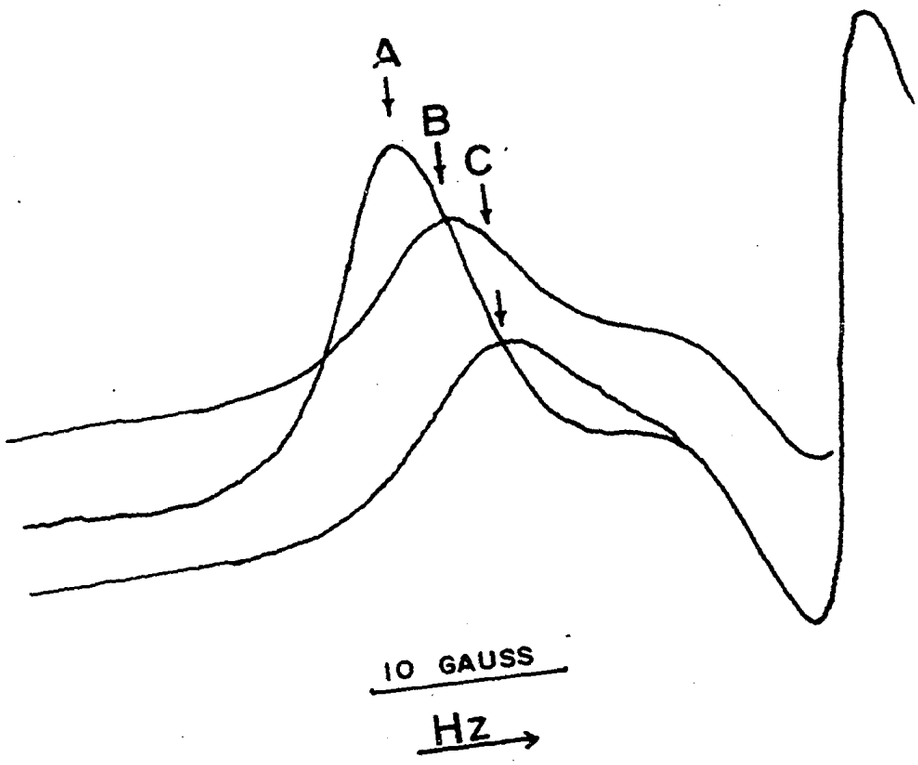
A
B
C
10 GAUSS
Hz

FIG. 2-27: Difference in spectra of PNP-5-A (P), ONP-5-A (O), and DNP-5-A (D) at antibody active site.

(A) AB-D

(B) AB-T

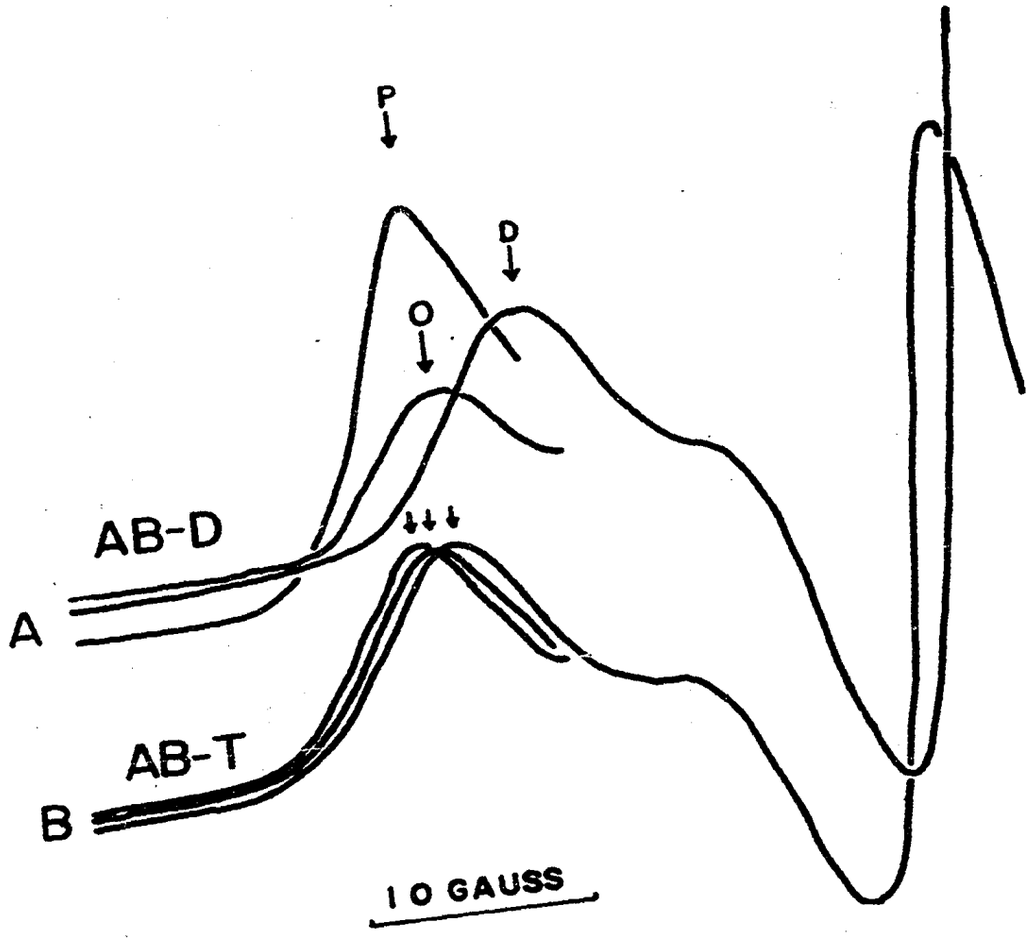
P
D
O
AB-D
A
AB-T
B
10 GAUSS

The dimension of the Fab fragment of anti-DNP antibodies, on which the HCS is presumed to be located, was found to be 60 Å x 34 Å x 34 Å, assuming a cylindrical-shaped fragment using electromicrograph techniques (Valentine and Green, 1967).

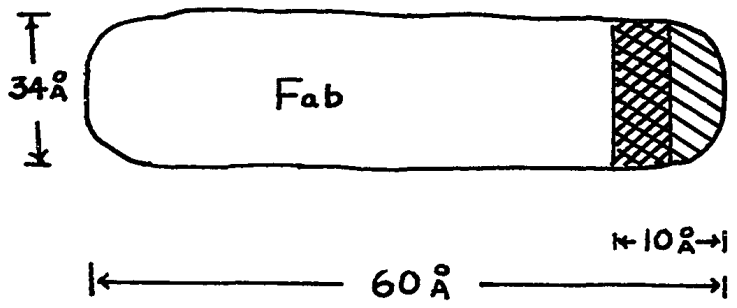

The HCS from our measurements is approximately 10 Å in depth, of which 5.5 Å is assigned to the rigid charge transfer complex region, where the direct complex formation of the nitrobenzene and the tryptophane ring occurs. The para- and ortho-nitrobenzenes are less electron deficient than the di- or tri-nitrobenzenes; thus forming a weaker complex with the tryptophane. These complexes are stabilized if a favorable hydrophobic interaction of the spin-label moiety and the HCS is available. Therefore, the p-nitro group can react with the anti-ortho-nitro site and allow the SL moiety to turn some 120° and interact with a more hydrophobic cross reacting site (C). The homologous

hapten DNP-5-A interacts more favorably with simultaneous binding of both para and ortho sites. Thus the spin-label moiety stays in a less hydrophobic region (H) with less immobilization. The difference among the antibody immobilized spin-labeled ortho, para, tri and di nitrobenzene derivatives can be explained by the equilibrium between the two binding orientations, C and H. The cross reactivity is most pronounced with AB-D; hence, we may conclude that the AB-D HCS has less hydrophobic interaction in both H and C region or that the hapten combining site of AB-D is shallower than AB-T. Since the depth of HCS is so critical, the spin-labeled haptens are more immobilized in all cases with AB-T than with AB-D, which is another indication that AB-T binding site is generally deeper than AB-D. This could be interpreted in terms of antibody active site formation in relation to hapten structure, although the D and L isomers of the labeled haptens may have some effect to the extent of immobilization.

The hapten-conjugated antigen used in the immunization of the rabbit for AB-T was DNP-BSA and for AB-D was DNP-BγG. The environment of the DNP groups on the two protein carriers were found to be different. (see Figs. 2-2 and 2-3)

This would indicate that the DNP groups on BγG were either in a less hydrophobic environment or less buried than on BSA. The direct evidence of the morphological difference of the two hapten carriers (BγG and BSA) may provide an explanation as to why antibodies prepared with the procedure of Cheng and Talmage (1965) has higher specificity than with the procedure of Eisen (1964). Also, the fact that antibodies having higher affinity for DNP-Lysine usually have lower affinity for $DNPO^-$ indicates that the hydrophobic region of the HCS interacts more favorably with the norleucine moiety of the DNP-Lysine than with the ionic phenolic group of $DNPO^-$.

CHAPTER III

DEVELOPMENT OF THE DOUBLE SPIN-LABEL METHOD

(A) Introduction

The single spin-labeling method developed by Ohnishi and McConnell (1965) has proven invaluable in studying longitudinal dimensions and conformational variation of a macromolecular active site in solution. However, its spectra are solely dependent for their basis on tumbling rate, and change in the size of the label is limited to longitudinal variation, with the result that sensitivity is somewhat narrowed in studying the transverse dimensions. It would be very interesting if a series of double spin-labels could be prepared where the interactions between the two paramagnetic centers serve as a measure of the width and rigidity of a binding site.

(B) Review of Stable Iminoxyl Biradicals

The first kinetically stable iminoxyl biradicals were prepared by E.G. Rozantzev and his co-workers (1965) where exchange interaction between the two radicals was observed. This exchange interaction was subsequently studied with nine biradicals with variable distance between the radical centers, prepared by reacting the kinetically stable monoradical 1-oxyl-2,2,6,6-tetramethyl-4-hydroxyl piperidine (E.G. Rozantzev, 1964) with dicarboxylic acid chlorides, with phosgene, and with diisocyanates, to form the diesters of the acids,

possessing two unpaired electrons. The exchange interaction between the two radicals was found to be a function of distance between the two radicals as well as the conformation or rigidity of the molecule.

The zero-field splittings of two of these biradicals (succinyl and Tere-pathalic derivative) were studied in a liquid crystal where each hyperfine absorption is further split into a doublet due to the zero-field generated by the adjacent radical centers. Similarly, this dipole-dipole interaction is a function of temperature, relative distance, and orientation.

The anisotropic spectra of these biradicals have not been extensively studied.

(C) Formulation of Research Problem

The objective of the double spin-labeling (DSL) technique is to study the flexibility, width, and shape of a protein active site in solution. Differing from the single spin-labeling (SSL) technique, DSL carries two stable nitroxide radicals (SL_1 and SL_2) and is labeled at a desired site onto a biomacromolecule via a biofunctional group R where

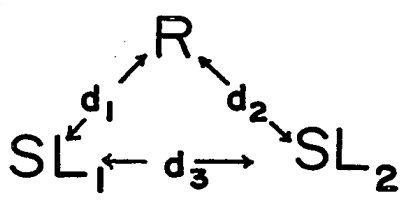

FIG. 3-1
Diagram of Double Spin-Label

d_1 and d_2 are the length of a covalent linkage between the SL and the biofunctional group R. They can be identical or different in order to vary d_3, the average distance between SL_1 and SL_2, to achieve the proper range of sensitivity.

In the isotropic phase, its spin Hamiltonian is

$$\mathcal{H} = g|\beta|S_zH + a(S_{1z}I_{1z} + S_{2z}I_{2z}) + J(S_1 \cdot S_2) \qquad (3\text{-}1)$$

where three right-hand terms are the Zeeman, hyperfine, and exchange energies. The electron spin operators, S_i and S_{iz}, refer to an electron spin wavefunction on the ith side of the biradical. I_{iz} is the corresponding N^{14} nuclear spin operator. The exchange integral J is dependent on the distance between the electrons and on the orientation of their orbitals. If $J \gg a$, then complete exchange will be observed with a hyperfine splitting of $a/2$ and a typical quintet with a ratio of 1:2:3:2:1. Intermediate exchange can be observed by varying either the distance or the orientation of the two axial symmetric hyperfine tensors (see Figs. 3-4, 3-5, and 3-7).

Since the two unpaired electrons of the DSL are highly localized and if it is a rigid molecule where the long axis of the hyperfine tensor has a fixed (average) orientation with respect to each other, shown in Fig. 3-2,

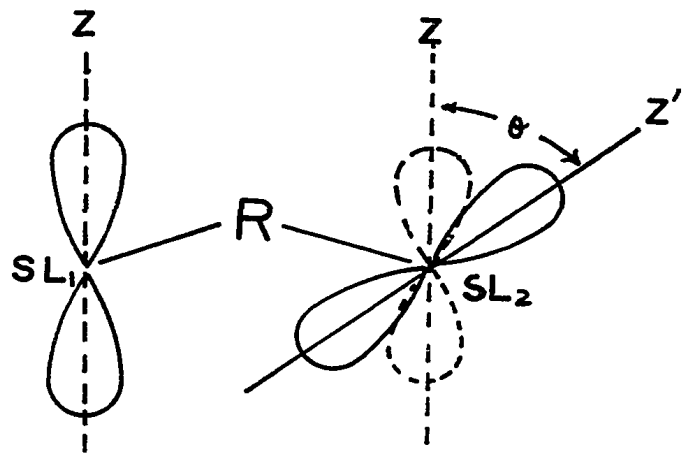

FIG. 3-2
Diagram of Rigid Double Spin-Label

the approximate spin hyperfine Hamiltonian is

$$\mathcal{H} = |\beta| \hat{\underset{\sim}{S}} \cdot \underset{\approx}{g} \cdot \underset{\sim}{H} + \hat{\underset{\sim}{S}}^{(1)} \cdot \underset{\approx}{T} \cdot \hat{\underset{\sim}{I}}^{(1)} + \hat{\underset{\sim}{S}}^{(2)} \cdot \underset{\approx}{T}' \cdot \hat{\underset{\sim}{I}}^{(2)} + \underset{\approx}{J} \hat{\underset{\sim}{S}}^{(1)} \cdot \hat{\underset{\sim}{S}}^{(2)} \quad (3\text{-}2)$$

The rotations used here are essentially identical to Eq. 1-3. The effective hyperfine tensor $\underset{\approx}{T}'$ is the projection of the hyperfine tensor ($\underset{\approx}{T}$) of $SL_{(2)}$ with respect to the principle axis of $SL_{(1)}$ as illustrated in Fig. 3-2.

In the anisotropic phase (Eq. 3-2) for a rigid DSL, the maximum splitting (A_{max}) of the ESR spectrum is a function of the relative angle (θ) (Fig. 3-2) between the two hyperfine tensors. The resultant maximum splitting is equal to $\frac{1}{2}(2T_z + 2T_z')$. Depending on θ, the A_{max} varies from $2T_z$($\theta = 180^\circ$) to T_z($\theta = 90^\circ$) shown in Fig. 3-3(A) and (B).

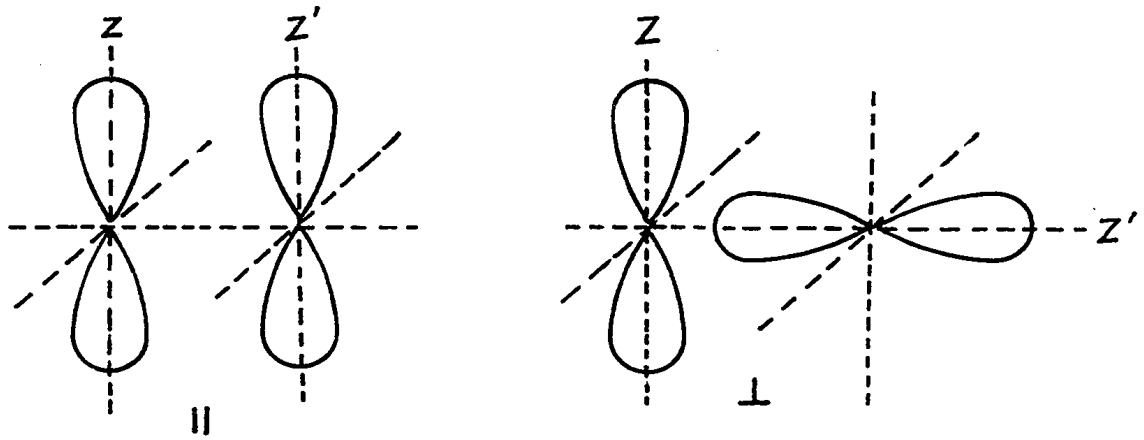

FIG. 3-3
Diagram of N^{14} 2p-orbitals of Idealized Double Spin-Label

Thus, the maximum splitting of the anisotropic spectrum can vary from a maximum of $2T_z$ to a minimum of T_z. The line shape and maximum splitting of the anisotropic spectrum of DSL are dependent on the extent of direct overlapping of the two unpaired electron wave functions. Thus a deviation from the native average configuration upon binding of a DSL at the HCS would be reflected in its anisotropic spectra. This will serve as a measure of the flexibility of the HCS as well as the extent of external distortion of the DSL.

The extent of immobilization of the DSL can be estimated from the binding of a double-labeled hapten which carries only one unpaired electron.

(D) Experimental

Preparation of Double Spin-Labeled Haptens.

<u>DSL (VIa)</u>: Yellow isomer; 1,5-di-N,N'-(2,2,5,5-tetramethyl-3-amino-pyrrolidine-1-oxyl)-2,4-dinitrobenzene was prepared by reacting 1,5-difluoro-2,4-dinitrobenzene with an excess of VI in chloroform. The orange-yellow residue was washed three times to remove the unreacted amine. Upon recrystallization from chloroform and ether, a flaky-yellow isomer was obtained which was recrystallized twice, m.p. 225-226°.

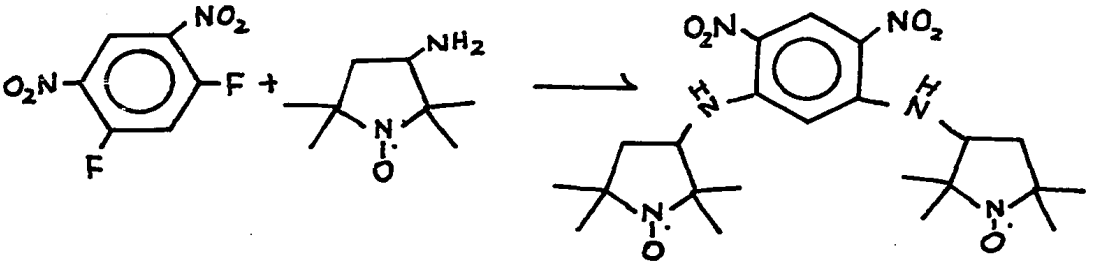

Anal: Calc. for $C_{22}H_{34}N_6O_6$: C, 55.5; H, 7.1; N, 17.5%

Found: C, 55.3; H, 7.1; N, 17.6%

<u>DSL (VIb)</u>: Red isomer: The remaining solution was evaporated under vacuum. The orange precipitate was recrystallized three times from dichloroethane and ether. An orange-red crystal was obtained, m.p. 234-235°.

Anal: Calc. for $C_{22}H_{34}N_6O_6$: C, 55.5; H, 7.1; N, 17.5%

Found: C, 54.8; H, 6.7; N, 17.4%

<u>MIX-DSL (VIc)</u>: 1-N-(2,2,6,6-tetramethyl-4-piperidine)-3-N'-(2,2,5,5-tetramethyl-3-pyrrolidine-1-oxyl)-2,4-

dinitrobenzene was synthesized by reacting equal molar of 1,3-difluoro-2,4-dinitrobenzene with 2,2,6,6-tetramethyl-4-amino-piperidine VII in chloroform. Yellow residue was recrystallized twice from chloroform and ether and then reacted with an excess of VI in a minimum amount of chloroform. After the reaction was over, chloroform was stripped off. The orange-yellow residue was recrystallized twice from di-chloroethane and heptane, and orange crystals were obtained, which melts between 195-196°.

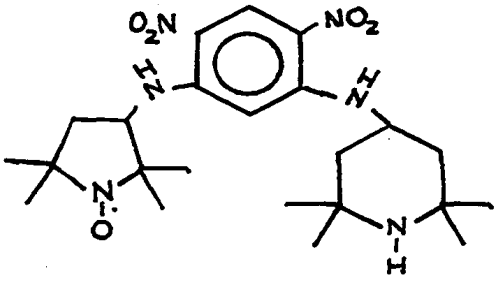

<u>DSL (VId)</u>: 1,5-di-N,N'-(2,2,5,5-tetramethyl-3-aminomethyl-pyrrolidine-1-oxyl)-2,4-dinitrobenzene was prepared according to the procedure of VIa.

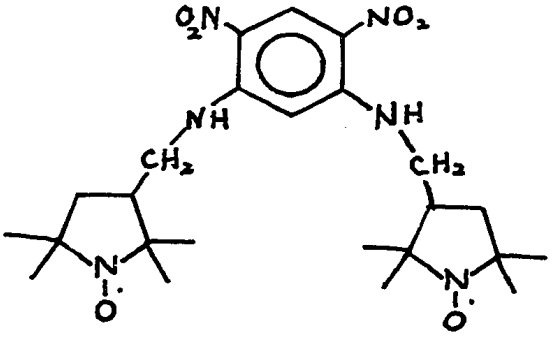

The recrystallized product melts between 202-203°.

(E) Results and Conclusions

(1) Spectral Properties of Double Spin-Label.

To demonstrate that the exchange integral J in Eq. 3-1 is a function of the probability of direct overlapping of the two unpaired electron wave functions, the oxalic biradical in 5% ethanol-95% H_2O is shown in Fig. 3-4(A) at 26°C and (B) at 98°C to be an identical triplet. This is because the rigidity of the linkage between the two radicals prevents the direct overlapping of orbitals, and thus, there is no exchange interaction. Fig. 3-5(A) shows the isotropic spectra of succinic biradicals at 26°C, where intermediate exchange was observed. This exchange interaction was much smaller at 98°C (Fig. 3-5(B)).

The reaction of 1,5-di-fluoro-2,4-dinitrobenzene with a mixture of the D and L forms of 5-Amine-NA results in a product which can exist in 4 possible configurations shown on the next page. The DD form and the LL form could be different. The DL and the LD forms are identical due to the inherently symmetric plane of the dinitrobenzene ring through C_3 and C_6. The ESR spectrum of a mixture of optical isomers at elevated temperatures (Fig. 3-6) is shown to have at least two species which were subsequently resolved into two crystalographic forms; an orange-red and a yellow

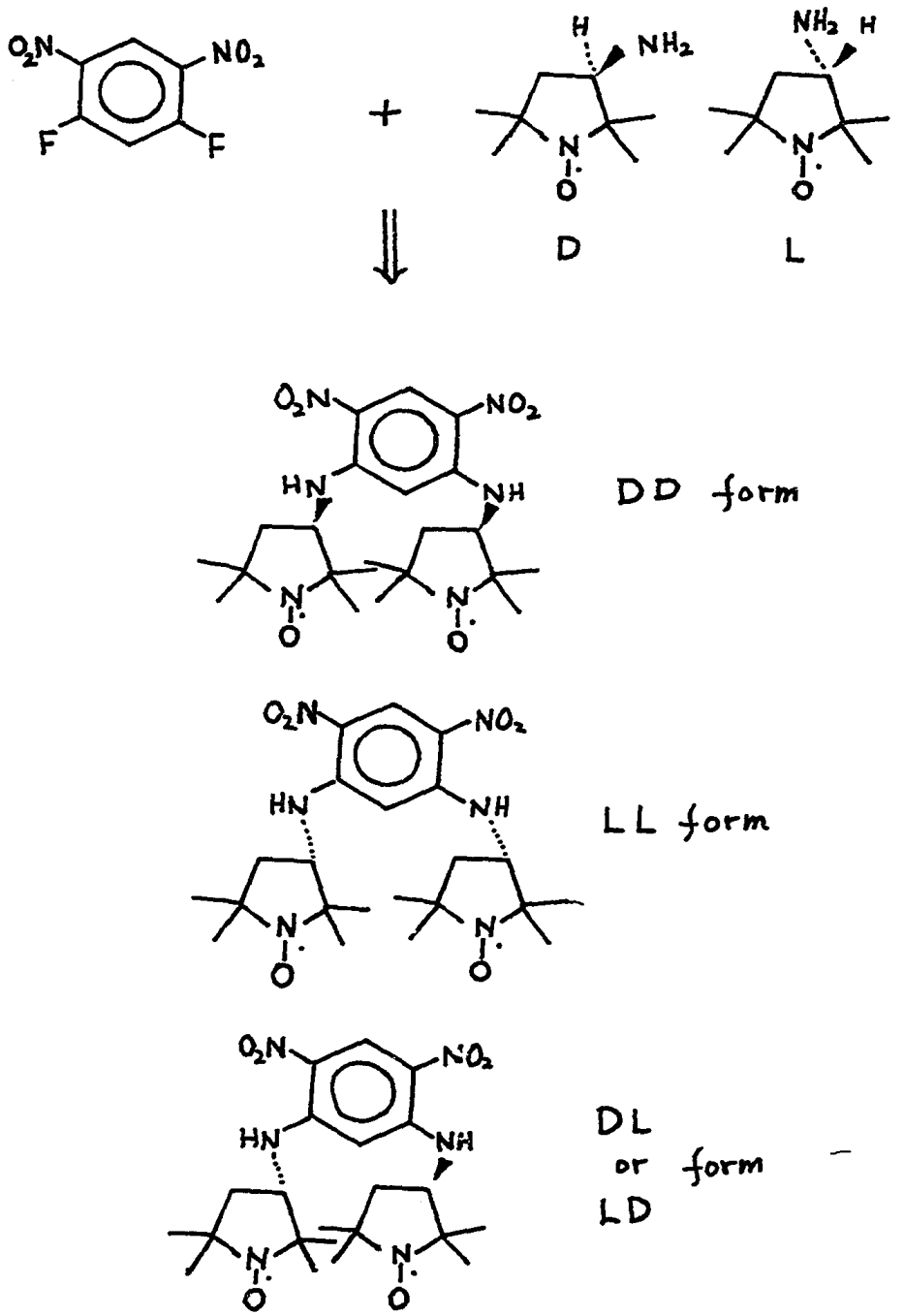
O2N
NO2
F
F
+
H
NH2
NH2
H
N
O
D
L
DD form
LL form
DL
or form
LD

FIG. 3-4: ESR spectra of di-2,2,6,6-tetramethyl piperidin-1-oxyl ester of oxalic acid in 5% ethanol 95% H_2O (A) at 26°C (B) at 98°C.

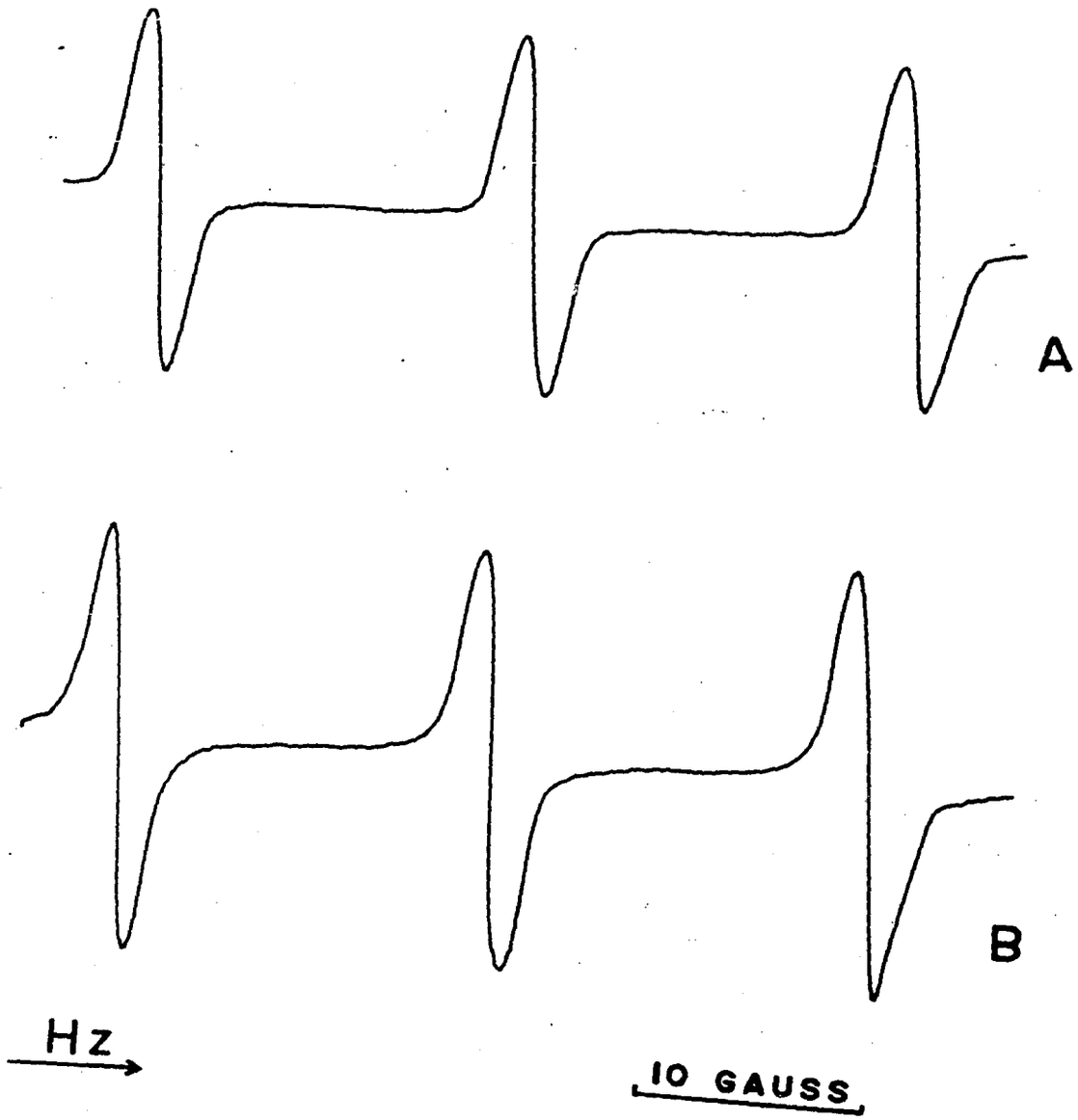
A
B
Hz
10 GAUSS

FIG. 3-5: ESR spectra of di-2,2,6,6-tetramethyl piperidin-1-oxyl ester of succinic acid in 5% ethanol 95% H_2O (A) at 26°C (B) 98°C.

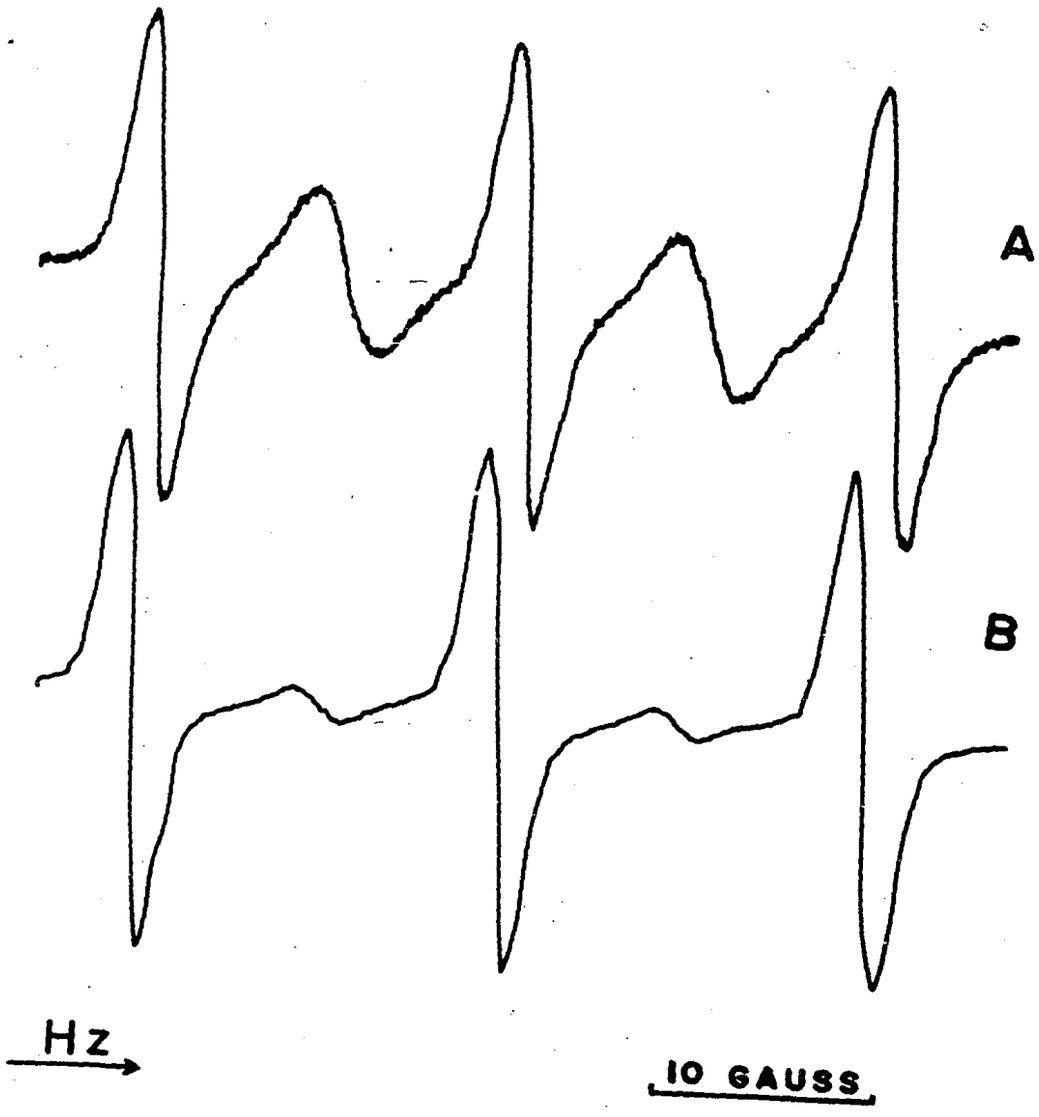
A
B
Hz
10 GAUSS

flaky crystal denoted as DSL-R and DSL-Y.

ESR spectra of DSL-R and DSL-Y in the isotropic phase are shown in Fig. 3-7(A) and (B). Although they are structural isomers, magnetically, they behave as two distinct species. Their differences are listed in Table 3-1.

	Peak Ratio	a in acetonitrile	a/2 in acetonitrile	Δw gauss
DSL-R	1:1.8:2.6:1.8:1	14.5	7.25	2.27
DSL-Y	1:1.4:1.5:1.4:1	14.5	7.25	3.23

TABLE 3-1
Spectral Difference of DSL-R and DSL-Y

The exchange integral J was found to be independent of temperature and viscosity effect. This indicate $J \gg a$ at all times. The most probable explanation for these phenomena is that there is a constant overlapping of the wave functions of the two unpaired electrons, and the difference in the peak ratio between the two racemic isomers is possibly due to the orientational differences in the overlapping of the two wave functions.

This orientational difference is further substantiated by the difference in the maximum splitting of their anisotropic spectra. Assuming there is random orientation between the two paramagnetic centers, the

FIG. 3-6: ESR spectra of crude double spin labels in acetonitrile at 80°C. A & B indicate the presence of two magnetically distinct species.

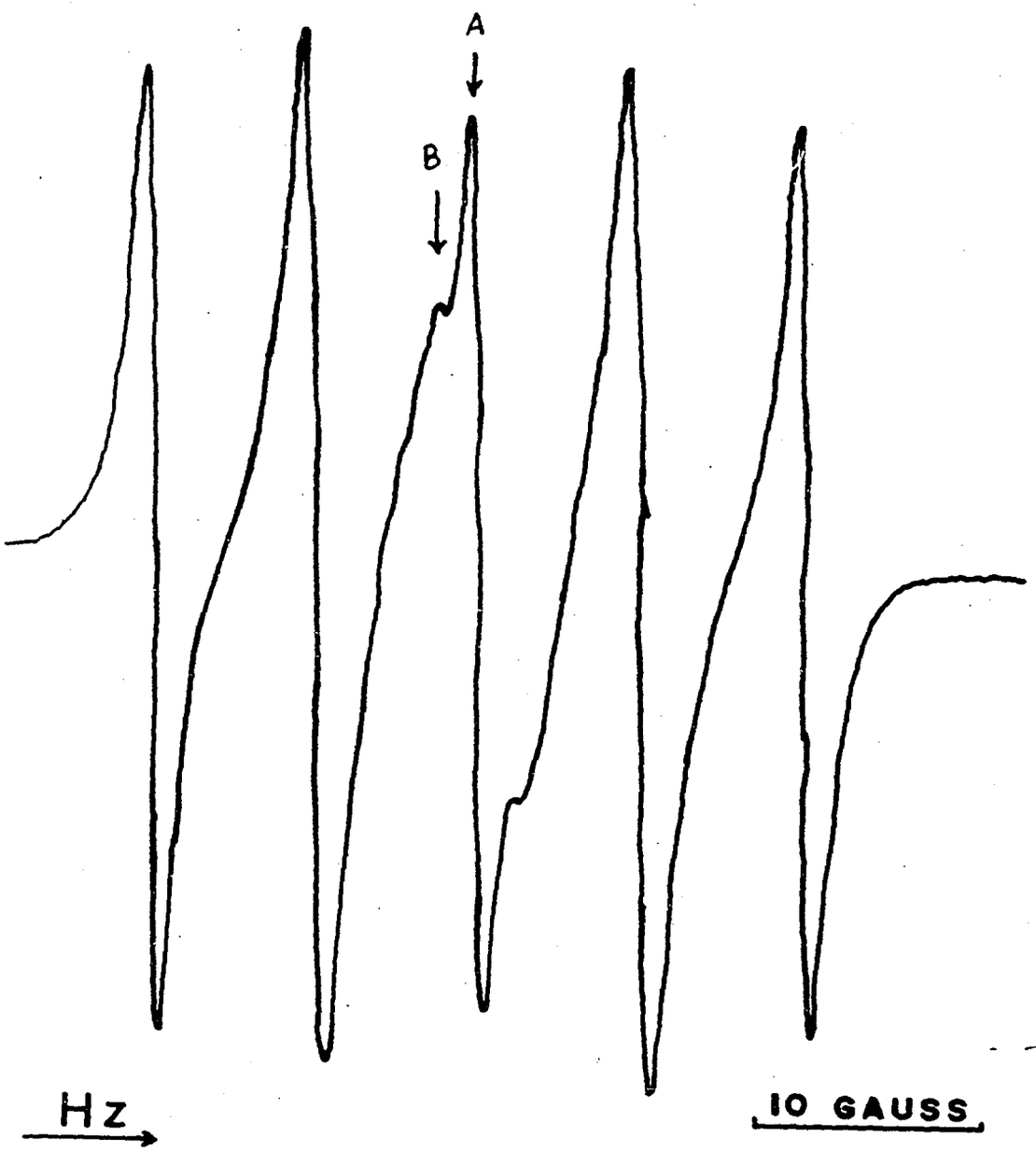
A
B
Hz
10 GAUSS

FIG. 3-7: ESR spectra of DSL-R and DSL-Y in the isotropic phase.

(A) DSL-Y in acetonitrile at 26°C.

(B) DSL-R in acetonitrile at 26°C.

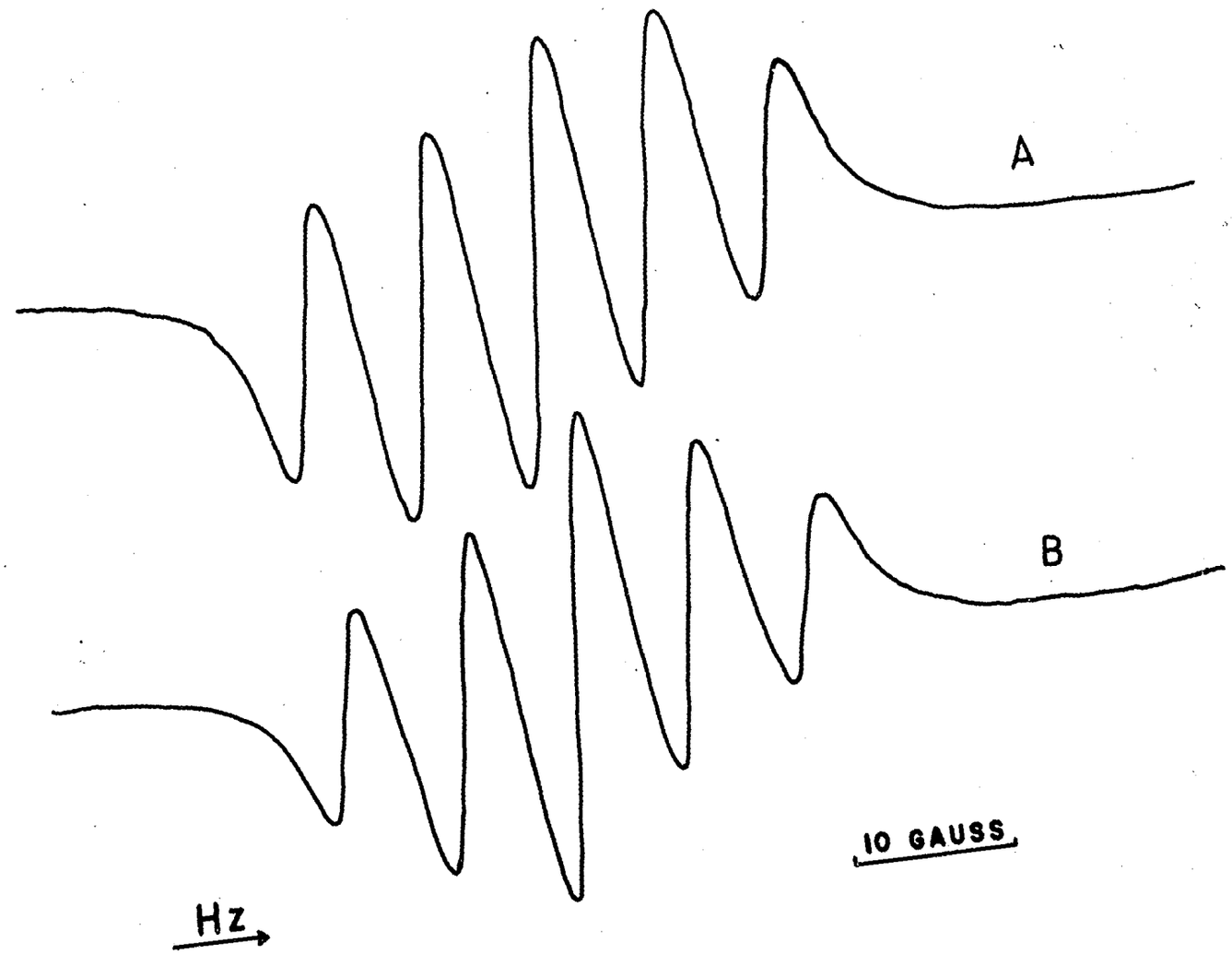
A
B
10 GAUSS
Hz

predicted maximum splitting should be $2T_z$ which has a value of approximately 68 gauss. If the molecule is rigid and has a preferred orientation, then the maximum splitting will be smaller than $2T_z$, depending on the relative angle of the long axis of the two hyperfine tensors. The anisotropic ESR spectra of DSL-R and DSL-Y are shown in Fig. 3-11(B) and Fig. 3-12(B) respectively.

In the case of DSL-Y, $A_{max} \simeq 66$ gauss; thus the two hyperfine tensors are approximately parallel ($\theta \simeq 180^{\circ}$ or 0°) while in the case of DSL-R, $A_{max} \simeq 60$ gauss, the angle between the two tensors deviate from the parallel orientation. This speculation agrees well with space-filling models. The racemic isomers (DD and DL form) were compared by keeping the relative bond angle of C-N-C linkage between the spin-label and the hapten constant, and the difference is shown in Fig. 3-8 (A) and (B).

(2) Studies of the Flexibility of HCS.

To demonstrate that DSL can be used to study the flexibility of HCS, it is necessary to establish that the DSL are specifically bound at the antibody active site. DSL-R was dissolved in acetonitrile (Fig. 3-9 (A)), then added to AB-T in buffer. Excess free spin was removed through dialysis. The resultant immobilized

FIG. 3-8: Molecular models of double spin labels.

(A) DL form.

(B) DD form.

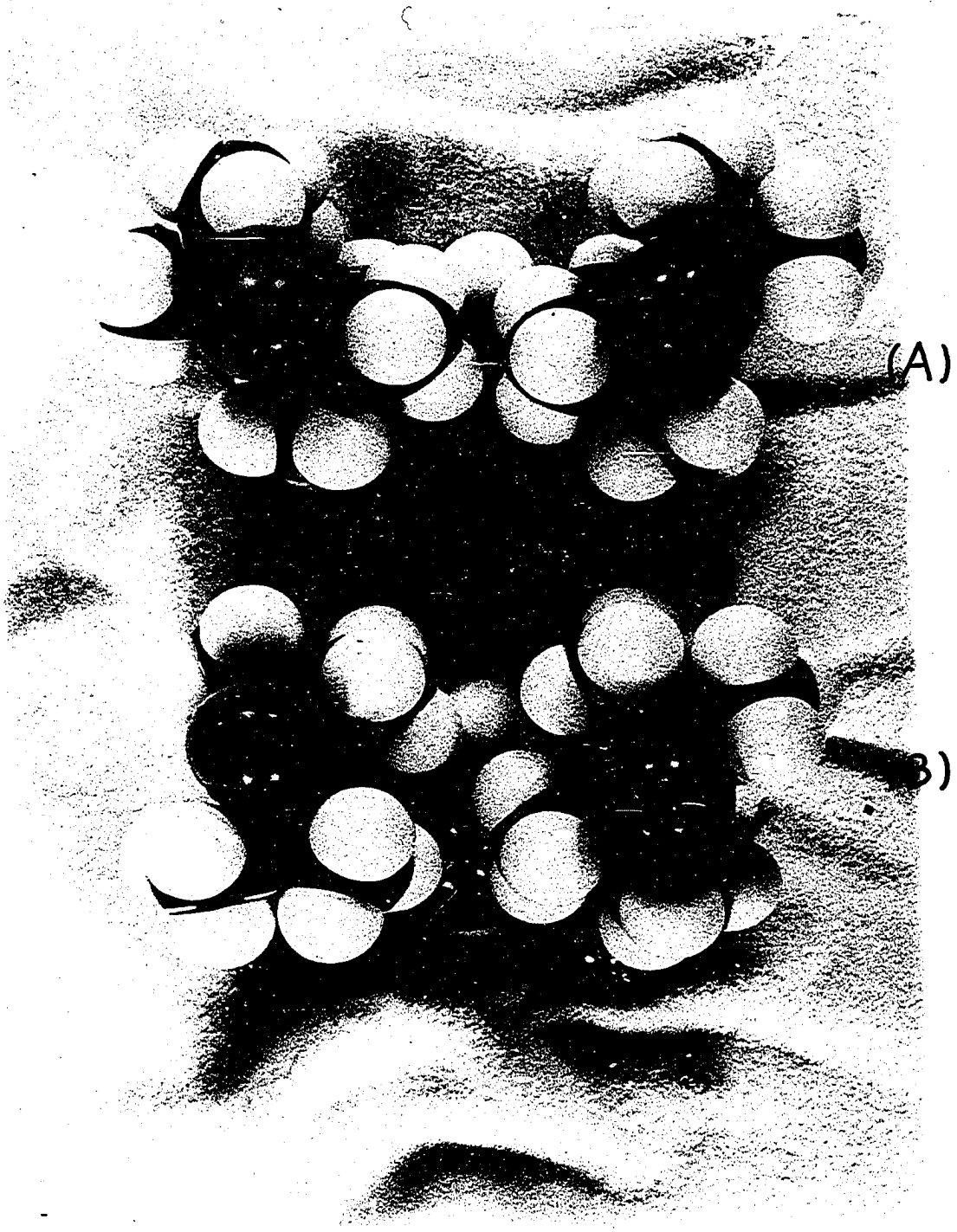
(A)
(B)

spectrum is shown in Fig. 3-9(B). To determine the extent of binding of DSL at the HCS, excess DNP-Lysine was used to back titrate the bound DSL. The resultant spectrum is shown in Fig. 3-9(C). The same procedure was used in the binding of DSL-Y (Fig. 3-10(A), (B) and (C)). These results indicate that the HCS is large enough to accommodate double spin-labeled haptens.

To understand the flexibility of the HCS, a higher resolution of the immobilized spectra of DSL at the HCS was desired. The immobilized spectra of DSL-R at AB-T concentration of approximately 20 mg/ml (Fig. 3-11 (A)) and DSL-R in 95% glycerol and 5% ethanol (Fig. 3-11 (B)) were compared and found to have almost identical maximum splittings of approximately 60 gauss each.

The immobilized and anisotropic spectra of DSL-Y were similarly compared and both found to have a maximum splitting of approximately 66 gauss (Fig. 3-12(A) and (B)).

To determine the extent to which the two spin-labels on the hapten moiety were immobilized at the HCS, a singlet-state double-labeled hapten or MIX-DSL (1-(2,2,6,6-tetramethyl-4-piperidine)-3-(2,2,5,5-tetramethyl-3-pyrrolindine-1-oxyl)-2,4-dinitrobenzene with approximately the same basic structure as DSL but carrying only one unpaired electron was prepared

according to the following scheme:

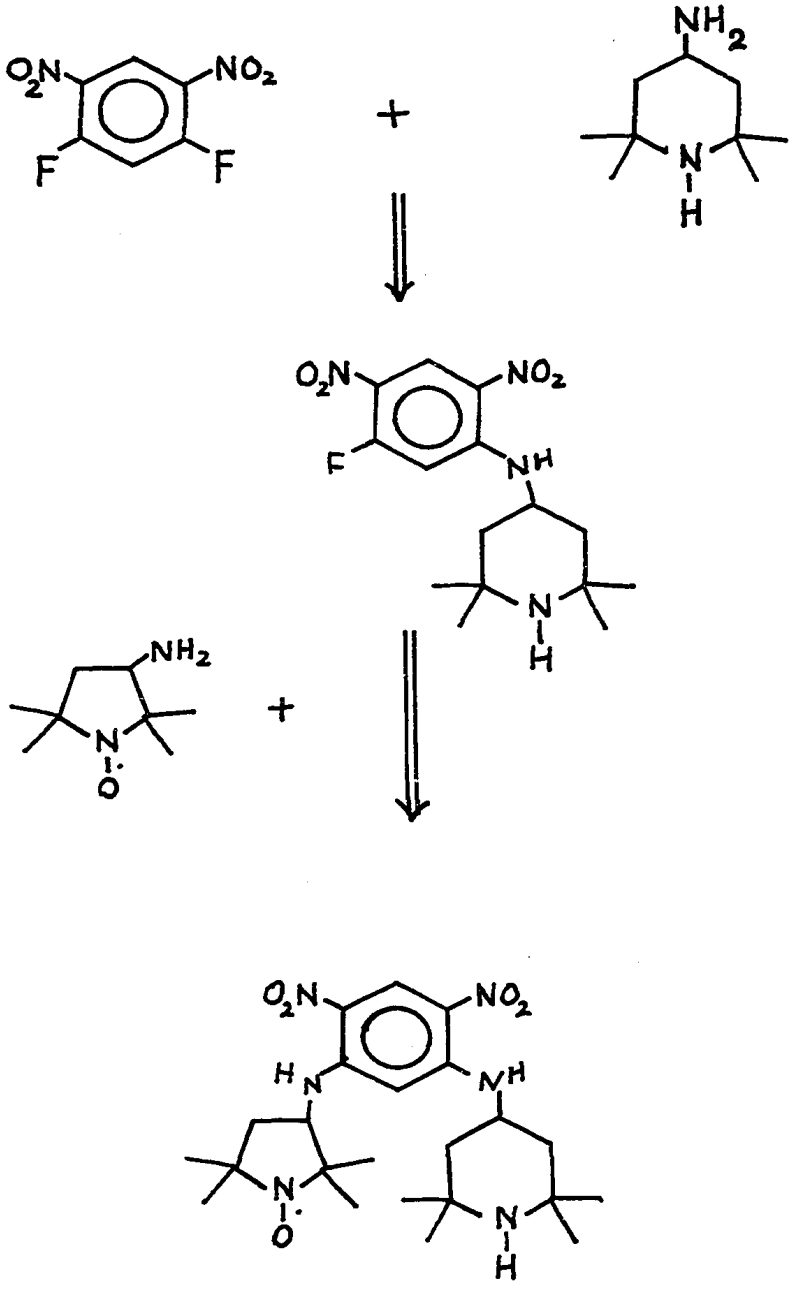

FIG. 3-9: ESR spectra of DSL-R.

(A) Free DSL-R in acetonitrile.

(B) Complexed spectrum of DSL-R bound at antibody HCS.

(C) Back titration of (B) with excess of DNP-Lysine.

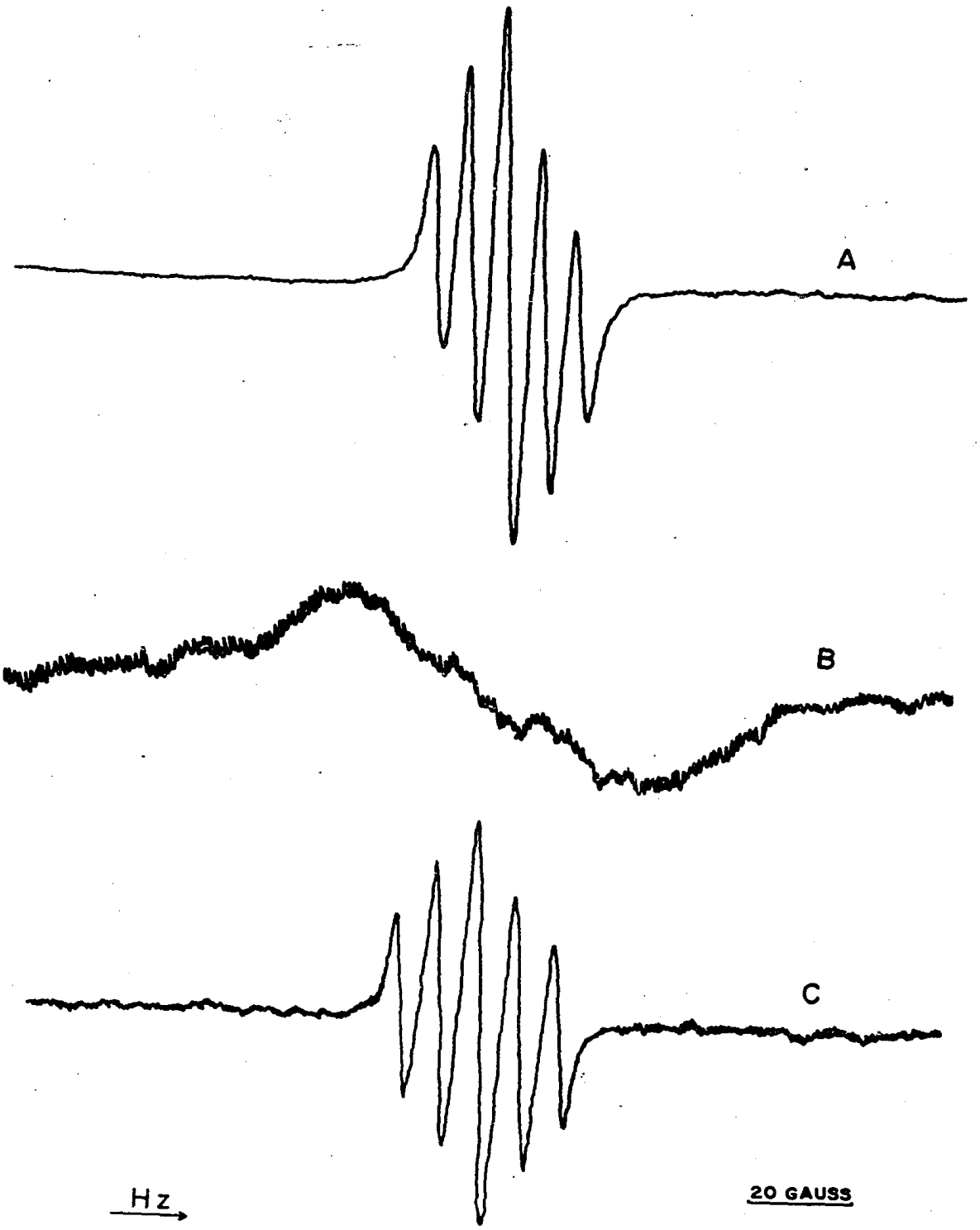
A
B
C
Hz
20 GAUSS

FIG. 3-10: ESR spectra of DSL-Y.

(A) Free DSL-Y in acetonitrile.

(B) Immobilized spectrum of DSL-Y at HCS.

(C) Back titration of (B) with excess DNP-Lysine.

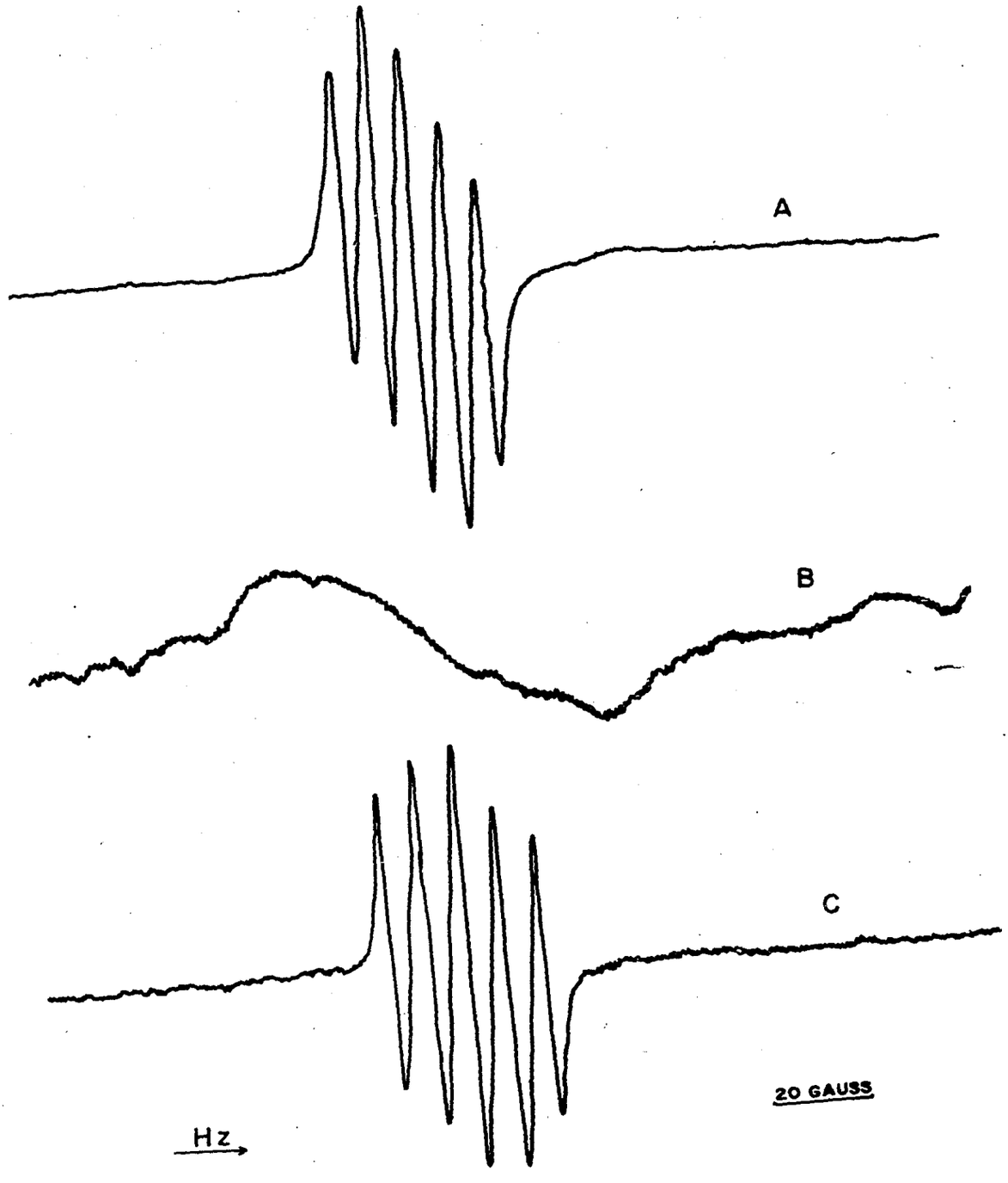
A
B
C
20 GAUSS
Hz

FIG. 3-11: Anisotropic ESR spectra of DSL-R.

(A) DSL-R-ABT complex spectrum. ABT concentration is approximately 20 mg/ml.

(B) DSL-R in 2.5% ethanol 97.5% glycerol.

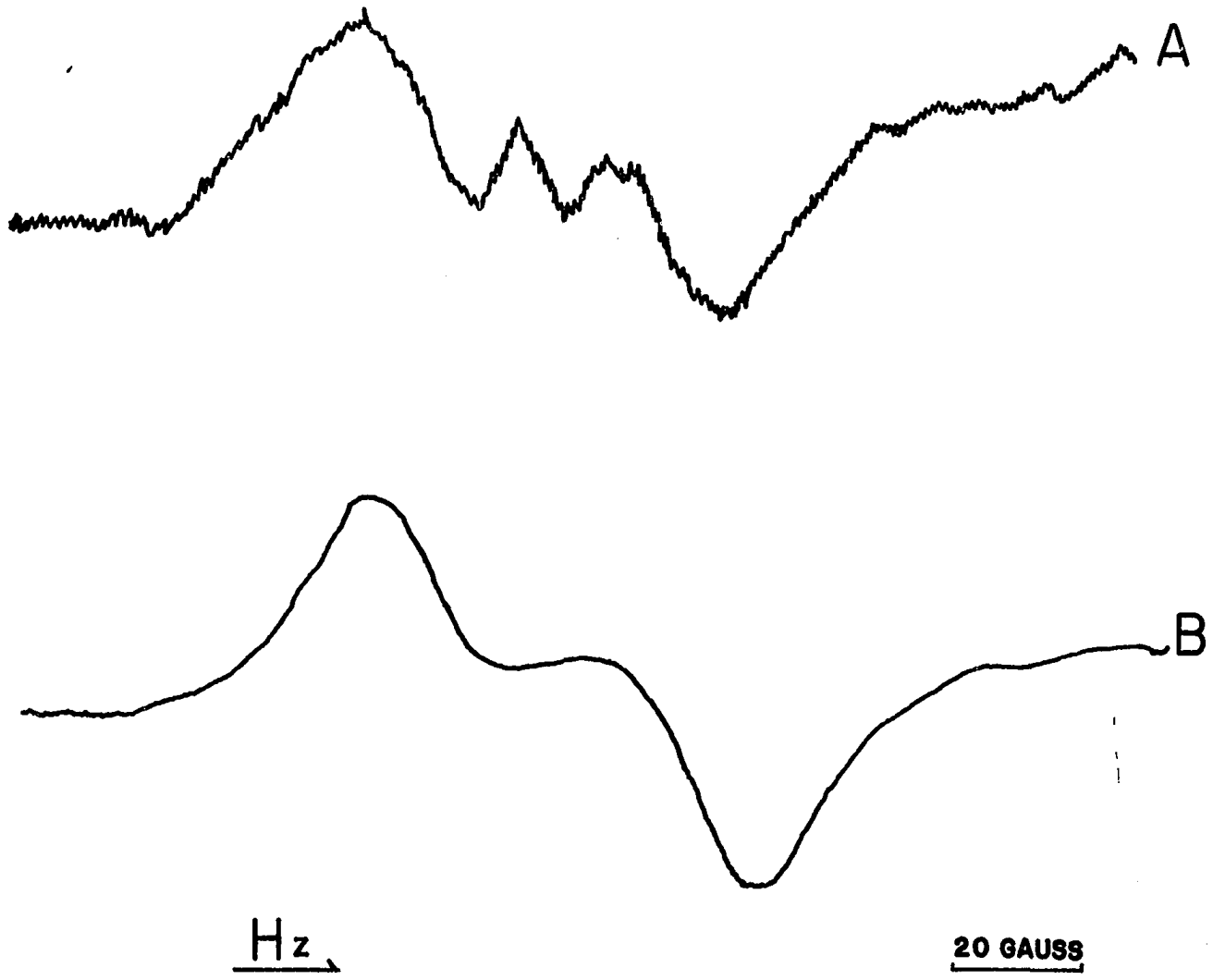
A
B
Hz
20 GAUSS

FIG. 3-12: Anisotropic ESR spectra of DSL-Y.

(A) DSL-Y-ABT complex spectrum ABT concentration is approximately 20 mg/ml.

(B) DSL-Y in 2.5% ethanol 97.5% glycerol.

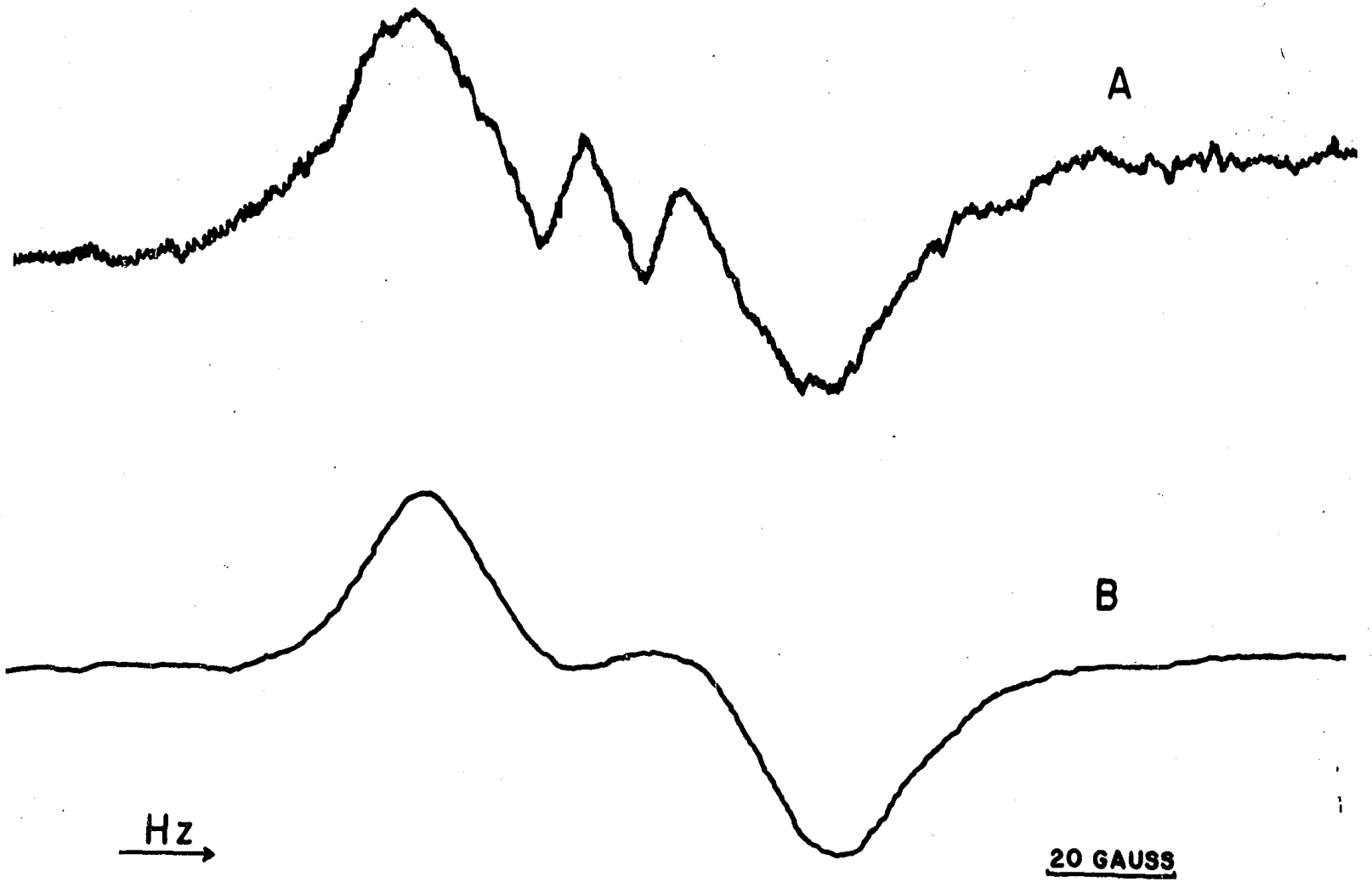
A
B
Hz
20 GAUSS

FIG. 3-13: NMR spectrum of 1-fluoro-5-(N-2,2,6,6-tetramethyl-4-piperidinyl)-2,4-dinitrobenzene.

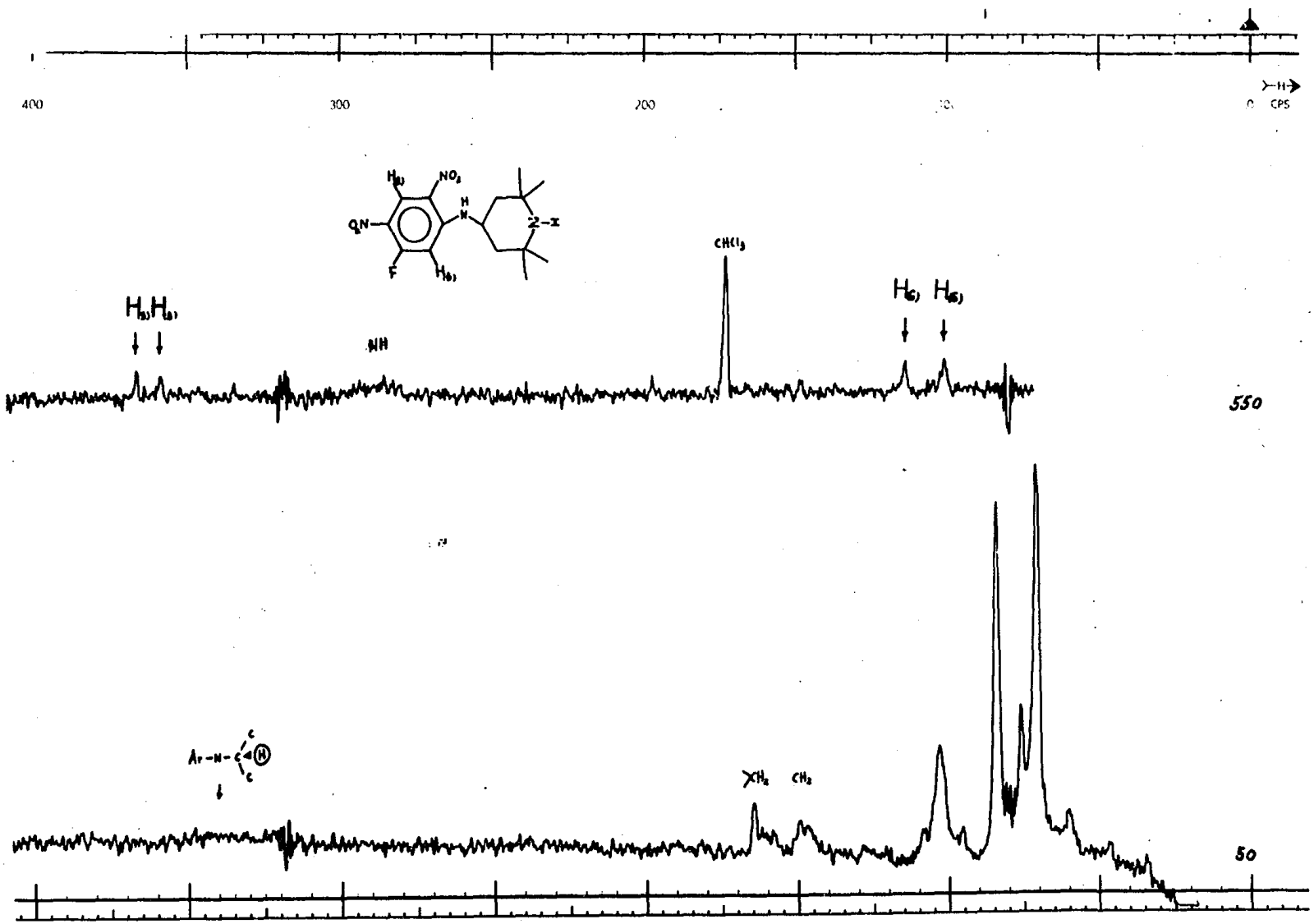
400
300
200
0 CPS
NO2
F
CHCl3
NH
550
50

FIG. 3-14: ESR spectra of 1-(2,2,6,6-tetramethyl-4-piperidin)-3-(2,2,5,5-tetramethyl-3-pyrrolindin)-2,4-dinitrodianiline.

(A) In 5% ethanol 95% phosphate buffer at pH 7.6.

(B) Antibody immobilized spectrum.

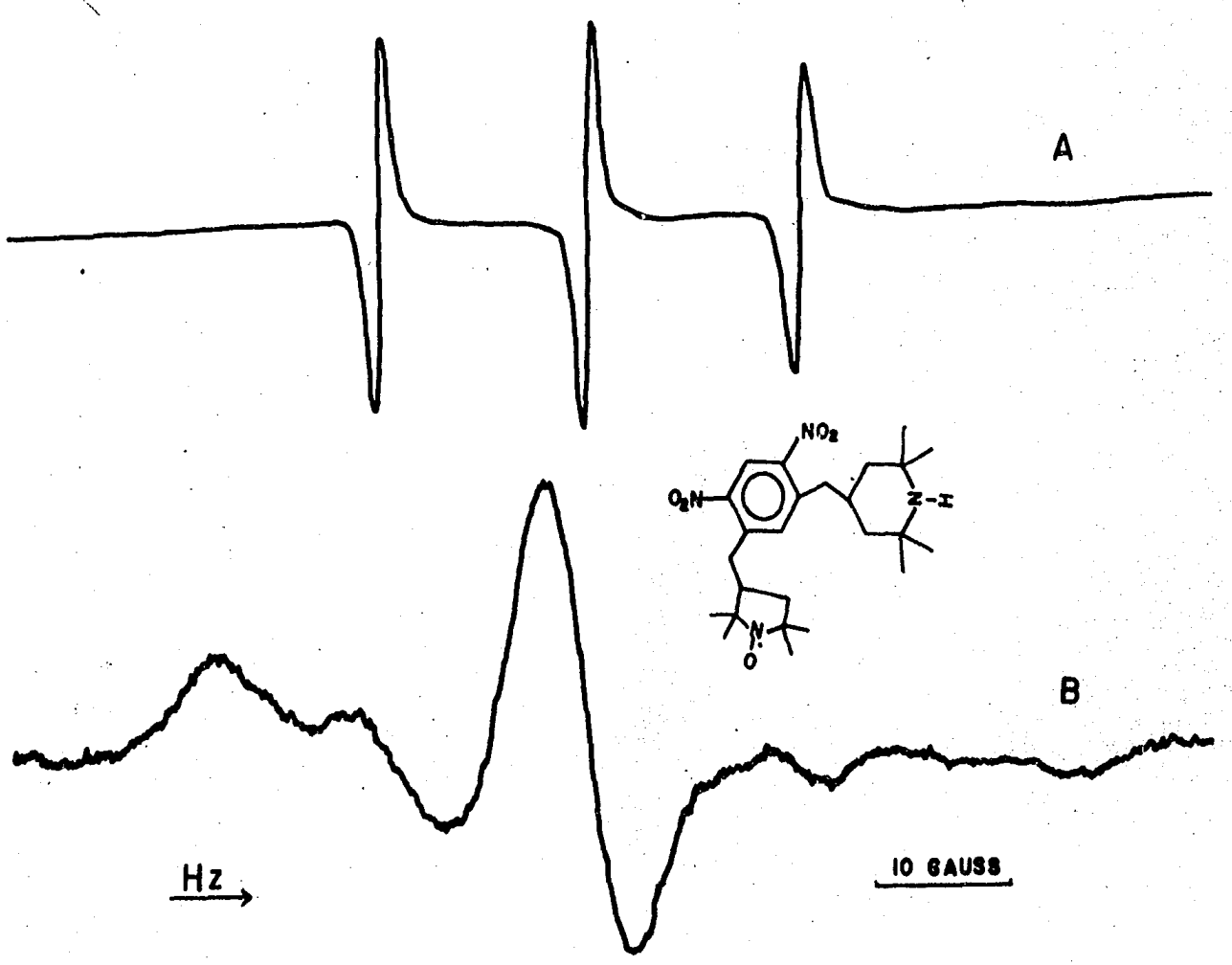
A
B
NO_2
O_2N
Z-I
N
O
Hz
10 GAUSS

(F) Discussion

Although ESR has been a very powerful technique in studying triplet states in solids, very few triplets have been observed in solution because of their short life span and large anisotropic zero-field splitting (S.I. Weissman, 1958). The double spin-labels used in the present experiment are stable biradicals with rigid configurations and are in the ground triplet state. This is due to the localization of the two unpaired electrons on separate nitrogen nuclear centers enabling full exchange of the two unpaired electrons without large zero-field broadening of the anisotropic spectra. The dependence, A_{max}, of the anisotropic spectra on the relative orientations of the two hyperfine tensors has been used as a measurement of external distortion, which in effect reflects the flexibility of the local environment. This method can be extended by varying d_1 and d_2 (see Fig. 3-1) so that d_3 can be varied. Then the exchange interaction between the two unpaired electrons will be highly dependent on d_3, the average distance between the two radical centers. Preliminary results indicate DSL-5-MA has a very weak binding to the HCS of AB-T as compared to DSL-R or DSL-Y shown in Figs. 3-9 and 3-10. Analogous to DSL-R and DSL-Y, the isotropic spectra of red and yellow crystals of DSL-5-MA are different (Fig. 3-15). When the two isomers were added to AB-T, the red

FIG. 3-15: ESR spectra of DSL-5-MA

(A) Red isomer of DSL-5-MA

(B) Yellow isomer of DSL-5-MA

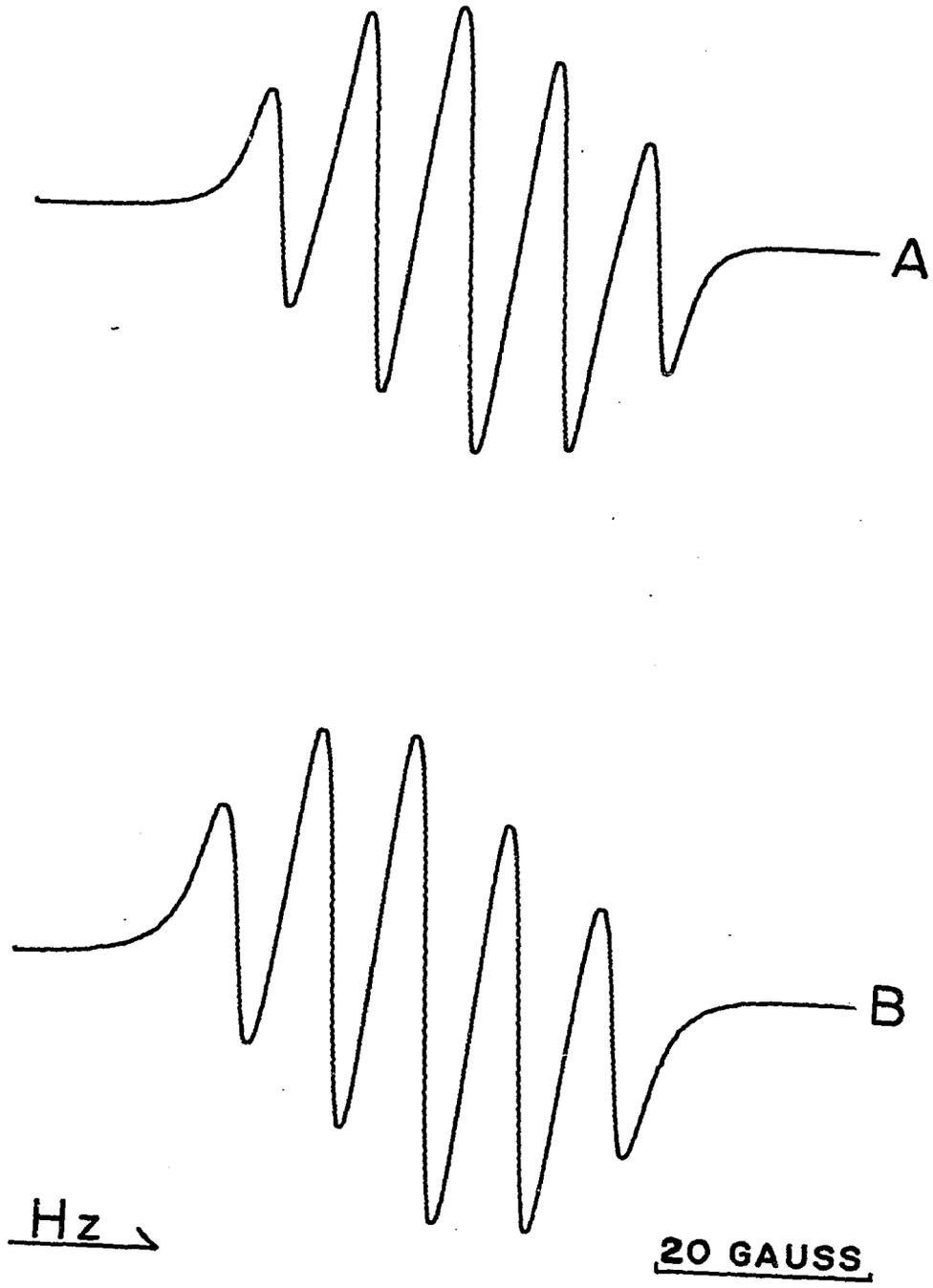
A
B
Hz
20 GAUSS

isomer appears to have very little binding while the yellow isomer has some affinity to the HCS. These are contrary to the result of Fig. 2-7 where DNP-5-MA has very well-resolved anisotropic spectra (i.e. indicate high affinity). The anisotropic spectrum of the yellow isomer appears to be an exchange-narrowed single-line spectrum, which is quite different than its anisotropic spectrum in viscous medium. These results then would suggest the HCS has limited flexibility.

In summary, the DSL technique developed here makes use of the exchange interaction and orientation dependence of the two unpaired electron hyperfine tensors. In general, the DSL has the advantage of being very sensitive to external distortion and still preserve all the qualities of a single spin-label. For every DSL, an appropriate singlet state double label can be prepared which has the same basic structural configuration as DSL but carries only one unpaired electron. Therefore, the anisotropic ESR spectrum of singlet-state double label like the SSL is a function of τ_c.

(G) Suggestions for Further Experiments

The preceding work can be fairly said to have demonstrated the validity and usefulness of spin-labeling as a general method for determining the dimensions of the combining site of any antibody directed towards a hapten to which a spin-label can be attached. Certain enzyme active sites could be probed in a similar manner by constructing labels of varying dimensions that are either substrates, specific inhibitors, or cofactors.

(1) Further investigations of the anti-DNP antibody system.

(a) Correlation of the formation of the HCS to the hapten-protein carrier used in the immunization of the rabbit.

(b) Evaluation of the binding contribution of the H and L chains to the HCS by the study of individual peptides chains, and compare the recombined HCS with relation to the intact site.

(c) Comparison of the HCS of Fab, $F(ab')^2$ and that of the intact antibody.

(d) Studies of the antibody binding affinity and its HCS structure in preparations fractionated according to binding constant and antibodies produced at different stages of the immuni-

zation process.

(2) Spin-labeled organophosphate studies of esterase active sites.

Much progress has been made in the elucidation of the primary structure around the active site of esterases. However, much more work needs to be done, since the knowledge of the primary structure of esterases, though extremely important, is in itself not sufficient for the understanding of the mode of action of these enzymes. Further progress in the immediate future will depend on our ingenuity in devising methods to analyze the physicochemical parameters which specify the active native site.

It would be interesting to prepare a series of spin-labeled organophosphates of the following general formula:

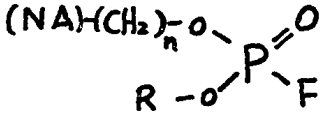

where $n = 0, 1, 2 \cdots$

(NA): 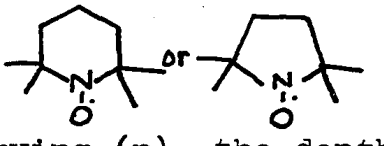

(R): $CH_3-\overset{|}{C}H-CH_3$

(a) By varying (n), the depth of the active site can be detected for each individual esterase.

(b) By varying (NA) and (R), namely, varying the fitness of the label to the esterase active site,

one can physically distinguish the dimensional differences in the active sites of the various esterases.

(c) If NA and R are both spin-labels, then the class of double-labeled inhibitors will be able to distinguish the configurational differences of the active site of various esterases.

In conclusion, the dimensions, and any change in the configuration of a specific protein binding site could, in theory, be probed in solution provided a suitable spin-label could be prepared.

BIBLIOGRAPHY

1. Berliner, L.J. and McConnell, H.M. (1966), Proc. Natl. Acad. Sci. U.S., 55, 708.

2. Buckley, C.E., Whitney, P.L. and Tanford, C. (1963), Proc. Natl. Acad. Sci. U.S., 50, 827.

3. Carsten, M.E. and Eisen, H.N. (1955), J. Am. Chem. Soc., 77, 1273.

4. Cheng, W.C. and Talmage, D.W. (1965), J. Biol. Chem., 240, 3530.

5. Cheng, W.C. and Talmage, D.W. (1966), J. Immunol., 97, 778.

6. Dupeyre, R.M., Lemaire, H. and Rassat, A. (1964), Tetrahedron Letters, 27, 1781.

7. Dupeyre, R.M. and Rassat, A. and Rey, P. (1965), Bull. Soc. Chim. France, 32, 3643.

8. Dupeyre, R.M. and Rassat, A. (1966), J. Am. Chem. Soc., 88, 3180.

9. Eisen, H.N. and Siskind, G.W. (1964), Biochemistry, 3, 996.

10. Feinstein, A. and Rowe, A.J. (1965), Nature, 205, 147.

11. Fleischman, J.B. (1966), Am. Rev. Biochem., 35, 632.

12. Gitlin, D. (1966), Am. Rev. Med., 17, 1.

13. Griffith, O.H., Cornell, D.W. and McConnell, H.M. (1965), J. Chem. Phys., 43, 2909.

14. Haber, F. (1964), Proc. Natl. Acad. Sci. U.S., 52, 1099.

15. Hoffman, A.K. (1961), J. Am. Chem. Soc., 83, 4671.

16. Hooker, S.B. and Boyd, W.C., (1933), J. Immunol., 25, 61.

17. Hsia, J.C. and Piette, L.H. (1968), Recent developments of Magnetic Resonance in Biological System, Hirokawa Pub. Co., Inc., Tokyo, pp. 74-82.

18. Itzkowitz, Martin S. (1967), J. Chem. Phys. 46, 3048.

19. Jablonski, A. (1960), Bull. Acad. Polon. Sci., Ser. Sci. Math. Astron. Phys., 8, 259.

20. Kabat, E.A. (1954), J. Am. Chem. Soc., 76, 3709.

21. Kabat, E.A. (1956), J. Immunol., 77, 377.

22. Kabat, E.A. (1960), J. Immunol., 84, 82.

23. Kabat, E.A. (1961), Kabat and Mayer's Experimental Immunochemistry, 2nd edition, pp. 243-244.

24. Kivelson, D. (1960), J. Chem. Phys., 33, 1094.

25. Krause, S. and O'Konski, C.T. (1963), Biopolymers, 1, 503.

26. Landsteiner, K. (1945), The Specificity of Serological Reactions, rev. ed., Harvard Univ. Press, Cambridge, Massachusetts.

27. Landsteiner, K. and Lampl, H. (1917), Z. Immunitatsforsch, 26, 293.

28. Little, J.P. and Eisen, H.N. (1967), Biochemistry, 6, 3119.

29. Metzger, H., Wofsy, L. and Singer, S.J. (1963), Biochemistry, 2, 979.

30. Metzger, H., Wofsy, L. and Singer, S.J. (1963), Arch. Biochem. & Biophys., 103, 206.

31. Neolken, M.E. and Tanford, C. (1964), J. Biol. Chem., 239, 1828.

32. Ogawa, S. and McConnell, H.M. (1967), Proc. Natl. Acad. Sci. U.S., 58, 19.

33. Ohnishi, S. and McConnell, H.M. (1965), J. Am. Chem. Soc., 87, 2293.

34. Ohnishi, S.I., Maeda, T., Ito, T., Hwang, K.J. and Tyuma, I. (1968), Recent developments of Magnetic Resonance in Biological System, Hirokawa Pub. Co., Inc., Tokyo, pp. 83-87.

35. Parker, C.W., Kern, M., and Eisen, H.N. (1962), J. Exptl. Med., 115, 789.

36. Porter, R.R. (1959), Biochem. J., 73, 119.

37. Porter, R.R. (1962), Basic Problems of Neoplastic Disease, Gellhorn and Hirschberg editions, 177.

38. Rozantzev, E.G. (1964), Izvestiya Akademii Nauk SSSR Seriya Khimicheskaya, 2, 2137.

39. Rozantzev, E.G. and Neiman, M.B. (1964), Tetrahedron, 20, 131.

40. Rozantzev, E.G., Goluber, V.A., Neiman, M.B. and Kokhanov, Yu.V. (1965), Izvestiya Akademii Nauk SSSR Seriya Khimicheskaya, 3, 572.

41. Rozantzev, E.G. and Krinitzkaya, L.A. (1965), Tetrahedron, 21. 491.

42. Rozantzev, E.G. and Kokhanov, Yu.V. (1966), Akademii Nauk SSSR Bulletin Div. et Chemical Sciences, 8, 1422.

43. Pressman, D., Bryden, J.H., and Pauling, L. (1948), J. Am. Chem. Soc., 70, 1352.

44. Sandberg, H.E. and Piette, L.H. (1968), Agressologie, 9, 1.

45. Sips, R. (1948), J. Chem. Phys., 16, 490.

46. Smith, Ian C.P. and Yamane, Tetsuo (1967), Proc. Natl. Acad. Sci., 58, 885.

47. Stryer, L. and Griffith, O.H. (1965), Proc. Natl. Acad. Sci. U.S., 54, 1785.

48. Valentine, R.C. and Green, M.O. (1967), J. Mol. Biol., 27, 615.

49. Velick, S.F., Parker, C.W. and Eisen, H.N. (1960), Natl. Acad. of Sci., 46, 1470.

50. Weissman, S.I. (1958), J. Chem. Physics, 29, 1189.

51. Whitney, P.L. and Tanford, C. (1965a), Proc. Natl. Acad. Sci. U.S., 53, 524.

52. Whitney, P.L. and Tanford, C. (1965b), J. Biol. Chem., 240, 4271.

53. Wofsy, L., Metzger, H., and Singer, S.J. (1962), Biochemistry, 1, 1031.

54. Zerner, B., Bond, R.P.M. and Bender, M. (1964), J. Am. Chem. Soc., 86, 3674.

ACKNOWLEDGEMENTS

I am very grateful for the predoctoral fellowship I have received from the Institute of Student Interchange, East-West Center, from 1964 to 1968.

I also wish to acknowledge the working experience of spin-labeling technique I have acquired during a brief visit to Dr. H. McConnell's laboratory at Stanford University in 1966, which later served as a spark for the development of this work. This experience could never be so vivid without the friendship of Dr. Ian Smith and Mr. Ralph Young.

Comments from Dr. Lubert Stryer of Stanford University were also very helpful.

The technical assistance from Mr. Herbert Nakagawa, Mr. David Moriguchi, Mr. Robert Green, Dr. Dan Kosman, Dr. Gary Rabold, Dr. Howard Sandberg, Dr. A.A. Benedict, Miss May Robertson, Mrs. Monica Winnick, and Mrs. Ellen Wildman during certain phases of this work are gratefully acknowledged. I also would like to thank Miss Janet Kawata for her patience in typing out this manuscript.

The production of this work would not have been possible without the untiring effort of my wife, Mary.

BIOGRAPHICAL

1938 --Born in I-Yang, Hu-nan, China.
1962 --B.S., National Taiwan University, Taipei Taiwan, China.
1964-1968 --East-West Center Predoctoral Fellowship, Department of Biochemistry and Biophysics, University of Hawaii.

GRADUATE STUDIES

Graduate Field: Biophysics.
University of Hawaii, Honolulu, Hawaii.
660 Special Instrumental Methods. Professor Lawrence H. Piette.
~~(Advanced Enzymology. Associate Professor Robert H. McKay.)~~
621 Chemistry of Proteins. Assistant Professor John B. Hall.
750 Topics in Biophysics. Professor Lawrence H. Piette

Other Studies.
Quantum Chemistry. Assistant Professor
754 J. Adin Mann, Jr.

PUBLICATIONS

"ESR Spin-Labeling Studies of Hapten Antibody Interactions." (With L.H. Piette). Symposium on Application of Magnetic Resonance Biological Systems. Tokyo, August 1967. Pub., Hirakawa.

"Structural Characteristics of Antibody-Hapten Combining Sites from ESR Spin-Labeling Studies." (With L.H. Piette). Archives of Biochemistry and Biophysics. 1968. In print.